Politecnico di Torino

Master's Degree in Energy and Nuclear Engineering

Renewable Energy Systems

March 2025

Techno-Economic Modelling and Comparative Analysis of Horizontal Axis Tidal Energy Converters

Supervisors:
Giuseppe Giorgi
Emiliano Nelson Gorr

Candidate:
Petri Mattia

Acknowledgements

First of all, I would like to thank Professor Giuseppe Giorgi for suggesting a thesis topic that was originally unknown to me, which proved to be very interesting.

Special thanks go to my co-supervisor Dr. Emiliano Gorr for his constant support and continuous motivation provided during this work. His enthusiasm significantly contributed to the quality of the thesis.

I would also like to mention Blue-X, the European project of which this work is part, which aims to harness offshore potential by providing decision support services.

It was a hard work, but I'm really grateful for the opportunity I received.

Abstract

The increasing scarcity of onshore land and the rising efficiency and competitiveness of marine renewable energies (MRE) are accelerating the offshore energy transition. However, the limited experience of commercial MRE deployments and the scarcity of detailed cost data availability often lead to unrepresentative economic models. This work proposes a cost model based on the bottom-up approach (BUA) to three tidal energy converters (TECs): monopile, floating, and gravity-based substructures (GBS), combined with a power assessment based on the available tidal current models and real meassurements. Cost functions for multiple TEC components were retreved from literature and adapted to tidal sector. Techno-economic analysis was performed to five marine locations: Fall of Warness (Scotland), Punta Pezzo (Italy), Cozumel (Mexico), Fromveur and Raz Blanchard (France), showing that monopile and floating TEC achieve the highest annual power output and capacity factor, equal to 393 kW and 39.35% in Fromveur, respectively, due to proximity to sea surface.

In all cases, an asymptotic decreasing trend in LCoE is observed as the installed capacity of the sites increases, with LCoE ranging between 840 and 50 €/MWh with 32 turbines installed. Among all the sites analyzed, Fall of Warness and Cozumel generated the lowest and highest LCoE values, respectively. In all case studies, except of Punta Pezzo, monopile TECs generated the lowest LCoE values followed by floating type. At Punta Pezzo, floating TEC proved more cost-effective due to greater water depth (100 m), explaining how monopile are preferable in shallow waters (<50 m) and floating TECs at greater depths.

Objective

The main objective of this work is to develop a techno-economic model that evaluates the feasibility and a comparison of the three stream tidal turbines, by firstly creating a cost model, furtherly assess a resource availability and power production, and finally combine them. For this purpose, the thesis is structured as follows:

Chapter 1 provides a background about tidal energy and its technologies, focusing on three main types of tidal energy converters (TECs): gravity-based, monopile, and floating. It outlines the research objectives, methodology, and the current state of tidal energy costs.

In Chapter 2 the cost model is developed for different TEC components, breaking it down into Capital Expenditures (CapEx), Operational Expenditures (OpEx), and decommissioning costs.

Chapter 3 examines different methodologies for assessing the tidal energy potential, using data from models and real measurements. Statistical analysis and power curves are applied to estimate energy output and capacity factor.

In Chapter 4 five case studies (Fall of Warness, Fromveur, Raz Blanchard, Punta Pezzo and Cozumel) are analysed to assess the viability of different TECs, comparing power production and economic feasibility indicators.

In the final part, Chapter 5, all the findings are summarized, highlighting the economic challenges and potential of TECs.

Table of Contents

List of Figures

List of Tables

1. Introduction

1.1. Background

Tidal energy has emerged as a promising renewable energy source with the potential to contribute to the global transition toward sustainable energy systems. Unlike other intermittent renewable energy sources such as wind and solar, tidal energy has a predictable and reliable power profile, making it attractive for grid stability and energy security.

1.2. Technology

Tidal energy converters can be generally classified in two categories: tidal range and tidal stream technologies. Tidal range or tidal barrage consists of a dam, typically built across a bay or estuary which experiences high tidal ranges, reaching up to 13.5 m as it occurs in La Rance in France, the largest operating tidal barrage with a generating capacity of 240 MW [1]. The working principle is the same as hydroelectric generation, but with the additional possibility of the turbine to operate in both current directions [2]. It utilizes the difference in water levels between high and low tides, which follow a cycle, to produce electricity.

The other main category is the tidal stream, which exploits the kinetic energy of the water current to generate electricity as it occurs in a wind turbine. In this context, horizontal water currents are generated by vertical variations of water levels by tides, that's why they're also called tidal currents. Tidal stream technologies can be further classified in [3]:

- Horizontal axis turbine (HAT): it has the same working principle of a wind turbine in which tidal stream passes through the turbine and make the blades to rotate around a horizontal axis;

Figure 1.2-1: Sabella D10 HAT tidal turbine [4]

- Vertical axis turbine: works in the same way of the HAT, but blades rotate around a vertical axis;

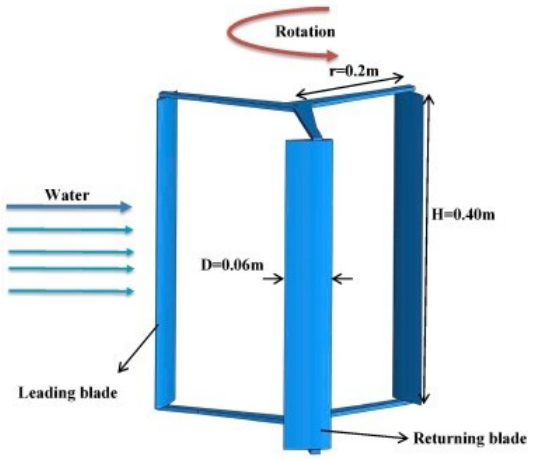

Figure 1.2-2: VAT tidal turbine scheme [5]

- Tidal kite: as the name says, a kite, with turbines attached below it, is attached to the seabed through a mooring line, and the kite flies in the tidal stream making the turbines to rotate.

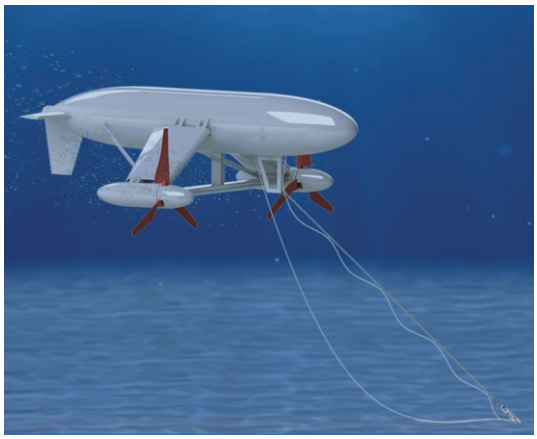

Figure 1.2-3: Gemstar tidal kite design [6]

Only the main stream technologies were previously described, but many other types are present, like the Archimede screw and the oscillating hydrofoil, which haven't been described because of being at a demonstration phase stage or haven't been a widespread technology.

The most prominent and popular technology is the HAT, which can be further classified in terms of foundation type, here described [7]:

- Gravity-based substructure: turbine is attached to a structure which is fixed to the seabed due to gravity, so friction. For this reason, it's needed a huge mass, which is typically composed of steel or concrete;

Figure 1.2-4: AR1500 GBS tidal turbine used in Meygen project [8]

- Monopile: the same wind turbine principle is involved in which the turbine is mounted on pile penetrating the seabed. In recent monopile TECs the turbine is attached to a crossarm which can be lifted up or down, allowing easier maintenance for example;

Figure 1.2-5: Seagen S-1.2 MW monopile tidal turbine [9]

- Floating platform: as the name suggests, the turbine is mounted on a floating platform which is moored to the seabed, and it may swing depending on the tidal current direction or remaining fixed in a certain position.

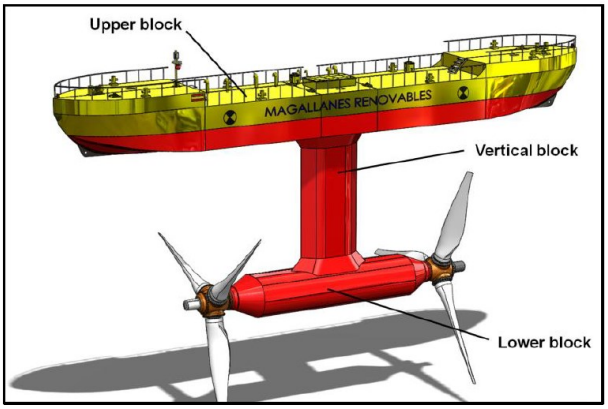

Figure 1.2-6: Atir floating platform tidal turbine owned by Magallanes Renovables [10]

These three technologies will be analysed in this work since they're the most popular ones and more projects involving these TECs are present around the world.

1.3. Objectives and Methodology

This work aims to develop a techno-economic model that evaluates the feasibility and a comparison of the three stream tidal turbines, by firstly creating a cost model, furtherly develop a resource and power assessment, and finally combine them.

The research employs a combination of literature review and data analysis to assess the techno-economic performance of TECs, involving a review of existing projects, in terms of turbine used and cost encountered, a cost model development incorporating CapEx, OpEx and decommissioning costs, and a result comparison between the technologies by evaluating different power and cost metrics.

1.4. Current status

Recent studies indicate that current Levelized Cost of Electricity (LCoE) ranges from 0.11 to 0.48 €/kWh for tidal stream converters, and the European commission set a LCoE of 0.1 €/kWh as target by 2030, as can be noted in Figure 1.4-1.

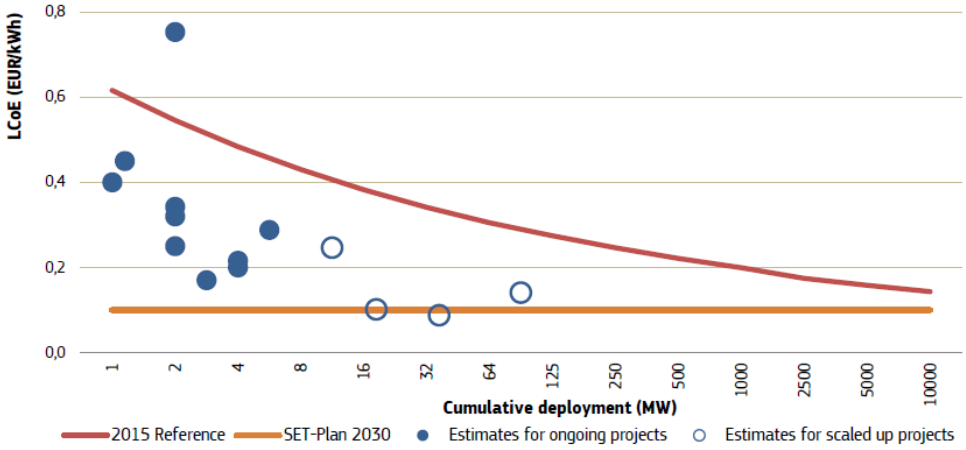

Figure 1.4-1: LCoE of estimated current and scaled up tidal energy devices [3]

In terms of financial indicators, the average CapEx is 3.4 m€/MW, while the average OpEx is estimated at 0.5 m€/MW every year. It's important to say that only TECs with a Technology Readiness Level (TRL) higher than 7 are considered in the costs since a lower value of TRL means that the technology is still at a demonstration phase.

Worldwide, around 521 MW of combined capacity of tidal and wave energy converters is installed, and 98% of this is accounted by the tidal range, with plants in Korea, France and Canada. Despite this large coverage, no tidal barrage power plants have been developed in the last decade, mainly due to the high investment costs and environmental impact.

2. Cost analysis

A detailed cost analysis of horizontal tidal energy converters (TECs) will be presented in this chapter in order to create a cost model for the three TEC technologies, i.e. gravity-based substructure (GBS), monopile and floating. The total cost breakdown includes Capital Expenditures (CapEx), Operational Expenditures (OpEx) and decommissioning costs, which will be described in detail in each subchapter to provide a comprehensive framework for assessing economic feasibility of tidal energy projects.

2.1. CapEx Cost Functions

In this section all the TEC components will be described, and one or more cost functions will be proposed for each. Most of these functions has been retrieved from literature regarding the wind energy sector, because almost no functions were available for the specific tidal sector. Considering the fact that these two technologies are really similar in terms of working principle, it could be possible to take wind cost functions and use them in the TEC cost analysis, if the range of validity of a given equation was in line with the TEC variable used in the function.

2.1.1. Blade

In [11] a simple cost function is present which requires only the rotor radius as input parameter. Unfortunately, this function is valid only for a radius higher than 25 m, which is not the case for TECs since rotor radius is in the order of 10 m. A linear scaling law was an option, but it has been discarded since the overall impact of scaling in terms of captured energy and load levels is unclear, and sophisticated scaling models are necessary for this [12]. Given this, another cost function is proposed, which requires the blade mass as input variable as

$$Cost_{blade} = 13.084 * M_{blade} - 4452.2\,, \qquad Eq.(1)$$

This equation considers a blade composed by different percentages of the following materials:

- Fiberglass fabric: 60% of the element;
- Vinyl type adhesives: 23% of the element;
- Metal fasteners: 8% of the element;
- Urethane and foam products: 9% of the element.

Unfortunately, there isn't a simple and direct way to calculate the mass of the blade other than knowing the geometry of it, so it's necessary to design the blade, such as with BEM method, define a thickness over chord ratio, so the overall volume and mass can be found. Compared to wind turbines, in the TEC the acting forces on the blades will be one or two order of magnitude higher, so a more resistant blade should be designed. Since the material involved in the tidal blade manufacturing is the same as for wind turbines, meaning fiberglass or carbon fibre in some cases, the only way to design a more resistant blade is to increase the thickness-chord ratio. This ratio varies along the blade, since close to the root a higher thickness is necessary, but it's possible to consider, in general, a ratio in the range of 0.1-0.2 for wind turbines, while for tidal turbines it's increased to 0.3. [13]
Since higher level of details is required, a simpler cost metric is proposed by [14], which requires the rotor diameter as variable, evaluating cost as,

$$Cost\ metric = 40\ €/m\ , \qquad Eq.(2)$$

$$COST_{blade} = 40 * \left(\frac{D}{2}\right)^{2.7} , \qquad Eq.(3)$$

2.1.2. Hub

The hub is the component that holds the blades and transfer the motion to the main shaft of the turbine. There are different shape designs of the hub, which depend on the type of generator and the design of the blades [15]. In the proposed equation only the mass of the blade will be used as a variable to calculate the mass of the hub. After that, by assuming a hub made of ductile iron casting, with a cost of 4.25 $/Kg, the cost of the hub can be calculated as, [12]

$$M_{hub} = 1.92 \cdot (0.954 \cdot M_{blade} + 5680.3)\ , \qquad Eq.(4)$$

$$COST_{hub} = 4.25 \cdot M_{hub}\ , \qquad Eq.(5)$$

Since the blade mass can't be found without a detailed analysis, as previously mentioned, a simpler way is required to obtain the cost, which is provided by [14], as,

$$Cost\ metric = 1000\ €/m\ , \qquad Eq.(6)$$

$$COST_{hub} = 1000 * \frac{D}{2}\ , \qquad Eq.(7)$$

2.1.3. Blade pitch mechanism and bearings

The pitch system is an important component of the turbine because it allows the blades to rotate in order to reach the optimal orientation at different flow speeds so that the maximum energy can be

extracted. In wind sector it's also used as a power control system when the wind speed reaches values too high that the turbine can't handle. In the case of tidal energy, the current velocities are predictable, so there is a much lower risk of reaching an excessive power above the nominal value compared to wind turbines. So, the pitch system may be used to keep the highest power coefficient at different current velocities and for safety reasons, but some commercial TECs do not include this system. In the cost function proposed also the bearings necessary to support the pitch system mass is included. In this case the only variable present is the rotor diameter and cost is evaluated as, [11]

$$COST_{pitch} = 2.28 \cdot (0.2106 \cdot D^{2.6578}) , \qquad Eq.(8)$$

and since no range of validity is present, it's assumed that this equation is valid also in the case of TECs where rotor diameters are about 20 m.

2.1.4. Main Bearings and Housing

The main bearings are components needed for supporting and guiding the main shaft of the turbine and providing low friction. A mass function is proposed in NREL study, in which main bearings mass is related to the rotor diameter. Since forces are different in a tidal turbine, it doesn't seem reasonable to consider rotor diameter as a variable. Current velocities are lower compared to wind velocities, but, on the other hand, density of water is 1000 times than air. As a simple model, it was possible to relate the bearing mass only to the thrust force, neglecting the other forces (radial and moment loads) since the most relevant is the axial one. First of all, the thrust force F_T was calculated, considering a thrust coefficient C_T for the wind turbine of 0.8 as,

$$F_T = \frac{1}{2}\rho C_T A U^2 , \qquad Eq.(9)$$

where ρ is the air density equal to 1 kg/m^3, A is the rotor area and U is the wind speed. The same equation is used for the tidal turbine, this time with a water density ρ=1025 kg/m^3 and U as the tidal current velocity.

In order to find a relationship between thrust force and mass of bearings, the original data has to be extrapolated from the original study [16]. From there, turbine diameter, bearings mass and wind speed are written down, and a linear relationship is found, as depicted in Figure 2.1-1.

Table 2.1-1: Original main bearings data

Cp	U [m/s]	Ct	Ft [kN]	Mass [kg]
0,43	12	0,8	115,9	103,1
0,44	12	0,8	227,2	339,6
0,44	12	0,8	454,5	1154,7

Cp=power coefficient, U=wind speed, Ct=thrust coefficient, Ft=thrust force

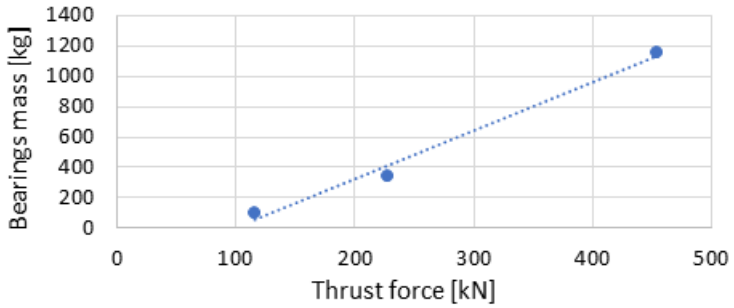

Figure 2.1-1: Relationship between bearing mass and thrust force

$$M_{bearing} = 3.1771 * F_T - 312.26 \ , \qquad Eq.(10)$$

After mass of the bearing is defined, it is supposed that only one main bearing is present, despite if different configurations may involve an additional one, and that the housing mass is the same as the main bearing one. Given this, the overall cost of main bearings is obtained by considering a mass price of 17.6 $/Kg for both components as stated in [16]:

$$C_{bearing} = 2 \cdot M_{bearing} \cdot 17.6 \ , \qquad Eq.(11)$$

2.1.5. Yaw Drive and Bearing

The yaw system is used to rotate the axis of the turbine so that the flow direction is directly facing the rotor, so that the maximum power can be extracted. Most of the tidal current flows are approximately bidirectional, which means that ebb and flow are 180°, so it can be easily predicted when the current will change direction, and so the TEC, and how many degrees it will rotate [17]. The cost and mass function include also the bearing that allows the turbine to rotate.

As well as in the case of main bearings, also in the yaw system an equation with rotor diameter is present in, but, as stated from the same paper, it's incorrect to consider that variable in the cost function [11]. From the study in which that paper refers to, a mass function for yaw bearings is extracted from [16], expressed as,

$$M_{yaw\ bearings} = 0.0152 \cdot \left(\frac{M_{max}}{D_{yaw}} - 36\right)^{1.489}, \qquad Eq.(12)$$

in which M_{max} is the maximum applied moment on the bearings in kNm and D is the yaw bearing diameter. By knowing the yaw bearings mass, the total cost of the yaw system is estimated to be twice the cost of the yaw bearings, so the cost function becomes as,

$$C_{yaw} = 2 \cdot \left(M_{yaw\ bearings} \cdot 6.689 + 953\right), \qquad Eq.(13)$$

The maximum applied moment is referred to the maximum moment between the one acting in the y direction M_y, so the one perpendicular to the yaw axis and parallel to the flow direction, and the one acting in the z direction M_z, so the one generated around the yaw axis during the rotation of the nacelle. From the data present in the study, M_y is the maximum applied moment on the yaw bearing, so this will be considered in the evaluation. M_y can be defined as the thrust force acting on the turbine multiplied by the vertical distance between the centre of the hub and the yaw bearing location. Since the yaw bearing is immediately down the nacelle, it can be assumed equal to the half of the height of nacelle cover.

By comparing the acting moment calculated in this way and the moment chosen for the bearing resistance using original data provided in Table 2.1-2, a coefficient around 3 is present, which may represent a safety factor, so SF equal to 3 is included in the equation:

$$M_y = F_T \cdot \frac{D_{cover}}{2} \cdot SF\ , \qquad Eq.(14)$$

Table 2.1-2: Windpact data of yaw bearings to find SF given M_y

Rotor Diameter [m]	U [m/s]	Heigth [m]	Thrust force [KN]	Moment applied [KNm]	Max Moment [KNm]	SF
50	11,24	2,31	151,96	350,51	1017	2,901
70	11,79	3,27	327,92	1071,27	3079	2,874
99	12,40	4,60	724,62	3335,62	10707	3,210

U=wind speed, Height=distance at which thrust force is applied to evaluate applied moment, SF= safety factor

In order to find the yaw bearing diameter, from the AVON bearings data present in the article and reported in Table 2.1-3, it's possible to find a linear relationship between the bolt circle diameter, which can be approximated to the bore diameter of the bearing, and maximum moment they can support.

Table 2.1-3: Avon yaw bearings data

Bolt circle diameter [m]	Max Moment [kNm]
1.45	1217
2.14	3773
2.548	11826
4.086	27646

So, the relationship obtained is the following:

$$D_{yaw} = 9 \cdot 10^{-5} \cdot M_y + 1.53 \qquad Eq.(15)$$

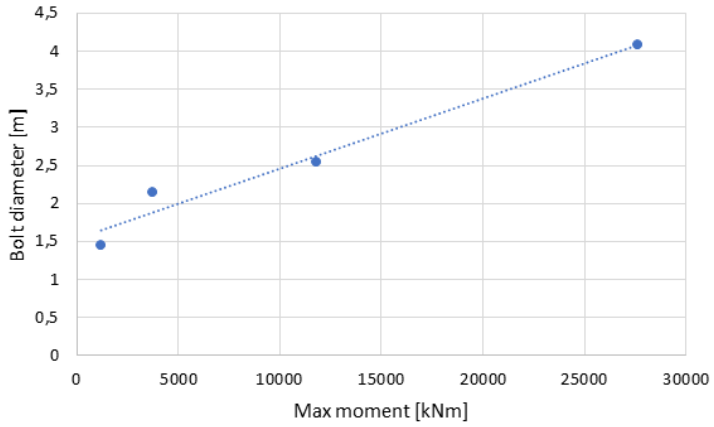

Figure 2.1-2: Relationship between yaw bearing bolt diameter and maximum moment

2.1.6. Mechanical Brake and High-Speed Coupling

The mechanical brake is a safety component used for slowing down and, in extreme conditions, stopping the shaft when the current speeds are higher than the rated one, or an emergency occurs, such as a fault in the electrical system which requires the turbine to be shut down [18]. Generally, in wind turbines, the brake is located on the high-speed shaft because it operates at a high-speed, so a lower torque compared to the low-speed shaft, so it's easier and more precise to control [19]. The same reasoning can be done for the TEC. In the cost function presented the cost associated to the coupling is included, which is needed to remove the brake in case of failure. The variable used this time is the rated power of the turbine (P_N), used to calculate the overall mass of the component. Then, it is assumed a cost of 10 \$/Kg for the component which includes material, labour and manufacturing [12].

$$M_{breake/coupling} = 0.19894 \cdot P_N\,, \qquad Eq.(16)$$

$$COST_{breake/coupling} = 10 \cdot M_{breake/coupling} \qquad Eq.(17)$$

2.1.7. Low-Speed Shaft

The low-speed shaft is a component that transmits the rotational motion from the rotor to the generator through the gearbox, if present. Also in this case, the cost function proposed is related to the rotor diameter, which is not a reliable metric for applying the equation to a tidal turbine. It's better to perform a structural analysis of the shaft by looking at the forces involved. Since the computation of the entire analysis requires input data that aren't easy to choose, and they would add variables to the entire work, a simplified cost metric is proposed by [14] and used.

$$Cost\ metric = 500\ €/m\ , \qquad Eq.(18)$$

$$COST_{shaft} = 500 * \frac{D}{2} \qquad Eq.(19)$$

2.1.8. Gearbox

Since the rotational speed of the rotor is really low, such as 14 rpm of the AR1500 tidal turbine[8] and most of the commercial generators require high rotational speeds, a gearbox is needed in order to transfer the load generated from a low-speed shaft to a high-speed shaft. Many types of gearboxes are commercially available, and they can be subdivided in planetary and multi-stage gearboxes.

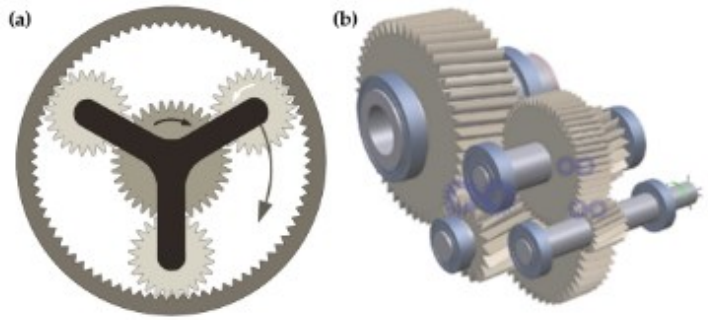

Figure 2.1-3: Schematic of (a) a planetary gear set and (b) a multi-stage gear set

Generally planetary gearboxes can reach higher speed ratios in a compact space and an efficiency around of 99%, while multi-stage gearboxes have a lower cost and an efficiency around 98%. A gear pair in the multistage gearbox can have a speed ratio up to 1:5, while a planetary gear set can reach up to 1:12. In a tidal turbine with a nominal power of the megawatt, the planetary gearbox is preferred since the high torque is better distributed on the gear pairs and costs are reduced due to their small size and mass [20]. As an example, the AR1500 turbine has multi-stage gearbox, with a ratio of 1/98.

Mass of the gearbox depends on the mechanical low-speed shaft torque, and two cases of gearboxes are provided for wind turbines, applicable also to TECs [11]. Since in the paper the cost functions are related to the rated power, it doesn't make so sense to use the same function in a tidal turbine, so a specific cost in €/Kg is provided by [21], which is different for both the two cases considered:

- Single-stage gearbox: this case focuses only on a planetary gearbox, whose characteristics were discussed previously. Single stage means that only a set of gears within the gearbox, so the multiplication of speed occurs in a single step.

$$M_{g1s} = 88.29 \cdot T_{lss}^{0.774} \ , \qquad Eq.(20)$$

$$COST_{g1s} = 6 \cdot M_{g1s} \qquad Eq.(21)$$

- Three-stage gearbox: this case proposed is a mix of a planetary gearbox and a multi-stage one in which helical gears are used, obtaining an overall three-stage gearbox.

$$M_{g3s} = 70.94 \cdot T_{lss}^{0.759} \ , \qquad Eq.(22)$$

$$COST_{g3s} = 10 \cdot M_{g3s} \qquad Eq.(23)$$

It's interesting to note that, at equal torque, the three-stage gearbox is lighter than the single one. It can be expected the opposite since the three-stage gearbox requires more steps, but, by noting the higher cost per unit of mass of this configuration (10 €/kg, contrary to 6 €/kg for single-stage), it may be concluded that advanced and lighter materials are used, and maybe the single-stage gearbox requires additional features or robustness. At the end, the three-stage gearbox results to be the more expensive among the two configurations.

2.1.9. Generator

The generator is the element that converts the mechanical energy into electrical energy that is exported after. Generators can be classified in synchronous and asynchronous. The main difference is that in synchronous generators the generated voltage is synchronized with the rotation of the high-speed shaft, so at each rotor physical position corresponds a peak of the sinusoidal waveform, which is related to the grid frequency, which translates to a fixed shaft speed based on the grid frequency, which can be 50 or 60 HZ depending on the location of the plant, and the number of poles. On the other hand, the asynchronous generator is not bound to the grid frequency and is able to slightly vary the rotational speed of the rotor with respect to the synchronous rotational speed. This flexibility is present due to the slip, which allows the rotor speed to vary while keeping the output frequency synchronized with the grid.

Additionally to this classification, regarding tidal energy, the most common generators used are the squirrel cage induction generator (SCIG), which is asynchronous, and the permanent magnet synchronous generator (PMSG), which, as the names says, it's synchronous [22]. For example, in existing projects there is a PMSG used in the AR1500 TEC [8], and a not specified induction generator in the Andritz Hammerfest TEC used in the Meygen project [23]. Since the size of the generator is proportional to the torque rating, these generators operate at high speed, so that a low torque is reached, and the machines are smaller. For this reason, a gearbox is necessary, as explained before. An alternative is to use the so called low-speed generators, which is a category of generators that operates at a low rotational speed and do not require a gearbox, so they're directly coupled to the turbine. In this way the overall reliability and efficiency is increased since the gearbox is avoided. In order to reach a low rotational speed at the generator, a high number of poles is required. Based on this, the choice between the induction generator or the PMSG is oriented towards the latter since the induction generator will result in a really inefficient design due to the high number of poles and the consequent lower power factor [22]. The disadvantage is that the direct drive generator is much more expensive than the high-speed one, but the cost of the gearbox can be saved, and the reliability is increased.

Cost models for three general types of generators are present in [24] and they used the shaft torque as variable (the low-speed shaft will be used in the direct drive generator). Unfortunately, not a specific cost function of the SCIG is present, but only for the doubly fed induction generator (DFIG), which is another type. Also the cost function related to the direct drive generator doesn't specify what kind of generator is used, if PMSG or induction.

1. Three-stage High-speed generator (DFIG):

$$M_{gen\_3s} = 6.47 \cdot \left(50 \cdot \pi \cdot T_{shaft}\right)^{0.9223}, \qquad Eq.(24)$$

$$Cost_{gen\_3s} = 65 \cdot (50 \cdot \pi \cdot T_{shaft}) \qquad Eq.(25)$$

2. Single-stage medium-speed generator (PMSG):

$$M_{gen\_1s} = 10.51 \cdot \left(\frac{10 \cdot \pi \cdot T_{shaft}}{3}\right)^{0.9223}, \qquad Eq.(26)$$

$$Cost_{gen\_1s} = 54.73 \cdot \left(\frac{10 \cdot \pi \cdot T_{shaft}}{3}\right) \qquad Eq.(27)$$

3. Direct Drive Generator:

$$M_{gen\_dd} = 661.25 \cdot \left(T_{shaft}\right)^{0.606}, \qquad Eq.(28)$$

$$Cost_{gen\_dd} = 219.33 \cdot \left(\frac{2 \cdot \pi \cdot T_{shaft}}{3}\right) \qquad Eq.(29)$$

The shaft torque can be easily calculated as,

$$T_{shaft} = \frac{P_N}{\omega_{shaft}} \qquad Eq.(30)$$

2.1.10. Nacelle Cover

The nacelle cover is the element that hosts all the generating components, so gearbox, shaft, generator and brake system. A cost model of the cover is present for the wind turbine, but it can't be applied to a TEC since different forces are present. In fact, mainly pressure forces are acting on the nacelle cover while designing it in a wind turbine, while in the case of TEC nacelle there is also the hydrostatic pressure to consider, since the turbine is positioned underwater, which is significant for gravity-based TECs.

Comparing hydrodynamic and hydrostatic pressure it can stated that the hydrostatic pressure is much higher than hydrodynamic one, so the nacelle cover can be designed as a pressure vessel, as proposed in [25], with only the hydrostatic pressure acting on it. In order to obtain the thickness, firstly it's necessary to calculate the hydrostatic pressure P as,

$$P = \rho \cdot g \cdot h \ , \qquad Eq.(31)$$

in which h is the depth of the nacelle.

By assuming the nacelle cover as an empty cylinder composed of a material with a given yield strength σ_y, it is possible to design the thickness by using the Mariotte equation, which assumes a thin cylinder. This assumption can be checked after the calculations [26].

$$t = \frac{P \cdot D}{2 \cdot \sigma} \ , \qquad Eq.(32)$$

in which is the outer diameter D is needed and σ is the acceptable working stress obtained by including a safety factor to the yield stress of that material as,

$$\sigma = \frac{\sigma_y}{SF} \qquad Eq.(33)$$

A SF value can be chosen around 1.6 as provided in some structural elements designed in [25], but it can be increased for safety purposes.

Now that the geometry is known and a length of the cylinder L is defined as a design parameter, the volume can be computed, and after that, depending on the material, the mass is obtained. It is assumed that a hemisphere, with same thickness of the cylinder, is covering one edge.

$$M_{nacelle} = \rho_{nacelle} \cdot \left[\left(D_o^2 - D_i^2 \right) \cdot \frac{\pi}{4} \cdot L + \frac{2}{3} \cdot \pi \cdot \left(\left(\frac{D_o}{2} \right)^3 - \left(\frac{D_i}{2} \right)^3 \right) \right], \qquad Eq.(34)$$

$$COST_{nacelle} = M_{nacelle} \cdot p_{mat\ nacelle} \qquad Eq.(35)$$

Once the mass is obtained, a price for the material employed is used and the cost calculated.
It's important to remark that this method is a strong simplification of the reality since the structural analysis of the element is complex, but it provides an easy and acceptable way to obtain the nacelle cover mass. For more detailed analysis and more accurate results, sophisticated methods are necessary.
Also in this case, since the additional variables required are many and have to be selected by an expert, another methodology is required. By analysing the case study of [14], related to a GBS TEC, its possible to find the cost fraction of the nacelle cover compared to the total cost of the nacelle, resulting in 21% of nacelle cost. This metric will be used in this work.

$$COST_{cover} = 21\% * \ COST_{nacelle} \qquad Eq.(36)$$

2.1.11. Power converter

Power converters are electrical components that allow to convert certain electrical energy characteristics to other ones, so to a different frequency and tension, allowing a variable speed operation of the turbine. Since the output of an electrical generator is AC, the power converter used can be an AC/DC converter or an AC/AC converter, depending on the specific design of the system.
[11] proposes a simple cost model of the power converter which depends only on the rated power. Different approaches of cost modelling are possible, but they require additional information and study.

$$COST_{power\ converter} = 79 \cdot P_N \qquad Eq.(37)$$

2.1.12. Transformer

Since the main purpose of the power converter is to change the frequency and it's only capable of changing the voltage a little bit, a transformer is necessary. It allows to adjust the voltage level by stepping it up to the desired value. The transformer may be located in the nacelle immediately after the generator or in an offshore substation in which all the power from different TECs is conveyed, or

both. The reason why there is the need to have a high voltage level is due to the fact that losses are inversely proportional to the voltage. Depending on the system location and configuration it may be needed or not to use a transformer if the output voltage from the generator is sufficiently high to accept those losses. For example, in the AR1500 turbine the rated output voltage is 4.1 KV [8], so a transformer may not be needed if distances to shore are low. On the contrary, in the Seagen-S 2MW turbine the output voltage from the generator is 690 V, so the use of transformer is practically mandatory [27].

Different approaches of cost modelling of the transformer are present. The NREL model provides a linear relationship between cost and apparent power S in MVA [28]:

$$C_{transformer} = 11879 \cdot S \qquad Eq.(38)$$

On the other side, another cost function is provided by [29] in which an exponential behaviour relates cost and apparent power as,

$$C_{transformer} = c_1 \cdot S^{c_2} + c_3 \ , \qquad Eq.(39)$$

in which the coefficients c_i depend on the voltage level of conversion, for example from low to medium voltage (LV-MV) and on the type of transformer, as reported in Table 2.1-4. In fact, the transformer can operate in a dry or wet environment depending on the design.

Table 2.1-4: Cost parameters for tranformer

Voltage	Type	Cost Coefficient			Range	Units	Year	Ref.
		c1	c2	c3	(MVA)			
LV:MV	Dry	6.496×10^4	0.6329	7.307×10^3	[0.1125, 3]	U.S. $	-	-
	Wet	45.48×10^4	0.6329	51.115×10^3	[0.1125, 3]	U.S. $	-	-
MV:MV	Dry	2.629×10^4	1	0	[5.0, 100]	U.S. $	-	-
	Wet	18.4×10^4	1	0	[5.0, 100]	U.S. $	-	-
MV:HV	Dry	2.156×10^4	1	0	[5, 100]	U.S. $	-	-
	Wet	15.09×10^4	1	0	[5, 100.0]	U.S. $	-	-

LV-MV-HV=low-medium-high voltage, c=transformer cost coefficient for exponential equation

Dry transformers are the most common ones, both in onshore and offshore applications, in particular in the latter situation, an offshore platform hosts the component. In the case of wet transformers, also known as subsea transformer, they are typically liquid-filled pressure compensated in order to withstand marine environment and high pressures, so a higher cost is expected. In the following table some coefficients are present for the different types of transformers. After that, a comparison of the two models considered is performed by simply plotting the cost functions at different power in Figure 2.1-4.

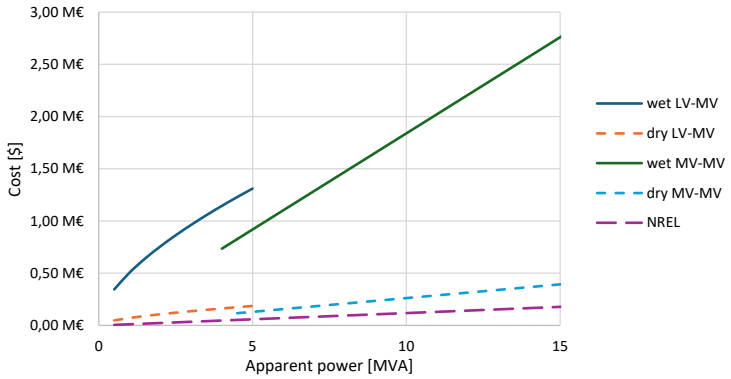

Figure 2.1-4: Comparison of two different transformer cost models

As it can be noted, there is a huge cost difference between dry and wet transformer, which has been calculated, and the results are that wet transformers are 600% more expensive than dry ones. Although NREL has not specified the type of transformer employed in the cost modelling, it can be assumed that the function evaluates the cost of the dry transformer since it has the same order of magnitude of the ones evaluated with the other model.

Despite the NREL model is easier compared to the exponential one, it will be used in the cost evaluation, if a dry transformer will be employed, due to its simplicity.

2.1.13. Offshore substation and other electrical components

An offshore substation is a specialized platform located above the sea level that houses many electrical components, that cannot fit inside the nacelle and are used for power quality and safety, such as switchgear, converter and others. Typically, an offshore substation is needed when the TEC farm size is large, and is more cost-effective to centralize all power generated in a single place, so using a single and larger electrical device, such as the transformer. The usage of a single electrical device per TEC may be applied to allow a local protection and isolating the turbine in case of faults or maintenance. A hybrid approach may be also applied by involving a substation with large components and a basic protection element for each TEC. For example, in the Meygen project all these electrical components, included the transformer are located in an onshore substation because up to now only 4 TECs are installed. The losses are acceptable since the plant is located not so far from the coast and the output voltage is sufficiently high.

A cost model proposed by the NREL [30] for the foundation of the offshore substation is present, and it only relates the array power capacity to the cost as,

$$COST_{base\ offshore} = 303.09 \cdot P_{array} \qquad Eq.(40)$$

The other electrical devices needed for a tidal energy plant are the following and their cost is dependent on the voltage rating (V) or the megavolt-ampere reactive (MVAR). This last quantity can be computed based on the rated power involved in the component, so P_{array} and the power factor PF, as,

$$MVAR = P_{array} \cdot tan\,(cos^{-1}(PF)) \qquad Eq.(41)$$

- Circuit breakers: protective devices that interrupt electric current during faults, so prevent damages to other components

$$COST_{circuit\ breaker} = 818.42 \cdot V \qquad Eq.(42)$$

- AC Switchgear: is the central control of the substation which enables an efficient switching, protection and control of the electrical circuits

$$COST_{AC\ switchgear} = 14018 \cdot V \qquad Eq.(43)$$

- Shunt Reactor: used to compensate for capacitive reactive power and to stabilize voltage levels. They may be or not present in a tidal energy plant depending on the design

$$COST_{shunt\ reactor} = 35226 \cdot MVAR \qquad Eq.(44)$$

- Static Var Compensator: used to stabilize the voltage by regulating the reactive power and to improve power quality. It can be noted that, since tidal power production is predictable, so less fluctuations, the need of the SVC is less crucial than for wind energy where flow speeds are not stable. It can be decided whether to install the device or not, but it's preferable to install it especially if the plant is directly connected to the grid

$$COST_{SVC} = 105060 \cdot MVAR \qquad Eq.(45)$$

- Series Capacitor: devices used to stabilize the voltage, as the SVC, by reducing the inductive reactance of the transmission line. Also for this component it can be decided whether or not to install it.

$$COST_{shunt\ reactor} = 22047 \cdot MVAR \qquad Eq.(46)$$

From the entire list of components, only some of these may be included in the cost evaluation, since it's not clear where and how many will be involved in the TEC array, and only a field expert may know the exact electrical configuration of the system.

2.1.14. Connectors

Connectors are the elements that allow a non-permanent connection between two components, such as turbine and power cable, facilitating the recovery and maintenance of the device. They can be classified in dry and wet mate connectors, as described for the transformer. The main difference between these two classifications relies on the ability to be mated in a dry or wet environment [29].

- Dry-Mate connectors: they can work in a wet environment as well as the wet-mate connectors, but they are mated/de-mated in a dry environment. For this reason, the mating procedure requires a deck area and a vessel lift capability to perform the connection. It's estimated that the cost of a connector varies between 100 and 200 k€, without any specification of voltage and current ratings.
- Wet-Mate connectors: differently from the dry-mate connectors, they can be mated directly under water by using ROVs or divers. They are a relatively new technology and the allow to dramatically reduce time and costs for maintenance work [31]. Costs of wet-mate connectors are estimated to be between 150 and 250 k€ per connector.

Dry-mate connectors are a more mature technology and are available at higher voltages and currents compared to wet-mate ones, but the latter reduce the O&M costs as proofed by Meygen project. Despite being more expensive, the wet-mate connectors are becoming adopted by all TEC manufacturers, so also in the cost evaluation they will be considered.

2.1.15. Power Cables

The power cables are the element that transmit the electrical power from the turbines to the shore. Submarine power cables are an established and mature technology for the offshore systems, and a lot of data is available. Generally, they are composed of three copper conductors, achieving a three-phase cable, and insulated with a cross linked polyethylene (XLPE). If power delivered is really large, the system may be composed of three single core cables, each one corresponding to one phase of the three. This solution is mainly due to thermal dissipation since high power is transmitted [32]. Cables can be also classified depending on the type of current they transport, that means AC or DC, or to be more precise HVAC and HVDC. High voltage direct current transmission systems have increased in recent years, especially in wind farms, since it requires fewer conductors, lower reactive power losses and cost-effective for long distances compared to HVAC, as reported in Table 2.1-5 [33]. In tidal energy sector the use of HVDC is limited because they are typically small-size farms and the distance

from the shore is relatively small, and it's not worth to install it for economic reasons. HVAC systems are simpler, more established and cheaper technology compared to HVDC.

Table 2.1-5: Cost-effectivenenss of type of export cables over distances

Installed Capacity (kW) \ Distance to Shore (m)	30,000	40,000	50,000	60,000	70,000	80,000	90,000	100,000	110,000	120,000	130,000	140,000	150,000
200,000	AC	AC	AC	AC	AC	AC	AC	AC	AC	AC	AC	AC	HVDC
300,000	AC	AC	AC	AC	AC	AC	AC	HVDC	HVDC	HVDC	HVDC	HVDC	HVDC
400,000	AC	AC	AC	AC	AC	AC	AC	HVDC	HVDC	HVDC	HVDC	HVDC	HVDC
500,000	AC	AC	AC	AC	AC	AC	HVDC	HVDC	HVDC	HVDC	HVDC	HVDC	HVDC
600,000	AC	AC	AC	AC	AC	HVDC	HVDC	HVDC	HVDC	HVDC	HVDC	HVDC	HVDC
700,000	AC	AC	AC	AC	AC	HVDC	HVDC	HVDC	HVDC	HVDC	HVDC	HVDC	HVDC
800,000	AC	AC	AC	AC	AC	HVDC	HVDC	HVDC	HVDC	HVDC	HVDC	HVDC	HVDC
900,000	AC	AC	AC	AC	AC	HVDC	HVDC	HVDC	HVDC	HVDC	HVDC	HVDC	HVDC
1,000,000	AC	AC	AC	AC	AC	HVDC	HVDC	HVDC	HVDC	HVDC	HVDC	HVDC	HVDC
1,100,000	AC	AC	AC	AC	HVDC	HVDC	HVDC	HVDC	HVDC	HVDC	HVDC	HVDC	HVDC
1,200,000	AC	AC	AC	AC	HVDC	HVDC	HVDC	HVDC	HVDC	HVDC	HVDC	HVDC	HVDC

AC=alternate current, HVDC=high voltage direct current

Now that it's been established that AC cables are used in tidal energy systems, a cost evaluation can be performed. As previously said, a lot of data is available, and many cost models are present in the literature, involving different approaches. Also for the export cables [29] exponential functions are proposed where the apparent power is used as variable, in which the coefficients are different and restricted to a limited range of power exported, as can be noted in Table 2.1-6.

Table 2.1-6: Cost parameters for power cables

Voltage (kV)		Cost Coefficient			Range	Units	Year	Ref.
Rated	Max	c1	c2	c3	(MVA)			
6.6	7.2	67.63	8.24	0.44	[2.9, 7.5]	k€/km	-	-
11	12	49.37	16.32	0.22	[4.8, 12.5]	k€/km	-	-
22	24	−1.27	50.66	0.07	[9.5, 27.2]	k€/km	-	-
33	36	−35.29	80.17	0.04	[17.0, 44.0]	k€/km	-	-
66	72.5	−57.35	105.20	0.02	[34.3, 94.3]	k€/km	-	-
132	145	−1337.00	1125.00	3.5×10^{-3}	[121.1, 188.6]	k€/km	-	-

c=power cable cost coefficient for exponential equation

An alternative method proposed by [34], and more elaborated by [35] involves a reference cost C_{ref}=200 €/m and two corrective coefficients:

- n_{CSA}: coefficient used to correct the conductor cross sectional area from the reference one.
- n_V: coefficient used to correct the cable voltage from the reference one.

In order to find the value of n_{CSA} it's mandatory to know the cross-sectional area of the conductor. To do so, data of current and CSA from a manufacturer was extrapolated. From ABB catalogue of XLPE 3-core cables [36] values of CSA were published for different current ratings valid for a voltage rating of 10-90 KV, and another table provided data for high voltage 3-core cables of 100-300 KV.

Table 2.1-7: ABB export power cables data

10-90 kV XLPE 3-core cables		
Cross section mm²	Copper conductor	Aluminium conductor
	A	A
95	300	235
120	340	265
150	375	300
185	420	335
240	480	385
300	530	430
400	590	485
500	655	540
630	715	600
800	775	660
1000	825	720

100-300 kV XLPE 3-core cables		
Cross section mm²	Copper conductor	Aluminium conductor
	A	A
300	530	430
400	590	485
500	655	540
630	715	600
800	775	660
1000	825	720

From the values provided in Table 2.1-7, it's possible to interpolate a function that relates CSA and current at different voltages, as can be noted in Figure 2.1-5 and an exponential interpolation resulted in the best fit of the data available.

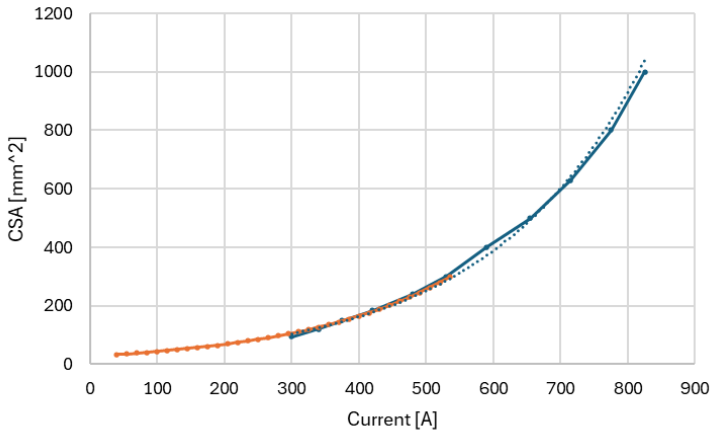

Figure 2.1-5: Interpolation of CSA with respect to current

$$CSA = 28.347 * e^{0.0044*I} \ , \qquad Eq.(47)$$

in which the current I used as variable to find CSA can be obtained directly from the rated apparent power and rated voltage as,

$$I = \frac{S}{\sqrt{3} \cdot V} \qquad Eq.(48)$$

Table 2.1-8: CSA and corresponsing corrective coefficient

CSAs (mm)	n_{CSA}
25	0.74
35	0.78
50	0.82
70	0.9
95	1
120	1.1
150	1.2
185	1.3
240	1.5

CSA=cross sectional area of cable, n_{CSA}=corrective coefficient for area of cable

After the CSA is obtained, it's possible to relate it to its corrective coefficient used in this method, whose values are reported in. In this case, a linear relationship is found given the data in Table 2.1-8.

$$n_{CSA} = 0.6553 + 0.0035 \cdot CSA \qquad Eq.(49)$$

Moving to the voltage corrective coefficient, two tables were available, reporting different coefficients at different voltages, resulting in a discontinuity at V=10 kV, as can be noted from Table 2.1-9 and Table 2.1-10.

Table 2.1-9: Cable voltage and corresponsing corrective coefficient for V≤10 kV

Cables Voltage (V)	n_V
400	0.637
900	0.657
3000	0.764
6000	0.901
10,000	1

n_V=corrective coefficient for voltage deviation from reference

Table 2.1-10: Cable voltage and corresponsing corrective coefficient for V>10 kV

Voltage	Lundberg Normalised Cost	Normalised Cost
10kV	1	1
20kV	~1.2	1.07-1.2 (CSA dependant)
33kV	~1.4	1.15-1.42 (CSA dependant)
132kV	~2.4	1.9-2.0 (CSA dependant)

Due to the discontinuity, two interpolations were performed, reported in the following equations, representing

$$n_V = 0.9819 + 0.0078 \cdot V\,[KV] \quad for \;\; V > 10\,KV\;, \qquad Eq.(50)$$

$$n_V = -0.0021 \cdot V^2 + 0.0607 \cdot V + 0.6076 \quad for \;\; V \leq 10\,KV \qquad Eq.(51)$$

Now that all the parameters are obtained, the cost of the export cable can be evaluated as:

$$COST_{cable} = C_{ref} \cdot n_{CSA} \cdot n_V \cdot L \;\; , \qquad Eq.(52)$$

where L is the total length of the cable, which can be the distance from the shore, or the array cable length, depending on the purpose of the power cable.

This method provides a unique way to calculate the cost for both the export cable and the inter-array cables, if present. The inter-array cables are the ones connecting different TECs, which are then coupled in a junction box, so that only one export cable is used to carry on the total power generated (at high voltage). At the beginning of the Meygen project no inter-array cables were present, and each turbine was directly connected to the onshore substation, but later they installed a subsea hub that allowed to connect different TECs into a single power export cable [37].

Generally, the export cables used are static cables since they remain fixed and do not experience movements, but, in the case of a floating TEC, dynamic or umbilical cables are necessary to connect the turbine to the export cable located on the seabed. These type of power cables are subject to mechanical loading due to current flows and floating structure movements. To provide more resistance their design is different from a static cable, and they are typically double armoured [38]. Based on this description it's intuitive that their cost will be higher than usual static cables. From [29] it's said that dynamic cables are approximately 30-50% more expensive than static cables, up to 33 KV, and it's possible to apply the same method used for static cables, and simply increase the cost of a certain %. The length of the umbilical cable required to calculate the cost will be the distance from the floating platform to the seabed where the connection with the static cable is present, so close to the depth of the sea.

2.1.16. Foundation

The foundation consists of the system that allows to keep the turbine stable and in place. Different designs are available and can be differentiated in 3 main types [39]:

- Gravity based foundation: it's a large structure which is placed on the seabed, and, thanks to its weight, they provide stability for the tidal turbine. Main advantage is that their installation is very easy, but, as a drawback, their maintenance costs are high due to the fact that the turbine must be raised back to the surface. The weight of the foundation is provided by the ballast blocks, typically made of concrete, and by the steel legs, as well as the turbine itself. Generally, they're used in a shallow water depth, up to 80 meters. Moving to the cost calculation of the

gravity-based foundation, not a proper cost function is present, since the design of the tripod is structurally complex, and would require an in-depth analysis, but a structural function can be based on the thrust force. By knowing the foundation mass of the AR1500 turbine, which is 1450 tons, and the calculated thrust force at the rated speed, it's assumed that a linear relationship is present (the other point is the origin) between the foundation mass and the thrust force. After mass is evaluated, only steel is considered to constitute the foundation, and the price can be freely selected.

$$M_{GBS} = 1.3726 * F_T \ , \qquad Eq.(53)$$

$$COST_{GBS} = p_{steel} \cdot M_{GBS} \qquad Eq.(54)$$

- Monopile: it's a cylindrical structure, widely used in wind sector, that can support two turbines by means of a cross beam that can go up and down, allowing easier maintenance to the turbines [40]. The monopile is typically made of steel, and part of it is buried into the seabed to provide stability. The main advantage is that maintenance costs are reduced and the design of the monopile is simple. Additionally, up to 90% of steel can be saved by using a monopile compared to a gravity-based foundation [41]. Also, monopiles are typically used in a shallow water depth, since it is a cheaper foundation compared to gravity-based one, and more forces and momentums are experiences at higher depths. For the cost calculation, it is assumed a structural analysis based on the total thrust force acting on the monopile, considered as a hollow cylinder. All the analysis is performed based on data and characteristics of the monopile considered in Figure 2.1-6 [25].

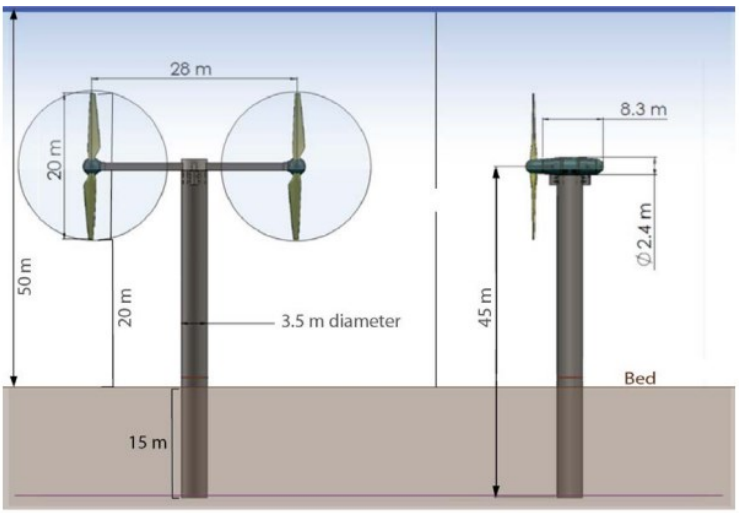

Figure 2.1-6: Monopile considered for the design of its foundation

First, the height of operation of the rotor has to be indicated as a variable. Form the figure, it's possible to assume that the length of monopile under the seabed is 50% of the length from the seabed to the rotor. It's not used the total length of the monopile because in this configuration it coincides with the rotor, but in Seagen configuration the monopile reaches the water surface, while the crossarm supporting the rotors is below it. A picture of this configuration is depicted in Figure 2.1-7 to better visualize it [27].

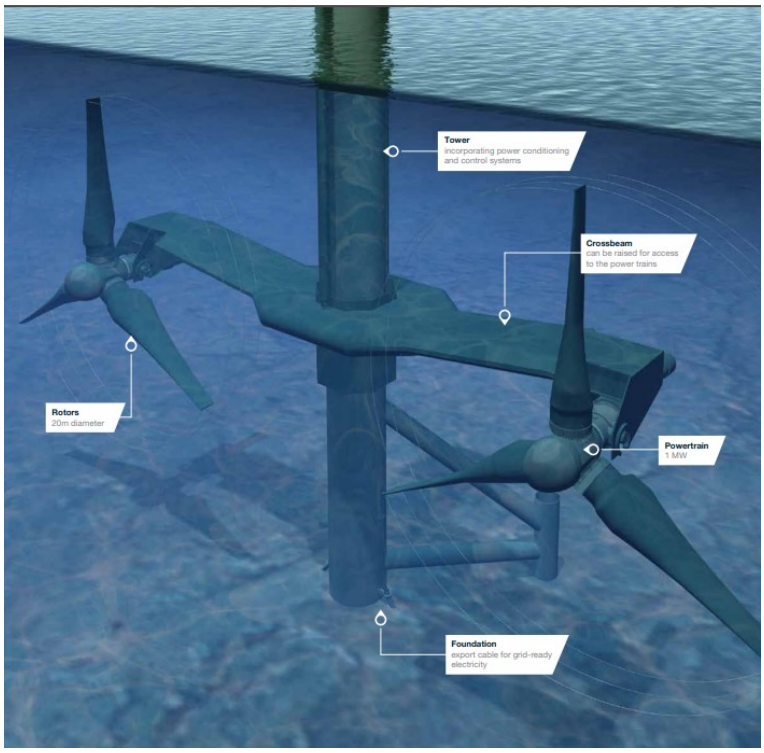

Figure 2.1-7: Monopile involved in Seagen S-2 MW tidal project

So, rotor height of operation is defined, 9 meters of monopile height above the average sea water level is assumed, so the total length of the monopile can be determined as,

$$H_{monopile} = 0.5 * H_{rotor} + H_{water\ depth} + 9 \qquad Eq.(55)$$

Moment generated by total thrust force is calculated as,

$$M_b = F_{T\_tot} * H_{rotor} \qquad Eq.(56)$$

Assuming a safety factor SF=2.6, an outer diameter of the monopile D_{out}=3.5 m, yield stress of A36 steel σ_{yield}=248 MPa and density of steel ρ=7850 kg/m^3, it's possible to determine the thickness of the monopile, so the mass, by following these steps:

$$\sigma_{amm} = \frac{\sigma_{yield}}{SF} \ , \qquad Eq.(57)$$

$$t = \sqrt[4]{1 - \frac{32 * M_b}{\pi * D_{out}^3 * \sigma_{amm}}} \quad , \qquad Eq.(58)$$

$$D_{in} = D_{out} - 2 * t \quad , \qquad Eq.(59)$$

$$M_{monopile} = \left(D_{out}^2 - D_{in}^2\right) * \frac{\pi}{4} * H_{monopile} * \rho_{steel} \qquad Eq.(60)$$

In order to consider the crossarm mass present mounted, also in this case a linear relationship between its mass and the total thrust force is assumed, based on data present in the same paper. Mass provided is 37200 kg and the corresponding thrust force is 1159 kN.

$$M_{crossarm} = 32.09 * F_{T\_tot} \qquad Eq.(61)$$

The overall cost is evaluated considering the price of the selected steel, in this case A36.

$$COST_{monopile} = \left(M_{monopile} + M_{crossarm}\right) * p_{steel} \qquad Eq.(62)$$

- Floating structure: it's a floating platform that hosts the turbines, and it's made of one or more hulls. In operating conditions, the turbines are underwater, while they can be lifted up during maintenance [42]. A floating platform allows to extract energy where water depths are high, more than 80 meters, and the use of a monopile or gravity-based foundation becomes too difficult. This alternative type of foundation is more expensive than the previous ones, but it allows a strong reduction of the O&M costs. In addition to the platform, a mooring system is required. Regarding the cost calculation of floating platform, data and models are not available to obtain a unique function relating different characteristics. Existing data from real projects was analysed, that means SR250, SR2000, orbital O2 and ATIR platform, but since there are many variables and only few data, it wasn't possible to find a correlation between the mass of the platform and the other variables, that could be the rated power or other geometrical characteristics. Due to this issue, the only option was to consider a given mass of the platform and perform a cost calculation based on this.

$$COST_{floating} = p_{steel} \cdot M_{platform} \qquad Eq.(63)$$

To have an idea of the weight of a floating platform, the orbital O2 weights 680 tonnes, while the ATIR platform weights 350 tonnes.

2.1.17. Mooring system

As previously said, the mooring system is necessary in a tidal floating platform to guarantee the fixing to the seabed. It is composed of different mooring lines, typically 4, kept steady to the seabed with anchors, and shackles that connect the line to the anchor [35].

- Chain line: it's the most common type of mooring line used in offshore plants. It can be made of different materials, depending on the mechanical properties required, and different diameters. The mass and cost of the chain is obtained by the following equations:

$$m_{chain} = 0.0219 \cdot 10^6 \cdot D^2 \cdot L \ , \qquad Eq.(64)$$

$$COST_{chain} = p_{steel} \cdot m_{chain} \qquad Eq.(65)$$

  in which D is the diameter of the chain, and L is the length of the line. Focusing on the length of the chain line, it's a common practice to consider a minimum scope ratio of 5:1, which means that the length of the chain line is 5 times higher than the water depth. In fact, in the case of orbital O2, the maximum water depth is 50 m, and each mooring line is around 225 m long [43]. Alternatively, it's possible to assume, in a more general way, a cost of the mooring line per unit length equal to 48 €/m [44].

- Anchor: different types of anchors exist, and the choice depends on seabed condition and costs, but the most common type is the drag embedded anchor. It is designed to penetrate the seabed, and the holding capacity is provided by the resistance of the latter. A function to calculate the anchor mass is the following:

$$m_{anchor} = 1000 \cdot \left(\frac{UHC}{a_1}\right)^{\frac{1}{a_2}} \ , \qquad Eq.(66)$$

$$COST_{anchor} = p_{steel} \cdot m_{anchor} \ , \qquad Eq.(67)$$

  in which UHC is the ultimate holding capacity in KN, which is the maximum capacity for the anchor before failure, so beginning of drag [45], while a_1 and a_2 are coefficients that depend on the seabed and anchor type. Three examples of anchors and types of seabed are provided in Table 2.1-11.

Table 2.1-11: Seabed parameters for anchor mass evaluation

Vryhof Anchor	Soil	a_1	a_2
Stevin MK3	Very Soft Clay	161.23	0.92
	Medium Clay	229.19	0.92
	Sand and Hard Clay	324.42	0.90
Stevpris Mk5	Very Soft Clay	392.28	0.92
	Medium Clay	552.53	0.92
	Sand and Hard Clay	686.49	0.93
Stevpris MK6	Very Soft Clay	509.96	0.93
	Medium Clay	701.49	0.93
	Sand and Hard Clay	904.21	0.93

a1 and a2=coefficients depending on seabed characteristics and anchor type

Since these detailed characteristics of the anchor can't be easily determined, a general mass of the anchor, used in existing projects, can be directly retrieved. For example, the ATIR platform manufactured by Magallanes is kept steady thanks to the use of an anchor, for each line, weighting 140 tons in wet conditions [10].

- Shackles: they allow the connection of the chain line to the hull and to the anchor. For these elements it's assumed that their cost is negligible compared to the rest of the mooring system, and their presence will affect the installation time. 3 shackles per line will be considered, meaning connection platform-chain, chain-chain (is not connected as a single chain line, but divided into 2 sections for easier installation), and chain-anchor.

2.1.18. Installation cost

All the costs analysed previously are related solely to the component itself, without considering the cost associated to its installation. In particular, this phase includes the installation of the turbine substructure, the turbine, the electrical infrastructure and the mooring system. The cost function depends on the time required for the corresponding installation phase and the type of vessel used since costs are different among vessels. A general cost function can be expressed for the turbine and substructure installation as [44]:

$$COST_{inst} = \frac{n}{n_{trip}} \cdot \left(t_{inst} + 2 \cdot \frac{d}{V_{vessel}} \right) \cdot C_{vessel} \ , \qquad Eq.(68)$$

in which:

- n is the total number of elements (turbine or TSS) to be installed;
- n_{trip} is the number of elements that can be carried per trip;
- d/ D_{vessel} is the time required to reach the place of installation of the turbine, which depends on the distance from the port and the speed of the vessel;

- t_{inst} is the time of installation of the element once the location has been reached;
- C_{vessel} is the total cost of the vessel, which depends on the characteristics required by the vessel, such as lifting capacity, which includes rental and fuel cost.

As previously said, many types of vessels exist whose selection depends on the purpose for which it is used and the harsh marine environment it can withstand. This latter point will not be discussed since it's very difficult to model because it's necessary to consider many variables. Different cost functions for different vessels are reported in Table 2.1-12, which were developed during the DTOceanPlus project [46], in which the variable used varies among the vessels.

Table 2.1-12: Vessel charter rate cost functions

Vessel type	Input Parameter	Domain validity	Function
Tug	Bollard Pull (tonnes)	$13 \leq x < 25$	$chart\_costs = 151.34x - 467.47$
		$25 \leq x < 70$	$chart\_costs = 2.18x + 3261.61$
		$70 \leq x \leq 80$	$chart\_costs = 508.57x - 32186$
Multicat	LOA (m)	$21 \leq x < 28$	$chart\_costs = 63.23x + 1812.4$
		$28 \leq x < 35$	$chart\_costs = 916.74x - 22086$
		$35 \leq x \leq 42$	$chart\_costs = 10000$
AHTS	Bollard Pull (tonnes)	$70 < x \leq 338$	$chart\_costs = -8.3 \times 10^{-3} x^2 + 114.90\, x - 261.87$
CLV	Total cable storage (ton)	$565 \leq x \leq 10000$	$chart\_costs = 2.46 \times 10^{-4} x^2 + 7.25\, x + 53090$
CTV	LOA (m)	$15 \leq x \leq 33$	$chart\_costs = -1.26\, x^2 + 179.16\, x - 85.57$
DSV	LOA (m)	$35 \leq x \leq 150$	$chart\_costs = 4308.81 \exp(0.02x)$
Guard Vessel	Service speed (knots)	$7 \leq x \leq 24$	$chart\_costs = 77.11x + 1345.48$
Non-propelled Transport Barge	Barge dimensions ($L \times B \times D$)	$1557 \leq x \leq 19950$	$x = ve.LOA \times ve.beam \times ve.draft$ $chart\_costs = 953.92 \log(x) - 6761.18$
Jack up vessel	Crane lift capacity (tonnes)	$50 \leq x < 755$	$chart\_costs = 64.71x + 21448.41$
		$755 \leq x < 896$	$chart\_costs = 586.18x - 372275$
		$896 \leq x \leq 4400$	$chart\_costs = 26.83x + 128892$
Non-propelled crane vessel	Crane lift capacity (tonnes)	$4 \leq x \leq 3300$	$chart\_costs = -5.44 \times 10^{-3} x^2 + 64.41x - 6974.10$
Propelled crane vessel	Crane lift capacity (tonnes)	$4 \leq x < 500$	$chart\_costs = 26.15x + 5842.59$
		$500 \leq x < 1500$	$chart\_costs = 56.33x - 9254.94$
		$1500 \leq x < 3300$	$chart\_costs = 42.24x + 11871.96$

LOA=length overall, bollard pull=vessel capacity of towing under full power

From the table it's possible to extract the vessels most widely used in tidal turbines installation phases, which are the following:

- Jack up vessel: it's a large vessel which uses legs to lift itself above the sea level, allowing a stable condition and operation. Due to this characteristic, it's the most used vessel for precise operations, like the turbine foundation deployment or the turbine installation. On the other hand, it's the most expensive vessel. In the cost modelling, the crane lifting capacity in tonnes is used as a variable. For the installation of the turbine support structure in the Meygen project, a jack up vessel was used, maybe because it's the longest installation phase and it's possible to operate also if weather conditions get worse [47]. For this reason, it's assumed that this type of vessel is used for the turbine foundation installation phase;

- Crane vessel: also this type of vessel is really common and it's able to lift heavy loads. It is cheaper than the jack up vessel, but it has a limited deck area, so it may be not able to carry the same amount of turbines as the jack up vessel, requiring additional trips, so additional time and cost. Crane vessel can be propelled or not propelled, but the first are preferred since they allow greater mobility, while the latter are cheaper and they require a tug vessel. Referring to the Meygen project, this type of vessel was used for the turbine and cable installation [48]. Also for the crane vessel, the lifting capacity is used as a variable in the cost function;
- CLV: the cable laying vessel, as the name says it's used for the underwater cable laying operation, in which cables can be simply laid on the seabed, buried or covered by rocks [49]. Since this vessel is specialized with the purpose of cable deployment, the choice of this installation phase falls on the CLV although Meygen used a crane vessel for the cable installation, because originally, they wanted to use only the crane vessel for the entire installation phase, probably due to economic reasons, but they ended up using a jack up vessel for the support structure installation phase. In the proposed cost function, the variable used is the total cable storage in tonnes, meaning the weight of the cable that has to be carried on the vessel;
- Tug vessel: is a ship primary designed for towing and assisting other vessels, so it's used for the floating platform installation or assisting the non-propelled crane vessel. Its cost function requires the bollard pull, which is the maximum pulling force that the tug can withstand;
- Multicat vessel: is a versatile and multi-purpose workboat designed for offshore works and transport. They are commonly used as support vessel but can also be used as main vessels for certain operations, such as the mooring system installation.

It's important to note that all these vessels are equipped with a dynamic positioning system, necessary to automatically maintain the vessel's position, and that the cost functions express the vessel daily charter rate in euros, so €/day.

The choice of the lifting capacity of the vessel depends on the weight of the turbine or the support structure that it has to lift. As a rule of thumb, the dry weight of the component to lift should be less than 65% of the crane lifting capacity, so given the overall mass of the turbine or the element to lift, it's possible to take it and evaluate the required lifting capacity of the vessel [48].

Additionally to the vessel charter rate, the fuel oil expenditure has to be included to obtain the total running cost. The fuel expenses can be calculated, as provided in [46], as,

$$C_{fuel} = p_{fuel} \cdot TIP \cdot ALF \cdot SFOC \cdot \frac{24}{10^6} \quad , \qquad Eq.(69)$$

in which:

- TIP: total installed power of the vessel in kW, which includes both main and auxiliary engines;
- ALF: average load factor, which is the average load experiences by the vessel during the entire operation phase. A value of 80% is suggested;
- SFOC: specific fuel oil consumption, which is taken equal to 210 g/kWh;
- p_{fuel}: price of the fuel in €/ton, for example a fuel price of 515 €/ton is indicated.

Then the overall cost can be computed as:

$$C_{vessel} = C_{vessel\,rent} + C_{fuel} \qquad Eq.(70)$$

As an example, in Table 2.1-13 some real vessel data is presented.

Table 2.1-13: Real vesssel data employed in case studies

Name	MV C-Odyssey [50]	Neptune [51]	Aker Wayfarer [52]	Thor [53]	MV Uskmoor [54]	Rambiz [55]
Type	Multicat	Jack Up	Crane propelled	Tug	Support vessel	Crane propelled
Total installed power [MW]	1.79	8.97	19.2	4.7	0.294	3
Crane capacity [tons]	/	600	400	/	/	1700
LOA [m]	26	/	/	/	16	/
Bollard pull [tons]	/	/	/	78	/	/
Deck space capacity [m^2]	120	2000	1850	/	/	/
Transit speed [km/h]	18.5	0.027	17.6	20	16.5	13

Additionally, workers cost is included, in which it is assumed that 3 workers are present in each vessel, while only 2 in the support vessel, and they're paid 50 €/h [35].

Remembering the equation of the installation cost, other variables are present which have not been discussed yet. n and d are design features of the tidal plant to be installed, while n_{trip}, as already mentioned, depends on the free deck space capacity available in the vessel and the size and layout of the component to be installed. As a really rough estimation, it's possible to obtain the number of turbines/substructures that can be carried in a single trip by dividing the free deck area by the area occupied by a single component, and rounding it to the lower integer value as,

$$n_{trip} = roundown\left(\frac{A_{deck}}{A}\right) \qquad Eq.(71)$$

It's important to remind that this is a rough estimation since width and length of the available area is really vessel dependent, as well as the turbine/substructure area. In fact, in some configuration, it's possible to decompose the entire substructure of a gravity-based foundation in subgroups, such as ballast blocks and steel structure, or the turbine in blades and nacelle.

Last variable to consider is the time required for the installation of the components. As reported in [56], the installation of the turbine substructure can last between 1 or 2 days each, assuming 24 hours of working on site, for a gravity-based turbine, while the monopile installation requires between 3 and 4 days of operation. It's reasonable that monopile installation requires more time than gravity-based since subsea drilling is necessary, while no seabed preparation is needed for the other.

After that, the turbine is mounted on the support structure and it's been stated that the duration of this phase lasted less than 60 minutes for the AR1500 turbine of Meygen, so it may be possible to consider 1 hour as duration of turbine deployment [57].

During the validation phase of the costs, which will be analysed in next sections, it was found out that 2 h for blade connection, retrieved from a wind turbine [58], in the floating TEC case, was not sufficient, so it was increased to 6 h in order to make installation cost closer to real value.

The installation time of the power cables depend on the speed at which the cable is laid on the seabed, which is vessel dependent, but some can reach 1 km/h [59]. For example, it was possible to install 11 km of export cable in 12 hours in the Meygen site [60]. In reality, for a better simplicity, the installation cost of the power cables was computed following the metrics proposed by [61], meaning that 1/3 of the export cable length is buried below the seabed, so a drilled duct creation is needed, while for the other part the cable is simply laid on the seabed. To summarize it, the cable installation cost procedure is the following:

$$Cost\ metric_{cable\ laid} = 100\ €/m\ , \qquad Eq.(72)$$

$$Cost\ metric_{cable\ drilled\ duct} = 282\ €/m\ , \qquad Eq.(73)$$

$$COST_{cable\ inst} = 100 * \frac{2}{3} * L + 282 * \frac{1}{3} * L \qquad Eq.(74)$$

Considering the installation process of a floating tidal turbine, no support structures are required, but only the towing of the platform and the mooring installation, as well as power cables, are needed. The towing phase involves the use of a tug vessel to bring the floating platform to the tidal site, generally with towing speeds around 7.4-9.3 km/h [62], which was already assembled onshore. The mooring

line installation phase involves the use of a multicat vessel. Firstly, the mooring pre-lay phase is performed, which involves the installation of the anchors, which lasts about 12 h for each anchor, and the mooring installation, with a duration of 22 h per line [58]. After that, there's the mooring connection phase, which lasts 10 h for each line.
In addition to this, the workers cost for the onshore element preparation is evaluated considering that 6 workers are present, and each element preparation requires 1 h. based on this, the elements involved in time evaluation are:

$$N_{elements} = N_{blades} + N_{foundation} + N_{chain\ lines} + N_{anchor} + N_{shackles} \qquad Eq.(75)$$

2.1.19. General costs

Besides costs related to manufacturing and installation, discussed in the previously, some general costs have to be included due to costs related to development and design, so the so-called Development Expenditures (DevEx), and costs of surveying and harbour. General costs can be assumed to be 5% of the CapEx [63].

2.2. OpEx

OpEx means operational expenditure and is a category of costs that includes the operating and maintenance costs of the plant over its lifecycle. Tasks included have an important repercussion on the energy production, and cost, in fact, a reduction of these tasks strongly influences the reduction of energy cost [14]. The tasks are performed typically in good weather conditions and small tidal currents hours, during which the vessel and the crew can easily retrieve the components to be maintained. OpEx can be divided into different categories:

- Preventive maintenance: includes regular and scheduled maintenance activities to prevent component failures. Examples are inspections, cleaning, and minor components replacement. Since activities are planned over the year, it's possible to choose good weather days to perform them in the most efficient way, reducing costs;
- Corrective maintenance: it's the opposite of the preventive one because it includes unscheduled repair and replacements due to component failure. Failure can occur at any time, and weather conditions may be not favourable to perform the maintenance, leading to a loss of energy production, or further damages;
- Insurance: as the name suggests, it's a cost that the owner of the energy farm has to pay to the insurance company to be covered by a range of potential risks associated with the

manufacturing, installation and maintenance of the energy farm. Typically, insurance costs are expressed in terms of a % of the CapEx or €/MWh, but in this work it will be assumed equal to 1% of the CapEx, which is more or less the % of what was spent during Meygen project (0.87%) [48].

Maintenance costs are really strong dependant on sea and weather conditions and are really difficult to evaluate in a proper way. In many papers the costs associated to OpEx category is expressed in the same way as insurance costs, so a fraction of CapEx or in terms of power/energy of the array, but in this way it's not possible to distinguish between different configurations adopted in the system, and everything would be directly related to CapEx. Since a detailed evaluation is required and the aim of the work is to remain as simple as possible, while keeping a sufficient validity of the costs, different assumptions were considered. As previously said, the insurance will be considered equal to 1% of the CapEx, while maintenance category will be evaluated in terms of the cost associated to the repair of the single component. To better explain it, a spare part cost of each component is considered and assumed to be 15% of the component cost, and it's assumed that a multicat vessel is used to retrieve the component, bring it to the shore facility, and bring it back again to the farm. Same number of workers on the vessel is assumed to be as the n° of technicians required for the maintenance, with a cost of 50 €/h, and it is assumed that the rent of the vessel and the cost of the workers lasts not only for the trip time to retrieve the component, but also for the entire maintenance process. This assumption is performed only for simplicity, since the cost of workers working on the vessel is negligible compared to the cost of technicians performing the maintenance. A failure rate is associated to each component, so it's possible to evaluate, with this probability, the yearly cost associated to maintenance of each component, so the total system cost. Failure rates and time repair cost were retrieved from a study related to a fixed tidal turbine, meaning a GBS TEC [64]. Since floating and monopile TECs are designed to reduce the maintenance costs, it doesn't make so sense to consider the same time of repair required as the GBS, since the turbine can be easily analysed and inspected above the water, and it's not necessary it from the bottom of the sea. For this reason, another strong assumption is necessary, meaning that the time of repair, for floating and monopile tidal turbines, is reduced by 30% compared to gravity-based one. A summary of failure rates and time of repairs in reported in Table 2.2-1.

Table 2.2-1: Failure rates and reparing time of main turbine components

Component	Annual failure rate	Time to repair GBS [h]	Time to repair floating and monopile [h]	N° of workers
Drivetrain	44%	60	42	4
Electric system	17%	5	3,5	2
Nacelle	12%	60	42	6
Blade	9%	7	4,9	2
Foundation	6%	500	350	8
Pitch system	4%	44	30,8	4
Gearbox	4%	45	31,5	4
Power converter	2%	50	35	4
Generator	2%	140	98	4
Control system	1%	45	31,5	2

2.3. Decommissioning

The final cost that has to be included in the entire cost model is the decommissioning, which refers to the expenses associated with the removal of the tidal plant at the end of its operational life. It depends largely on the type of TEC foundation since different removal methodologies and vessel characteristics are required [65]. For these reasons, decommissioning costs varies between the three technologies and are expressed in Table 2.3-1 as cost for a single device/foundation.

Table 2.3-1: Decommissioning cost data

Device type	Decommissioning cost per device
Gravity-based foundation	200 k£ (~300k €)
Monopile	500 k£ (~750 k€)
Floating	100 k£ (~150 k€)

Originally costs were found from a report in £ for that specific year of publication (2018), and they were corrected with the CPI, as done in the cost functions, and converted in € by using a conversion of 1 £=1.2 €.

Data included in the report was obtained from a review study performed by Arup company, in which these cost estimates were proposed. It's important to note that they are given independently of the size of the device and do not consider the distance from the shore.

2.4. Variables

Many cost functions were proposed previously, so many variables were required to perform the calculation. Some of the variables employed are affected by others, which will be defined as primary variables, so proper correlation is necessary in order to minimize the number of primary variables. These primary variables can be furtherly subdivided in different categories.

2.4.1. Environmental variables

Only two variables are included in this category, which are the water depth h and the distance from the shore L, and they only depend on the site location of the tidal plant, so it's a user free decision.

2.4.2. Technical variables

In this category all the variables related to the technical part of the plant are required, including characteristics of the turbine. A summary of these variables is presented in Table 2.4-1, in which is also reported a general range of values, retrieved from literature and existing projects. Moving to the description of some of these variables, it's possible to start from the characteristics of the turbine.

1. N° of blades: most common values are 2 and 3, but Sabella D10 tidal turbine was characterized by 6 blades [66].

- Rated current U_{rated}: the choice is determined after a resource analysis of the potential tidal current site, which will be discussed in detail in the power assessment chapter. By analysing different TEC power curves, typical values are between 2 and 3.5 m/s, but a configuration of the Tocardo T2 reaches 4.5 m/s [67].
- Rotor diameter D: the larger it is, the more current flow is investing the turbine. Also in this case, by analysing TECs with the corresponding power curve, a range of D is determined, which goes from 4 to 24 m, in which the last one is reached by the latest tidal turbine AR2000 [68].
- Rated power P_{rated}: is the most important parameter of the turbine, which allows to understand the power produced, and the capacity factor of the tidal plant by involving the power assessment. Obviously, power is related to the previous parameters with the use of the power coefficient by the following equation:

$$P = \frac{1}{2} * \rho * A * Cp * U^3 \qquad Eq.(76)$$

The best way to make all of these parameters coherent each other is to have a power curve to utilize.

- Export voltage: typically, in offshore farms, the voltage is 11 or 33 kV, a further increase to 66 kV may be possible, if large array is installed [29], or a decrease if small size array is involved.

Table 2.4-1: Technical variables

n° of blades	/	2—6
Rated current	m/s	2—4.5
Rotor diameter	m	5—24
Rater power	kW	100—2000
N° of turbines per structure	/	1 or 2
N° of structures	/	array dependent
Export voltage	kV	11—33
N° of export cables	/	array dependent
N° of rows for array	/	array dependent
N° of columns for array	/	array dependent

2.4.3. Assumed variables

These variables may be considered as technical, but they will be not freely selected in this model, but their value is assumed based on existing projects. Most of these variables are referred to the floating platform case study since it wasn't possible to correlate, for example, the mass of the platform to another variable, so becoming necessarily an input variable. These variables are summarized in Table 2.4-2. The decision of assuming certain variables was made because not a proper way to select the values could be found, and probably also the user of the model would have difficulties in the selection of the proper input value for these variables. An expert of the sector may vary these values if competent.

Table 2.4-2: Assumed variables

Output voltage from generator/array voltage	0,69	kV
Power factor	0,95	/
Gearbox ratio	1/98	/
Thrust coefficient	0,9	/
Ratio of cover and rotor diameter	0,1333	/
Safety factor for yaw	3	/
Floating platform mass	360	tons
Anchor weight	140	tons
Chain diameter	0,076	m
Scope ratio (length/depth)	5	/
Steel price for anchor and chain	0,5	€/kg
Steel price for floating platform	2,5	€/kg
Steel price for GBS	0,8	€/kg
A36 steel price for monopile	1,2	€/kg
Monopile outer diameter	3.5	m
n° mooring lines	4	/
DevEx of CapEx	5%	/
Spare part cost	15%	/
Repair time reduction (only for floating and monopile)	30%	/
Insurance cost of CapEx	1%	/

2.4.4. Vessel variables

This category includes all the parameters of the vessel that are employed in the cost evaluation. They were already explained in the installation section, but are summarized in Table 2.4-3.

Table 2.4-3: Vessel variables

Overall length of multicat	m
Bollard pull of tug	tons
Crane capacity for crane and jack-up	tons
Total installed power	kW
Deck area	m^2
Speed	km/h

2.4.5. Installation time variables

This is the last category of primary variables, and values of required time on installation were retrieved from a wind turbine installation paper [58] and from [56], which were already explained in chapter 2.1.18. Only the blade installation time was modified in order to get an installation cost value closer to the one of an existing project (ATIR).

2.4.6. Secondary variables

Finally, there's the other macro category of variables which are the secondary variables, meaning that they are all dependent on a primary one, so there's no need to input a value, and are discussed here just to present how they were obtained. All of secondary variables are reported in Table 2.4-4 and only the less intuitive correlation ones will be discussed.

Table 2.4-4: Secondary variables

TSR	/
low-speed shaft Speed	rad/s
low-speed shaft Torque	kN*m
high-speed shaft Speed	rad/s
high-speed shaft Torque	kN*m
Apparent Power	kVA
Array Rated Power	kW
Array Apparent Power	kVA
Current single turbine (array line)	A
Array cable voltage	kV
Current export cable	A
Cover diameter	m
Thrust force on rotor	kN
Device spacing along row	m
Device spacing along column	m
length each array line per row	m
Total array cable length	m
N° of transformers and switchgear	/

- TSR: is the acronym of Tip-Speed Ratio, and is an important parameter, defined as,

$$\lambda = \frac{\omega * R}{U} \quad , \qquad Eq.(77)$$

where ω is the rotational speed, R is the radius of the blade and U is the tidal current. Additionally, the TSR affects the Cp of the turbine, depending on if it is 2 or 3 bladed. In fact, from the below pictures, retrieved from their relative tidal study, it's possible to notice that the maximum Cp is reached at TSR=4.5 for a 3-bladed turbine [69] (Figure 2.4-1), while for a 2-bladed turbine is reached at TSR=6 [70] (Figure 2.4-2).

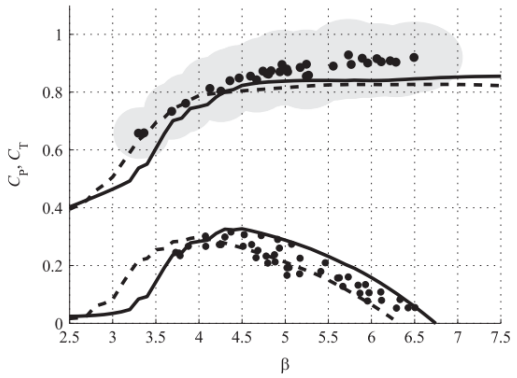

Figure 2.4-1: Cp and CT trend at different TSR for a 3-bladed tidal turbine

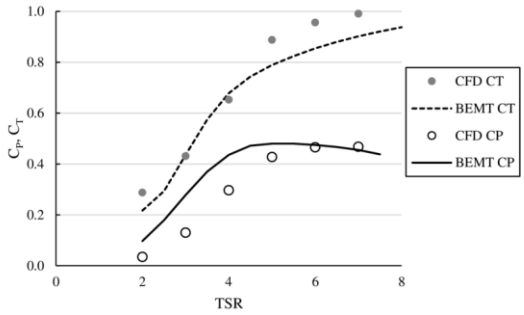

Figure 2.4-2: Cp and CT trend at different TSR for a 2-bladed tidal turbine

- Low-speed shaft speed ω: it can be easily calculated from the TSR equation previously mentioned;
- Low-speed shaft torque: given the rated power of the turbine, it is obtained with the following equation:

$$T_{lss} = \frac{P}{\omega_{lss}} \qquad Eq.(78)$$

- High-speed shaft speed and torque: they can be obtained by introducing the gearbox ratio;
- Array apparent power: it's the total rated power of the array simply divided by the power factor.

$$P_{app\ array} = P_{app} * n_{turb} = \frac{P * n_{turb}}{PF} \qquad Eq.(79)$$

- Output current from turbine: given apparent power of the turbine and the generator voltage, it can be calculated as:

$$I_{turb} = I_{array\ line} = \frac{P_{app}}{\sqrt{3} * V_{turb}} \qquad Eq.(80)$$

- Array cable voltage: if turbines are connected each other through an array power cable, supposing a radial configuration, the voltage of each turbine connected in series, in the same line, is summed up;
- Thrust force: as already mentioned in previous chapters, the thrust force is used in different cost functions, and for its calculation a fixed thrust coefficient C_T=0.9 is considered for a tidal turbine;
- Device spacing: in an array configuration, a spacing between each turbine is necessary, particularly in the case of a GBS TEC. Different measures of this spacing may be found in literature, but the European Marine Energy Centre (EMEC) suggests a lateral spacing (row) d_{lat}=2.5*D and a vertical spacing (column) of d_{vert}=10*D [71];
- Total array cable length: to determine the array cable cost, its length has to be determined, and can be easily calculated as:

$$L_{array\ cable} = L_{array\ line} * n_{rows} = d_{lat} * (n_{columns} - 1) * n_{rows} \qquad Eq.(81)$$

- N° of transformers and switchgear: it is assumed that in the GBS array, only 1 of each of these components is present for the entire array, while in the floating and monopile TEC, 1 component is present in each structure since electronics is installed directly inside it.

It's important to remark that the cost metrics weren't included in the variable list, since they were retrieved from literature, and aren't parameters that can be included in it. Only the steel and fuel price are considered as a variable since huge variability is present, depending on location, supplier and other geographical factors. The steel price has been defined based on the ATIR TEC case study, that has been used to validate the data, and from the analysis those prices were obtained.

2.5. Standardizing cost functions

Cost functions and data were originally retrieved from research papers published in different years, countries, and in some cases in a different currency. To enable a meaningful comparison and a uniform baseline, the cost functions were adjusted using the consumer price index (CPI). The CPI is an index that measures the average change in the prices of goods and services [72]. It accounts for inflation fluctuations and is referred to a specific region and time. By considering the CPI of a country at a specific year, the cost was corrected by using the CPI of the same country of the recent year, in this case 2024 was selected. If necessary, a currency correction is also performed in order the have the

same currency. The other currency present was only U.S dollar, and for the case studies a conversion of 1 $ = 0.92 € is considered.

$$COST_{year\ new} = COST_{year\ old} * \frac{CPI_{year\ new}}{CPI_{year\ old}} \qquad Eq.(82)$$

A summary of the countries involved, the specific year of cost functions, with the respective component, is reported in Table 2.5-1.

Table 2.5-1: CPI correction for cost functions

Country	Year	CPI of year	CPI 2024	Component
USA	2002	179.9	313.1	Hub
				Pitch
				Main bearings
				Yaw
				Brake
				Gearbox
				Generator
				Power converter
	2021	270.97	313.1	Transformer
				Circuit breakers
				Switchgear
				Base offshore
Spain	2017	95	115	Blade
				Shaft
England	2013	98.52	133.4	Connectors
Ireland	2015	82.8	100.5	Power cables
Denmark	2020	103.4	118.7	Cable installation
Europe	2020	106.1	130.6	Vessel charter rate

CPI=consumer price index, referred to a specific year and country

After the correction, all cost data are presented in real terms relative to a consistent base year, in this case 2024.

2.6. Validation of cost functions through real case study comparison

This chapter presents the validation of the cost functions by applying them to a real-world case study. The objective is to compare the predicted costs derived from the functions with the actual cost data provided by an existing tidal energy project, in this case the ATIR floating platform. This comparative analysis evaluates the accuracy and reliability of the proposed cost functions in reflecting real-world scenarios, both to CapEx and OpEx, and, if necessary, adjust the cost functions accordingly.

The Atir tidal floating platform was developed by the Spanish company Magallanes Renovables [73], and was installed in the Fall of Warness tidal test site owned by EMEC. Turbine and platform characteristics of Atir were obtained from different online sources and are reported and summarized in Table 2.6-1.

Table 2.6-1: Atir floating TEC characteristics

Parameter	Value	Measure unit
Water depth [74]	49	m
Distance from shore [75]	3500	m
Platform mass	360	tons
Mooring system mass (chain and anchor)	762	tons
n° of blades [76]	3	/
Rated current	2,9	m/s
Rotor diameter	19	m
Rater power (per turbine)	750	kW
N° of turbines per structure	2	/
Export voltage	11	kV
Output voltage from generator	0.69	kV
Gearbox ratio	1/98	/

Given the data provided in the table, further considerations and adjustments, compared to the cost functions model, have to be made. Firstly, it's unclear what rotor diameter was used, in fact some articles say 19 m, while other 21 m. From EMEC project description [77], it's written that the rotor diameter of ATIR can reach up to 24 m, so probably different turbines were tested in the same platform. Also in the Magallanes cost breakdown description it's not specified for which diameter costs are referred to [78], for this reason 19 m will be selected, since the value comes from the same source of the rated speed of the turbine. Additionally, some of the secondary variables were modified

because they were explicitly provided, so for a more accurate validation of the cost functions, these values were chosen. Modified secondary variables are reported in Table 2.6-2.

Table 2.6-2: Secondary variables modified for cost analysis

Parameter	Value	Measure unit
Rotor speed [76]	17	rpm
Generator rated power	850	kW
Power converter rated power	900	kW
Umbilical cable length	400	m
Mooring chain length [77]	372.5	m

No export cable is included in the cost evaluation because the platform was directly connected to the EMEC tidal test site power cable. Now it's possible to perform the economic assessment on the ATIR tidal platform, keeping in mind the previous considerations, and compare the results to the real costs provided by Magallanes Renovables.

Table 2.6-3: CapEx comparison between model costs and Atir project data

Component	**Cost from model**	**Cost from real project**
PLATFORM	**2.801.801 €**	**2.876.562 €**
Structure	900.000 €	912.787 €
Mechanical	911.900 €	1.217.391 €
Electrical	360.779 €	327.244 €
Control	231.538 €	102.448 €
Auxiliary	270.808 €	123.258 €
Blades	126.777 €	193.434 €
INSTALLATION	**654.377 €**	**519.169 €**
Mooring Design	/	10.000 €
Mooring Materials	374.238 €	200.000 €
Cable	107.576 €	106.830 €
Installation	113.681 €	83.339 €
Transport	44.801 €	100.000 €
Blade installation	14.080 €	19.000 €
Engineering (DevEx)	181.904 €	**158.747 €**
Design	/	100.909 €
Construction	/	57.838 €
TOTAL	**3.638.083 €**	**3.554.478 €**

The cost obtained from cost functions of each component was grouped into categories based on the framework presented in the paper. However, the paper does not explicitly specify which components belong to each category. Therefore, the categorization was conducted thoughtfully, ensuring that the modelled costs matched as close as possible the real-world cost data. Only a deviation was performed, meaning that the power converter was not included in the electrical category, otherwise the price was too high, but in the control one. In fact, the power converter is an electrical component which regulates the flow of power, so it could be considered part of both categories.

As can be noted from the Table 2.6-3, most of the component match the real cost data, while others deviate more, such as control and auxiliary category, in which power converter and pitch, and wet-mate connector were included respectively. Possible reasons of this deviation include an overestimation of the cost, particularly for the wet-mate connector, for which the cost was retrieved from a paper of 2017 [29], so possibly the cost has been reduced over the years. For the power converter, other cost functions were found in literature, but they resulted in a higher cost.

Another important deviation is the mooring material cost. To remember, the mooring cost is dependent on the mass of the mooring system (chain + anchor) and the steel price. Since the mooring system mass was already provided, as well as the mooring material cost, it's possible to easily determine the cost of steel by reversing the equation provided in the appropriate section, considering an equal price for both chain and anchor. By doing so, a steel price of 0.26 €/kg is obtained. As can be immediately understood, a so low price is not reasonable, and it couldn't be used in the cost function because not representative of real price, which is in the order of magnitude of few €/kg, depending on the quality of the steel used. For example, 3 €/kg is suggested for a wind turbine floating platform structure [79]. In the model calculation, a cost of 0.5 €/kg is used, which is close to the cost of raw steel [80]. Possible reasons of this cost difference are that some elements of the mooring system were provided by EMEC, so the company didn't have to buy them, as it happened for the export power cable.

Globally, the cost of the entire system is very similar to the real cost data, so it's possible to say that overall, the cost model works, keeping in mind the considerations previously explained.

As the validation has been performed to the CapEx, it can be done also to the OpEx, whose results are reported in Table 2.6-4.

Table 2.6-4: OpEx comparison between model costs and Atir project data

Component	Cost from model	Cost from real project
Maintenance	89.656 €	/
Insurance	36.377 €	/
OpEx	**126.033 €**	**96.000 €**

A single case study cost validation would be not sufficient to guarantee the validity of the model, so it would be necessary to consider another project, possibly of a different type of TEC. One of the first tidal projects developed was the Meygen project, an array of 4 fixed tidal turbines installed in Pentland Firth, in Scotland [48]. Costs of the project are reported, but as can be noted, the values are really high compared to the floating platform case study, and also much higher than the results that could be obtained from the cost model built. The main reason why a good comparison for cost validation is not possible is that, as previously mentioned, Meygen was a pioneering tidal energy project, and, as one of the world's first large-scale tidal energy arrays, faced the challenges inherent in deploying unproven technology. To secure financial backing, Meygen had to assume contractual risks associated with cost increases due to adverse weather conditions, which led to higher insurance premiums and contingency allocations. Additionally, the project's location featured a fractured rock seabed subjected to significant tidal and wave forces, and at that time, there was no suitable guidance for ensuring cable stability under such conditions, so custom engineering solutions were developed, increase project's cost. About the OpEx, from Figure 2.6-1, it's possible to notice that most of the operational cost was attributed to lease and insurance, which was really high due to the pioneering nature of the tidal project.

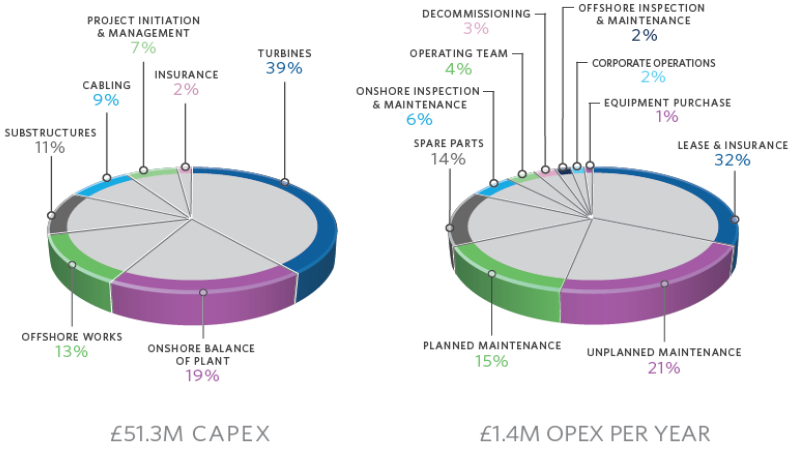

Figure 2.6-1: CapEx and OpEx distribution over different cost categories for Meygen project

Despite only a real case study has been analysed, meaning the Atir floating TEC, the model can be considered validated to existing data because Meygen project couldn't represent nowadays costs and knowledge of tidal energy, and no additional real cost data is present in literature.

3. Tidal energy resource assessment

A fundamental stage in developing a tidal energy plant project is the assessment of tidal energy resources, to understand the project feasibility. Different methodologies are included, depending on tidal data available.

3.1. Tidal current data retrieval

Unlikely wind speed data, which is widely available due to established measurement infrastructure, tidal current data retrieval presents more difficulties, despite being a predictable phenomenon: the complexity of oceanic conditions and the scarcity of measurement stations for example [81]. In order to measure tidal current, particular measure instruments are involved, called acoustic doppler current profiler (ADCP). They are usually deployed on the seafloor, at the bottom of a boat or directly at the rotor of the tidal turbine. It works by sending an acoustic signal into the water column, which bounces back when hitting water particles, and the instrument calculate the speed and direction of the current by retrieving different information, like travel time, frequency of return signal, etc [82]. Since these instruments are costly, provide a localized measure, and most of the time the measured data is not publicly available, models were developed to understand to spatial and temporal distribution of the tidal current.

For this work, Copernicus Marine Data Store [83] was mainly used to understand the tidal current, provided as an hourly value. Many models are present in the catalogue, depending on the variable of interest. For tidal current variable 2 models were considered, meaning a global model, with a resolution of 0.083°x0.083°, and a regional model (0.042°x0.042°) which varied depending on the location of interest.

It's important to note that the tidal current strongly varies with the location, in which high values are reached in flow restrictions, like ATIR floating platform is installed in a narrow channel of around 2 km in Fall of Warness. Considering a model resolution of 0.083° and using a conversion of 1°=111.1 km [84], just to have an order of magnitude, the resolution of the global model becomes ≈9.2 km, while for the regional model becomes ≈4.7 km, which it’s possible to immediately say that is not enough to capture all the details of the tidal resource.

Since the accuracy of tidal current provided by the model is unknown and using it directly in the power assessment of the turbine may lead to incorrect results, there’s the necessity of comparing the data with a measured value with ADCP in the location of interest. it’s possible to identify 4 resource

assessment cases depending on available tidal current data, which are later used in the cases studies. In all cases, no direction of current flow is considered, meaning the total velocity, because it's assumed that all the TECs have a yaw system included in the turbine itself, or the foundation can rotate following the current direction.

3.1.1. Case 1: Copernicus model bias correction

As previously mentioned, data collected by a model needs to be corrected with a measured value. Tidal current data is retrieved from Global Ocean Physics model from Copernicus by selecting the coordinates of the location of interest. To mention a case study location that falls into this category is the Fall of Warness site. Current data from model were available at a depth of z=0.494 m, while the measured data was the annual average velocity U_{z_mean}=1.5 m/s obtained from the ATIR floating platform at the rotor depth of z=13.9 m [75]. To assess the current speed at the depth of interest a power law equation is used as,

$$U(z) = U_{mean} * \left(\frac{h - z}{\beta * h}\right)^{\frac{1}{\alpha}}, \qquad Eq.(83)$$

where the bed roughens β=4 and power law exponent α=7 are given values from the study that proposed the equation [85], while U_{mean} is the depth averaged velocity, h is the water depth and z is the rotor depth.

Since U(z=0.494 m) is known, it's possible to find U_{mean} for the entire dataset. Then, U(z=13.9 m) is calculated, meaning a hourly value for all the years of data available (around 4 years) and averaged, obtaining $U_{z\_mean\_model}$. The result obtained is compared to the given value from literature, meaning U_{z_mean}=1.5 m/s. Since the result from the model was underestimating the velocities, the tidal current data was scaled upby the factor U_{z_mean}/ $U_{z\_mean\_model}$, in this way a new value of U_{mean} was obtained, and the procedure was performed again to check that $U_{z\_mean\_model} = U_{z\_mean}$.

Now, with the corrected value of U_{mean}, the equation is ready to be used to evaluate the tidal current speed at every z, depending on the turbine and type of TEC.

3.1.2. Case 2: Available tidal current timeseries

In this category, tidal current timeseries data was already available to be used, which was obtained from a model and already validated with ADCP measures. This is the case of Fromveur and Raz Blanchard case studies, in which timeseries of the respective location were retrieved from the DTOceanPlus project database [86]. Data and methodologies used in this project were publicly

available since the project ended in 2021, and it was possible to find the timeseries of these two locations, which were the most promising ones in terms of tidal current velocities. It is stated from the DTOceanPlus documentation that the timeseries were obtained from HOMERE model, developed by Ifremer, using an unstructured grid [87]. The advantage of having an unstructured grid is that it's possible to have a variable resolution across the modelling domain, meaning low resolution in less critical areas, and high resolution in areas of interest or with complex bathymetry. Furthermore, the modelled area refers to only the French territory, which may seem a disadvantage because it's a limited area, but it's a positive aspect since it's a regional model, with a better accuracy compared to having a global model. In conclusion, tidal current timeseries were already verified with a large set of in situ data from various sources, so no need of data validation step was necessary, they could be used directly in the power assessment evaluation [88].
Previous equation is still used to evaluate current speed at a certain water depth.

3.1.3. Case 3: Tidal current harmonic analysis

Instead of using a tidal model or a timeseries, harmonic components of tidal current are provided, in which Punta Pezzo case study falls into. To better explain it, data was acquired with ADCP in a period of approximately 24 days in the site of interest. After that, a harmonics analysis in time domain was performed on the data, in order to predict tidal current, so that tidal stream velocity could be estimated as a superposition of sine functions, in this case considering 20 harmonics, with different constituents (amplitude, period and phase) as reported Table 3.1-1 [6].

Table 3.1-1: Tidal current harmonic components in Punta Pezzo

Constituent name	A [m/s]	T [day]	ϕ [°]
M2	1,555	0,517	104,47
S2	0,443	0,5	147,1
K1	0,389	0,997	73,78
N2	0,243	0,528	84,87
O1	0,195	1076	30,06
M4	0,156	0,259	32,03
K2	0,147	0,499	147
P1	0,14	1,003	73,33
P2	0,129	1,003	80,85
K2	0,121	0,499	169,5
M6	0,064	0,172	313,74
2MS6	0,046	0,171	355,61
2MK5	0,034	0,206	284,7
2MN6	0,023	0,174	295,3
2MK6	0,016	0,17	354,84
MF	0,015	13,661	78,99
MK3	0,014	0,341	3,61
MK4	0,013	0,254	77,44
MS4	0,012	0,254	62,27
MSM	0,012	31,812	170,01

A=Amplitude of the harmonic, T=period of the harmonic, ϕ=phase angle of the harmonic

Given the harmonic components, it's possible to determine tidal current timeseries by sampling summing up all the waveforms by using the following equation:

$$U(t) = \sum_i A_i * sin\,(2\pi f_i t + \phi_i) \quad , \qquad Eq.(84)$$

in which frequency f is the inverse of the period, in h^{-1}, and t is the time of the year in hours.

It is stated that the measurements were taken with an ADCP positioned at a depth of 40 m, so it's necessary to calculate U_{mean} by reversing the exponential law equation, previously described in 3.1.1, at a depth z=40 m and a water depth h=100 m. After that, the equation is ready to be used.

3.1.4. Case 4: Yearly current frequency analysis

For the last case, tidal current data can't be accurately determined from Copernicus models because location of interest is really close to the shore and bathymetry strongly changes with distance to shore, and model resolution is too low to represent current speeds at that location. The case study of Cozumel Island falls into this category, in which the site of interest is located at a distance of 200 m from shore, in a water depth of 20 m [89], while by selecting the site coordinates in Copernicus model, the centroid of the cell is located at a water depth of 200 m.

For this reason, data was retrieved from literature and was available in terms of velocity relative frequency in a year, in which the velocity considered was the depth averaged velocity V_{mag}, obtained from ADCP measurements, and reported in the below histogram (Figure 3.1-1).

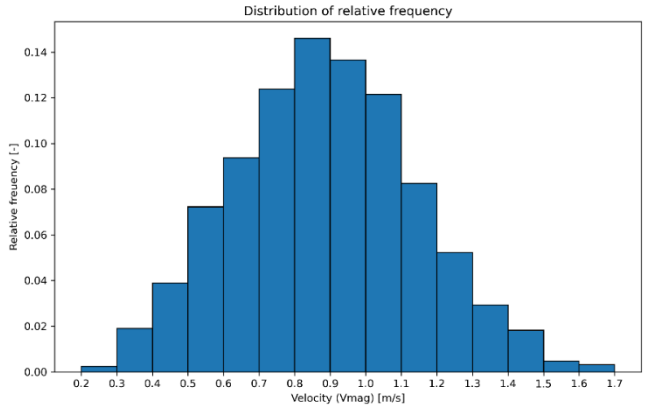

Figure 3.1-1: Relative frequency of depth-averaged velocity in Cozumel Island

A different power law equation is used in the paper and reported here:

$$U(z) = U_{mean} * (h - z)^{\frac{1}{b}} \quad , \qquad Eq.(85)$$

where the power law exponent is provided and equal to b=6.14, and no bed roughness is present this time. The depth averaged velocity can be written as:

$$V_{mag} = \frac{\int_h^0 U(z)\, dz}{h} \qquad Eq.(86)$$

By explicating U(z) and solving the integral, it's possible to find U_{mean} by considering the central value of each velocity bin of the histogram:

$$U_{mean} = V_{mag} * \frac{b+1}{b} * h^{\frac{1}{b}} \qquad Eq.(87)$$

Now all the parameters of the power law equation are known, and it's possible to determine the relative frequency of the tidal current at the specific depth of interest.

3.2. Statistical analysis and application of power curve

Tidal resource has been determined and it's possible to perform some statistical analysis in order to understand the magnitude of the current and choose the most suitable turbine for that site, taking into consideration the location constraints as well, such as bathymetry.
Important statistical elements that are computed are the following:

- Maximum current: it's the highest observed speed, important for structural load analysis;
- 90 percentile: it's the velocity at which 90% of the entire dataset stays below it;
- Histogram and Probability Density Function (PDF): it represents the density of probability of a random variable, in this context tidal current, over a specific range of values. It helps estimating the most probable tidal current velocities [90]. An example of PDF is reported in Figure 3.2-1 for the case of Fall of Warness at z=13.9 m.

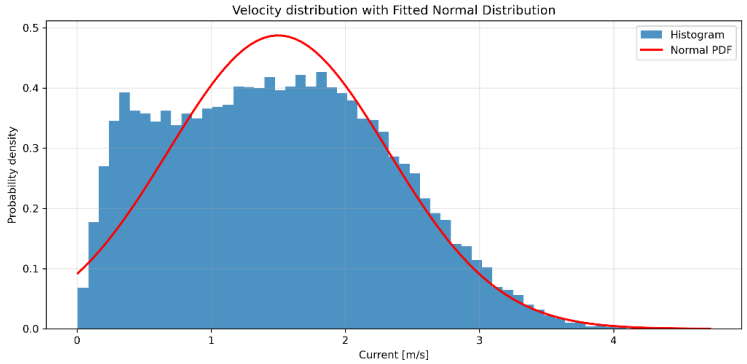

Figure 3.2-1: Histogram and PDF of Fall of Warness tidal site

Generally, it's possible to say that a narrow and high-peaked PDF shape means that a consistent velocity is present, so it's easier to determine the turbine choice, but with a wide and flat PDF shape, tidal velocities are highly variable, so a turbine that operates efficiently over a wide range is needed. From the reported plot, PDF shape seems to be wide, meaning high variability in tidal currents instead of a single dominant velocity. Due to this, the turbine should have a wide operational range to capture energy across a wide range of velocities, and, since there is a high frequency in low-speed currents, a turbine with a low cut-in velocity is preferred.

Once the proper turbine is selected, it's possible to apply its power curve to the tidal current resource and understand the yearly power/energy output and the capacity factor CF, which is defined as the ratio of the average yearly power output over the rated power of the turbine [91]. Important turbine parameters, necessary for the power curve implementation, are the following [92]:

- Rotor diameter D: it's the length of rotor blades, which determines the swept area of the turbine;
- Cut-in velocity U_{in}: it's the minimum speed at which the turbine begins to produce energy;
- Cut-out velocity U_{out}: it's the maximum speed above which the turbine stops working in order to prevent damages;
- Rated velocity U_{rated}: it's the speed at which maximum power is generated. Between rated and cut-out velocity, the power is kept at the rated level;
- Power rated P_{rated}: it's the power generated at the rated velocity.

Another important parameter to consider is the minimum clearance between the tip blade and the sea level, and the minimum clearance between tip blade and seabed for the case of GBS. These two values are the constraints of the position of the rotor along the water column, representing a top limit for the first case, and a bottom limit for the second one (blade tip-seabed).
Given the constraints of the rotor depth, and the determination of the tidal current resource at that depth for the different TEC configuration, it's possible to use the power curve of the selected turbine and evaluate the yearly power output. In this work, power curves of different turbines were retrieved from literature or existing projects, and not a wide collection was available.
After power curve implementation, the yearly mean power is computed, as well as the capacity factor as,

$$P_{yearly\ mean} = \frac{\sum_{i=1}^{8760} P_i}{8760} \quad , \qquad Eq.(88)$$

$$CF = \frac{P_{yearly\ mean}}{P_{rated}} \quad , \qquad Eq.(89)$$

in which 8760 values are considered in a year because hourly data is available.
An assumption that has been made is that the rotor depth is the same for the floating and monopile cases, satisfying the minimum clearance requirements. There's no reason for the monopile rotor to be lowered below this minimum clearance since higher tidal current velocities occur closer to the sea surface.

It’s important to note that in the power evaluation no power cable losses are considered in this model, so the entire power generated by the turbine reaches the shore.

4. Case studies

In this section the cost model and the power assessment methodologies previously proposed are developed in 5 real-world case studies with the aim to evaluate the feasibility and energy production potential of 3 TEC configurations, i.e. GBS, floating and monopile, in different geographical locations, whose selection was based on tidal current data availability or existing tidal projects.
Prior to the development of the techno-economic analysis, some considerations and hypothesis should be done.

- Minimum clearance: this constraint was previously mentioned without giving any quantification. Since it has been defined as the distance between the blade tip and the sea level or sea bottom, it's possible to write a simple equation defining the minimum or maximum rotor depth as function of the rotor diameter.

$$Depth_{rotor\ min} = Depth_{clearance} + \frac{D}{2} \qquad Eq.(90)$$

It's necessary to quantify the minimum clearance in order to determine the rotor depth. Considering the ATIR project information, a minimum clearance from the sea surface has been imposed to 4.4 m [10], and, despite being evaluated for a floating platform, the same value will be used for the monopile configuration. Regarding the GBS, a different clearance value is proposed, which is equal to 8 m [56]. For what concerns the minimum clearance from the sea bottom, it's necessary to analyse a GBS tidal turbine since this quantity is more relevant in this configuration. From AR1500 turbine, it's possible to notice that the rotor height is 15 m from the seabed, for a turbine with D=18 m. Given this data, it's possible to define a minimum clearance from the seabed by simply reversing the previous equation, leading to a value of 6 m [8]. Obviously, this value is specific for the AR1500 turbine, and each designer can decide to change the foundation height, in order to reach higher current values, but in this work that specific value will be considered. Minimum clearance distances are summarized in Table 3.2-1.

Table 3.2-1: Clearance TEC constraints

	GBS	Floating	Monopile
Minimum clearance from sea level [m]	8	4.4	4.4
Minimum clearance from sea bottom [m]	6	6	6

- Foundation weight: although the GBS and monopile foundations were designed following a procedure, the floating one didn't follow the same designing phase. In fact, a given platform mass was retrieved, from ATIR project, and kept fixed independently of the currents. In reality, a design phase is necessary also for the floating platform, but due to complexity of a possible structural and hydrodynamic analysis, and lack of information, the same platform weight was selected for all tidal sites.
- Footprint element area: considering the monopile and GBS configurations, to evaluate the installation costs, or to be more precise the n° of trips necessary for the entire array installation, the footprint element area has to be determined. Specific dimensions of the GBS foundation are not published, but a maximum footprint of 30x20 m is indicated in Meygen project description [56], while regarding both GBS and monopile turbine installation, a deck footprint of D^2 is considered, assuming nacelle cover length equal to rotor diameter.
- Vessel characteristics: many vessels are present in the market, each with different characteristics affecting the cost. In this work only few vessels were selected, whose characteristics are reported in Table 2.1-13,while in Table 3.2-2 is reported a summary of vessel usage in the different TEC configurations.

Table 3.2-2: Vessel employed for different TEC configurations

	GBS	Floating	Monopile
MV C-Odyssey	✓	✓	✓
Neptune	✓		
Aker Wayfarer	✓		✓
Thor		✓	
MV Uskmoor		✓	
Rambiz			✓

It's important to note that the MV C-Odyssey vessel has been selected for maintenance purposes for all the TECs, and in the case of the floating turbine it has been used for the mooring pre-lay and blade connection phases as well. Additionally, Rambiz heavy lift crane vessel was employed in monopile installation since it was used during the installation phase of Seagen [93].

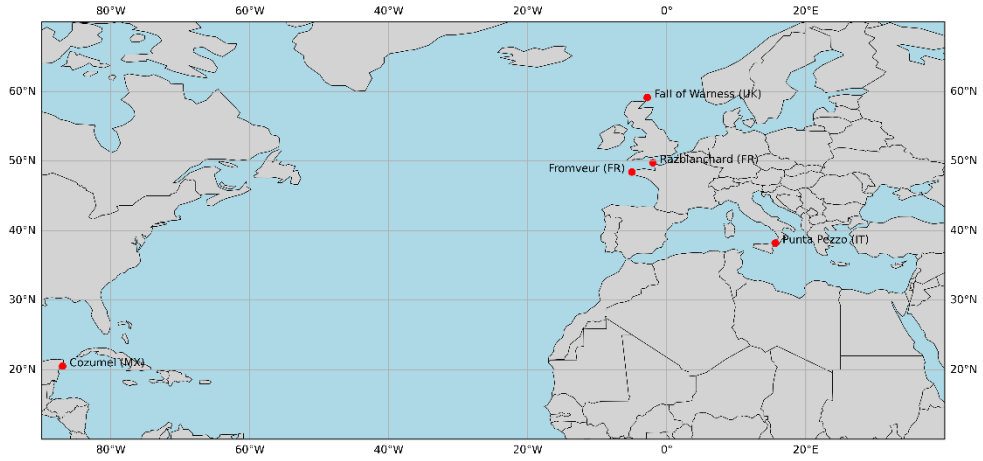

Figure 4-1: World map including markers with selected tidal site

In Figure 4-1 the map that includes all the case studies location is presented in order to have an overview of the spatial distribution of the tidal sites in which the techno-economic analysis will be performed.

4.1. Fall of Warness

Fall of Warness a well-known tidal test site owned by EMEC, in Scotland (UK), situated in a narrow channel between the Westray Firth and Stronsay Firth, in which very strong tidal current occurs, with a typical spring flow of 4 m/s, with depth ranging from 12 to 50 m [94].

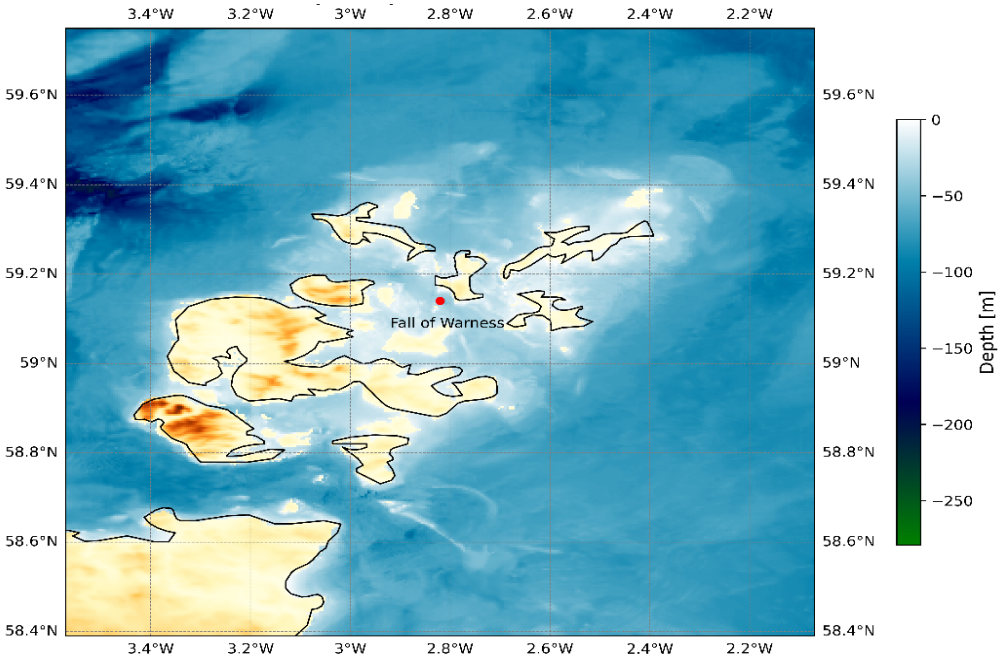

Figure 4.1-1: Bathymetry and location of Fall of Warness. The red dot represents the selected tidal test site

Figure 4.1-1 shows the bathymetry of the area, retrieved from the GEBCO's bathymetric dataset [95], and the red marker is the location of the site of interest, which corresponds to the location of the ATIR platform, meaning at latitude=59.14° and longitude=-2.82°, where a water depth of 45 m is provided by the database, which more or less in accordance with the 49 m indicated in ATIR project description [74].

To find the distance from the shore, SammysHP website map has been used [96], which is based on OpenStreetMap with the possibility to measure the distance on it.

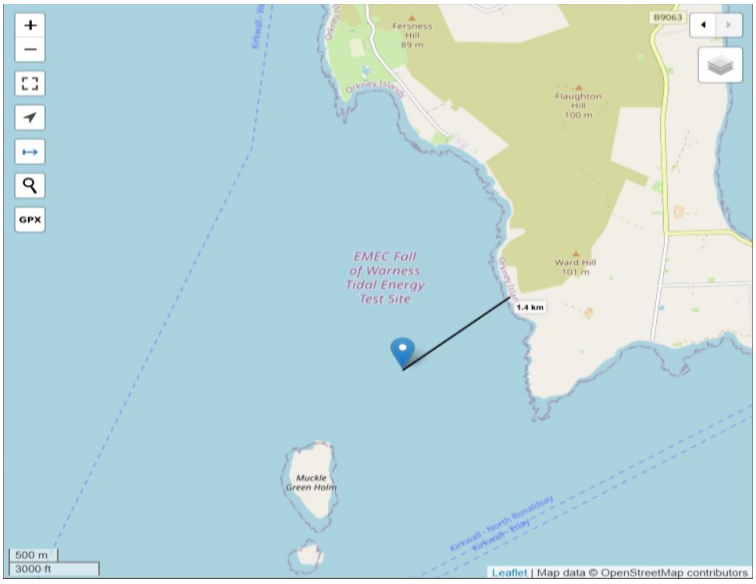

Figure 4.1-2: Fall of Warness tidal plant distance from the shore

As can be noted in Figure 4.1-2, it was possible to measure the distance from the tidal deployment site to the nearest shore, which in this case lead to 1.4 km.

Tidal current resource for that specific location has been retrieved from Copernicus model and corrected with real data values, as explained in Case 1: Copernicus model bias correction. The global model provided 4 years of tidal data, from 08/12/2020 to 08/12/2024, meaning 35065 data points, and results of the power assessment are summarised in Figure 4.1-3.

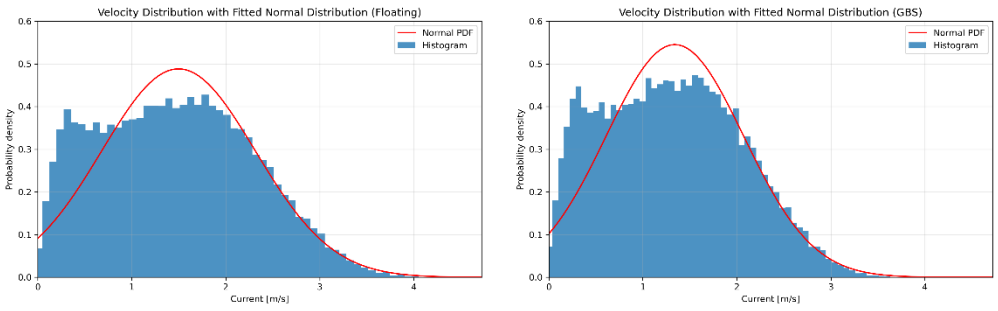

Figure 4.1-3: Resource assessment results (histogram and PDF) of Fall of Warness tidal site

Maximum tidal current reached in tidal site for Floating and GBS is 4.7 m/s and 4.2 m/s, respectively, while the 90-percentile is 2.6 m/s and 2.33 m/s. From Figure 4.1-3 it's possible to note that the probability density of the tidal current is different in the 2 cases since GBS turbine is deployed at a lower depth compared to floating one. The PDF is narrower and reaches higher values in the case of GBS, meaning that a specific current value is more likely to occur around the peak. To quantify it, the maximum probability density occurs at 1.48 m/s in floating configuration, while peak is reached at 1.33 m/s in the GBS.

Power performance is evaluated by using the tidal turbine employed in the Orbital O2 tidal floating platform, whose power curve has been retrieved from a conference video and reported in Figure 4.1-4 [97]. The flatform involves 2 large turbines, with a rotor diameter of 20 m each, 2 blades, and a rated power of 1 MW. Other important characteristics that can be extrapolated from the power curve are U_{rated}=2.65 m/s, U_{in}=1 m/s and U_{out}=4 m/s.

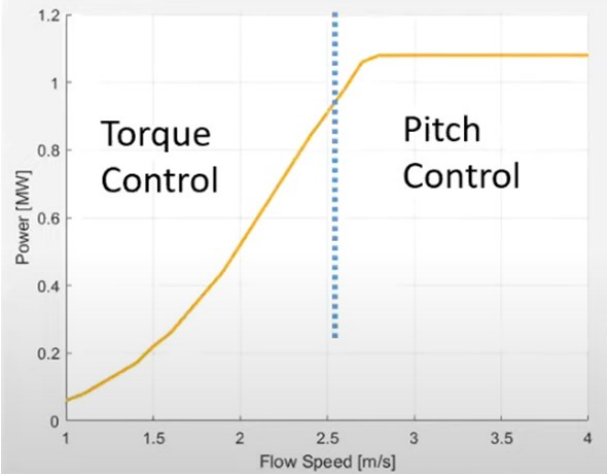

Figure 4.1-4: Original Orbital O2 power curve

From Orbital O2 power curve of a single turbine many points were picked up and for each a power coefficient was calculated, in order to understand if it was constant all over the velocity range. For this turbine it wasn't the situation, in fact Cp varies in the current domain, ranging from 0.34 to 0.4, keeping in mind the possibility of having a error in selecting the points of the curve. Due to the variability of Cp, a third power interpolation equation is performed on the points in order to easily apply it to the tidal resource data. Equation found is report here, in which power in kW is obtained:

$$P = -159.95 * U^3 + 1088 * U^2 - 1695.3 * U + 843.23 \qquad Eq.(91)$$

With the implementation of the power curve, the power trend is obtained, and results are presented in Figure 4.1-5 for the 2024 year.

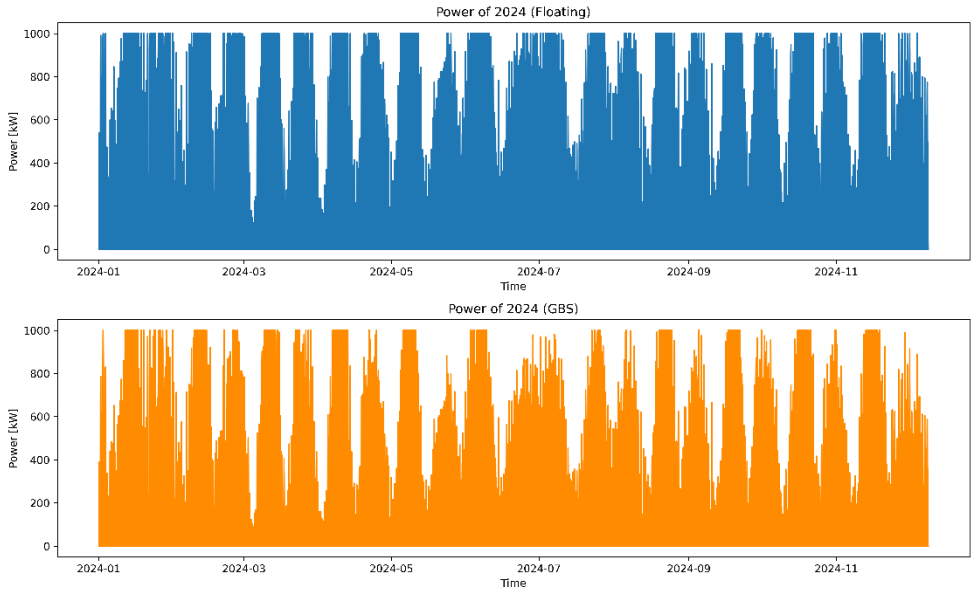

Figure 4.1-5: Power generated by GBS and floating TEC in 2024

As can be noted from the plot, lower power values are reached by the GBS turbine due to the lower values of current, and it's also possible to note that many times the rated power is reached and stopped at that level in both configurations, meaning that tidal currents are between the rated and the cut-out velocity. In fact, these 2 conditions are reflected by the average yearly power and the capacity factor, described in Statistical analysis and application of power curve, which resulted to be P_{yearly_mean}=332 kW and CF=33.24% for the floating configuration, while P_{yearly_mean}=262 kW and CF=26.17% for the GBS one.

Now the power assessment is concluded and it's possible to move to the economic analysis, this time considering all the 3 TEC configurations.

All the variables needed for the cost evaluation have been defined, but an additional consideration has to be made regarding the steel price. For the floating platform, steel cost has been obtained with a reverse procedure as explained in Validation of cost functions through real case study comparison, while price for monopile and gravity-based structures are missing. For the monopile structure, A36 raw steel cost has been found online for USA, corresponding to 702 $/kg [98]. By increasing this value of 80% to take into account manufacturing costs, and converting it in euros, a steel price of 1.2 €/kg has been obtained. For the GBS case, an average steel price has been considered based on its value of the other 2 configurations and the raw steel price [80] in USA. Steel price has been selected arbitrarily to a value of 0.8 €/kg, keeping in mind that most of the steel mass in the structure is used as a ballast, so a low-quality steel is supposed to be used.

Furthermore, the export voltage has been set to 11 kV, but an optimization could be performed in order to find the best voltage depending on the power to deliver. For the GBS, the voltage has been

increased to 33 kV for an array power higher than 16 MW, since the export cable unit cost increases a lot after that value.

Different financial metrics have been evaluated with different array capacities, ranging from 2 to 32 MW.

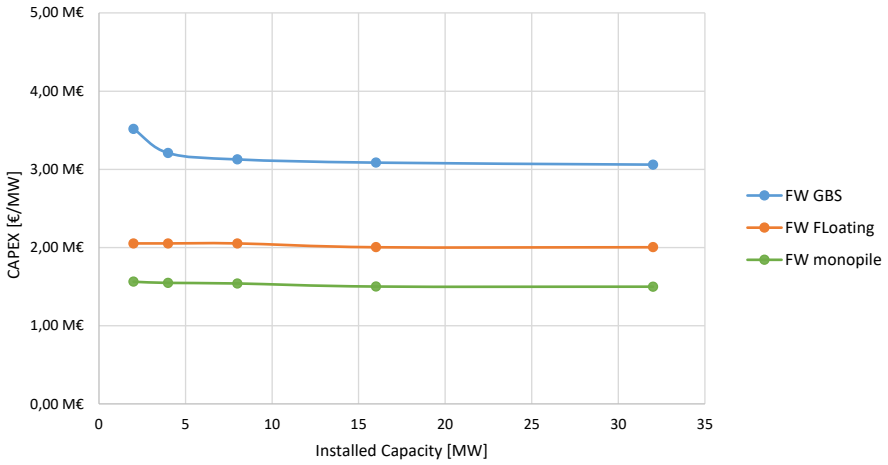

Figure 4.1-6: CapEx values as a function of Installed Capacity generated by GBS, Floating and Monopile TECs at Fall of Warness

In Figure 4.1-6, the CapEx per unit of installed power is reported in function of the installed capacity, where CapEx has been evaluated as the sum of all the component and labour costs. It's possible to note that the GBS array is more affected by a cost reduction with an increasing capacity, but it still remains the costliest technology these terms, while the monopile one is the cheapest. For the monopile case a slight reduction can be observed, while for the floating one cost remains the same since the platform is simply replicated in more to meet the desired array power, each of which has its own export power cable. A slight reduction in cost is noticed at 16 MW because the power cable voltage has been reduced to 6.5 kV, meaning that 11 kV was not the optimal voltage for this configuration. The fact of not using immediately 6.5 kV is due to the fact of wanting to show this behaviour.

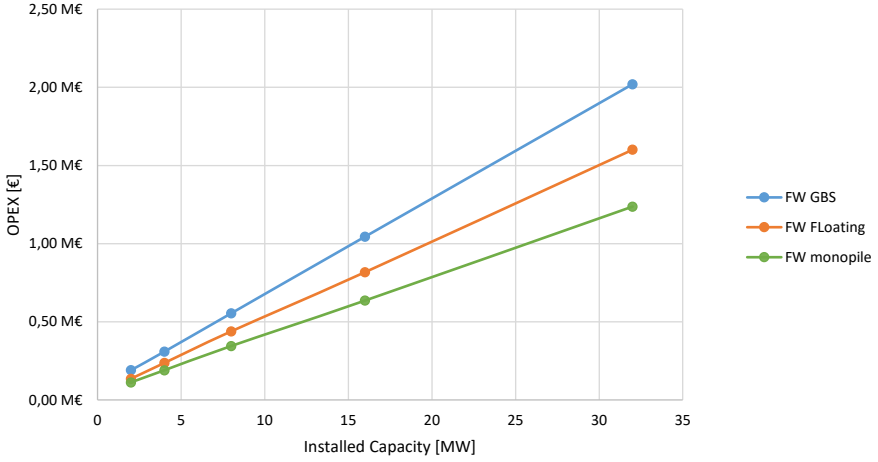

Figure 4.1-7: OpEx values as a function of Installed Capacity generated by GBS, Floating and Monopile TECs at Fall of Warness

The OpEx trend is shown in Figure 4.1-7, which is almost linear, and it's possible to note that the GBS TEC requires more money to do maintenance, in accordance with what literature says. Also in this situation, the monopile TEC has the cheapest OpEx.

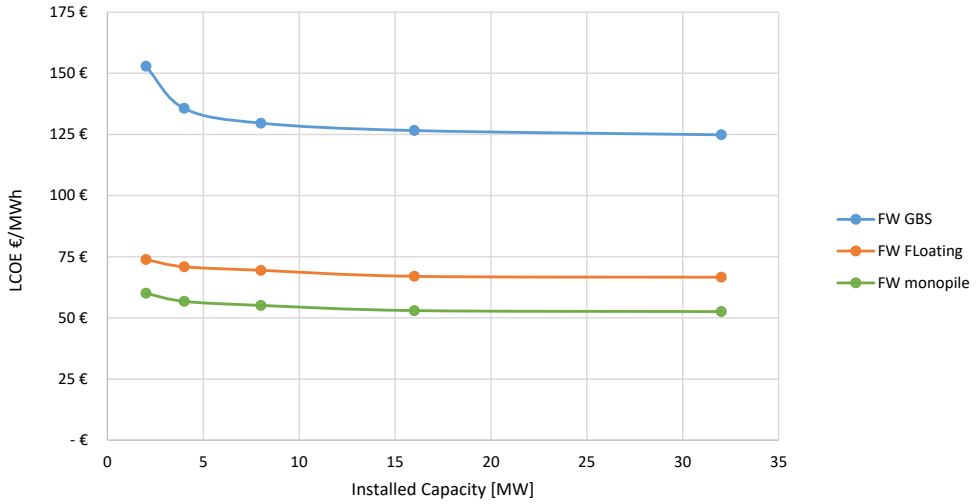

Figure 4.1-8: LCoE values as a function of Installed Capacity generated by GBS, Floating and Monopile TECs at Fall of Warness

The levelized cost of electricity (LCoE) is a common and important cost metric used for comparing different power production technologies [75]. It can be defined as the life-cycle cost divided by the total energy produced, which in mathematical terms become:

$$LCoE = \frac{CapEx + \sum_{t=1}^{n} \frac{OpEx_t}{(1+r)^t} + \frac{D_c}{(1+r)^n}}{\sum_{t=1}^{n} \frac{AEP_t}{(1+r)^t}} \quad , \qquad Eq.(92)$$

in which AEP is the annual energy production, obtained by multiplying the annual average power for 8760 h, Dc is the decommissioning cost, which is discounted at the end of the lifetime of the tidal plant after n years, in this work equal to 25 years, while r is the discount rate, imposed equal to 5%, and t is the time in years. Since OpEx and AEP are constant over the lifetime of the plant, it's possible to take them out of the sum and the equation becomes:

$$LCoE = \frac{CapEx + OpEx * f + \frac{D_c}{(1+r)^n}}{AEP * f} \quad , \qquad Eq.(93)$$

$$f = \sum_{t=1}^{n} \frac{1}{(1+r)^t} = \frac{1-(1+r)^{-n}}{r} \qquad Eq.(94)$$

From the Figure 4.1-8, LCoE trend follows the typical shape of this quantity, which decreases as the array capacity increases until a steady state behaviour is reached. It is less evident for the floating and

monopile technologies due to the previous reasons, meaning that power unit CapEx is little affected by array size increases, and the OpEx is the only term that influences on the LCoE trend for these 2 cases since it doesn't linearly increase with capacity as previously said.

As expected, the monopile technology is the most convenient one, reaching a minimum value of 52.5 €/MWh, while GBS is the least convenient TEC configuration.

Last 2 cost metrics that can be evaluated are the Net Present Value (NPV) and the Return of Investment (ROI). By definition, NPV is the present value of the cash flows at a certain time, in this work at the end of life, so 25 years, and it's important to be evaluated in order to calculate the ROI [99]. The following equation is used to calculate NPV:

$$NPV = -CapEx + \sum_{t=1}^{n} \frac{R_t - OpEx_t}{(1+r)^t} + \frac{D_c}{(1+r)^n} \quad , \qquad Eq.(95)$$

where R are the revenues from the project, which may include energy sold to the market, incentives, and whatever is an income. In this work only revenues from selling the electricity are considered, so:

$$R = AEP * p_{el} \quad , \qquad Eq.(96)$$

where p_{el} is the price at which electricity is sold into the grid, which is 207 €/MWh specifically for tidal energy in UK [100].

ROI is defined as the ratio between the NPV over the total cost [101], meaning the sum of CapEx, OpEx and decommissioning over the entire life of the plant, which in mathematical terms it becomes:

$$ROI\ \% = \frac{NPV}{C_{tot}} \quad , \qquad Eq.(97)$$

$$C_{tot} = CapEx + \sum_{t=1}^{n} \frac{OpEx_t}{(1+r)^t} + \frac{D_c}{(1+r)^n} \qquad Eq.(98)$$

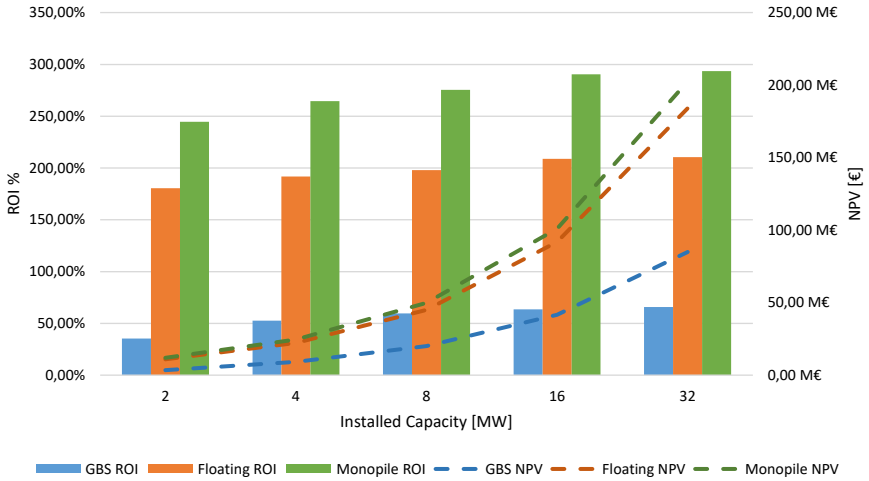

Figure 4.1-9: NPV and ROI as a function of Installed Capacity generated by GBS, Floating and Monopile TECs in Fall of Warness. Bars and dashed lines represent NPV and ROI values, respectively

In Figure 4.1-9 these two metrics are reported and is evident that the GBS technology has a significant lower ROI compared to the other 2 technologies, showing poorest financial performance, but still profitable. Monopile configuration appears to be the most economically viable one. In any case, all the technologies show a ROI improvement as the array capacity increases.

4.2. Fromveur

The Fromveur passage is located in Brittany, in France, and represents a promising location for tidal energy since it's characterized by powerful tidal currents. Additionally, a tidal energy plant installed in this location could support the off-grid community of Ushant Island, which historically relied mainly on fossil fuels for electricity production. This location has already demonstrated the opportunity of installing a tidal turbine in 2015, when the Sabella D10 turbine proved the feasibility of tidal energy technology [4].

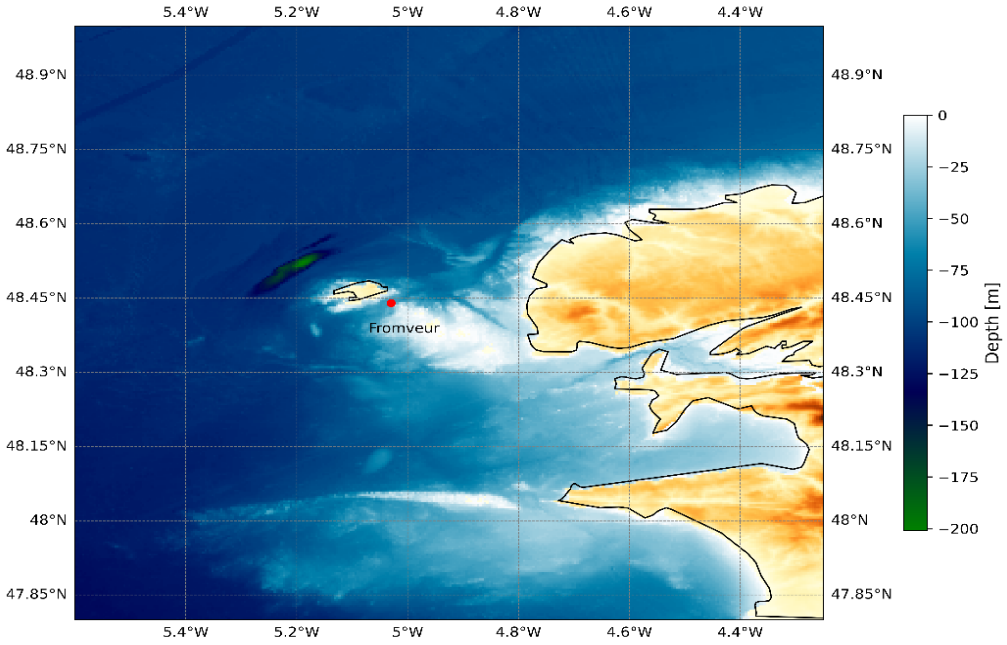

Figure 4.2-1: Bathymetry and location of Fromveur. The red dot represents the selected tidal test site

In Figure 4.2-1 the bathymetry map is reported, and for the red dot a water depth of 51 m is present. The exact location of the tidal site has been chosen depending on data availability also this time, meaning latitude=48.44° and longitude=-5.03°.

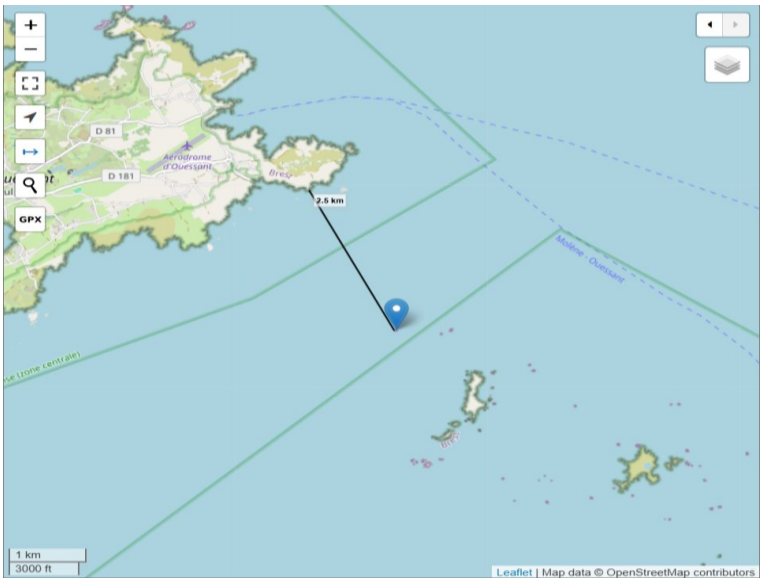

Figure 4.2-2: Fromveur tidal plant distance from the shore

Closest distance to the Ushant Island is 2.5 km s depicted in Figure 4.2-2.

Tidal current data has been retrieved from the DTOceanPlus database, in which a timeseries of 23 years was provided, from the beginning of 1994 to the end of 2016. Further details about this database and how the power assessment was performed is described in Case 2: Available tidal current timeseries, and results are reported in Figure 4.2-3.

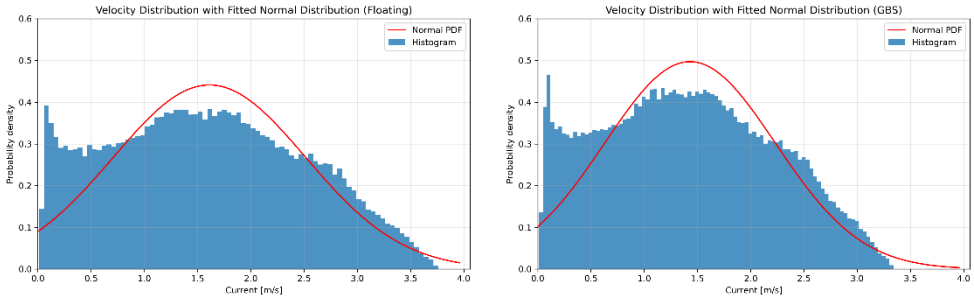

Figure 4.2-3: Resource assessment results (histogram and PDF) of Fromveur tidal site

Maximum tidal current reached in tidal site for Floating and GBS is 3.78 m/s and 3.36 m/s, respectively, while the 90-percentile is 2.87 m/s and 2.55 m/s. From Figure 4.2-3 it's possible to note that the PDF is narrower and reaches higher values in the case of GBS, and by comparing the shape of the PDF with the Fall of Warness case, it seems that the curve is wider in the case of Fromveur. In fact, lower values of PDF are reached, meaning that tidal current velocities are more variable in that location. To quantify the maximum probability density in Fromveur, it occurs at 1.6 m/s in floating configuration, while peak is reached at 1.44 m/s in the GBS.

Power performance is evaluated by using the tidal turbine used in Seagen S 2 MW tidal project, a monopile structure with a couple of 3-bladed tidal turbines mounted on it, each of 1 MW of rated

power and 20 m of rotor diameter. Power curve of the combination of the turbines has been retrieved directly from the company [27], and is reported in Figure 4.2-4. For the power assessment the values of the power curve have been divided by 2 in order to consider the characteristics of a single turbine.

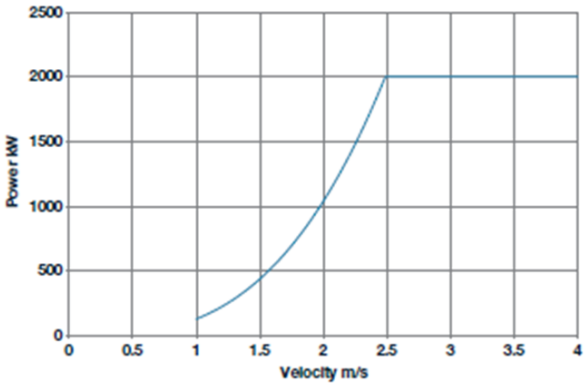

Figure 4.2-4: Original Seagen S-2 MW power curve

Seagen 2 MW power curve was analysed, and by picking up different points of the curve, it's been stated that the power coefficient is constant and equal to Cp=0.4 all over the curve, meaning that the pitch mechanism allows to keep the TSR at the optimal Cp. Other important characteristics that can be extrapolated from the power curve are U_{rated}=2.5 m/s, U_{in}=1 m/s and U_{out}=4 m/s.
The power curve is combined with the tidal resource and power is obtained, which is represented in Figure 4.2-5 for the 2008 year.

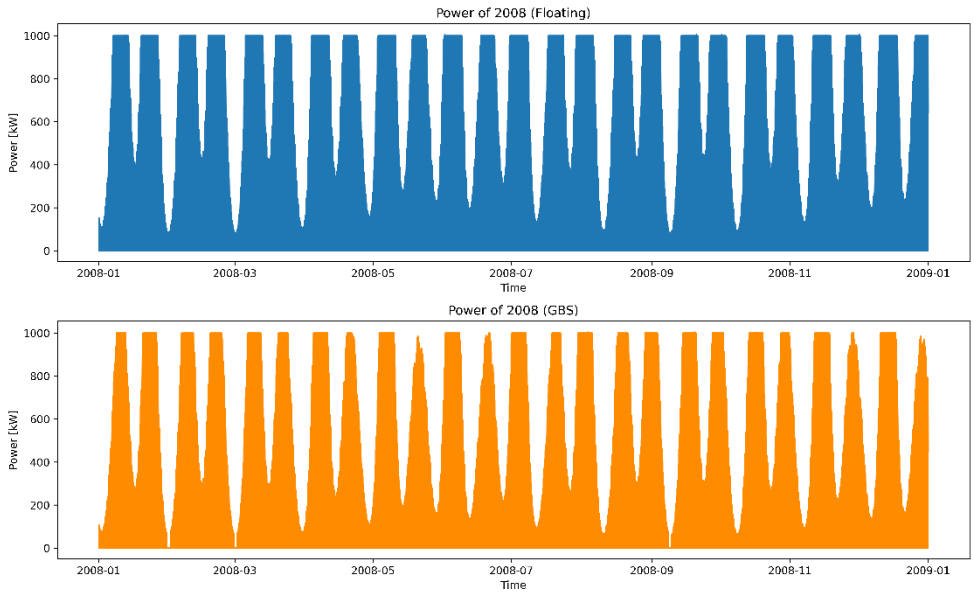

Figure 4.2-5: Power generated by GBS and floating TEC in Fromveur in 2008

The rated power is reached many times also in this case, and yearly average power and capacity factor resulted to be P_{yearly_mean}=393 kW and CF=39.35% for the floating TEC and P_{yearly_mean}=318 kW and CF=31.83% for the GBS one.

Moving to the cost analysis, same cost metrics were evaluated as in the previous case study and are here presented.

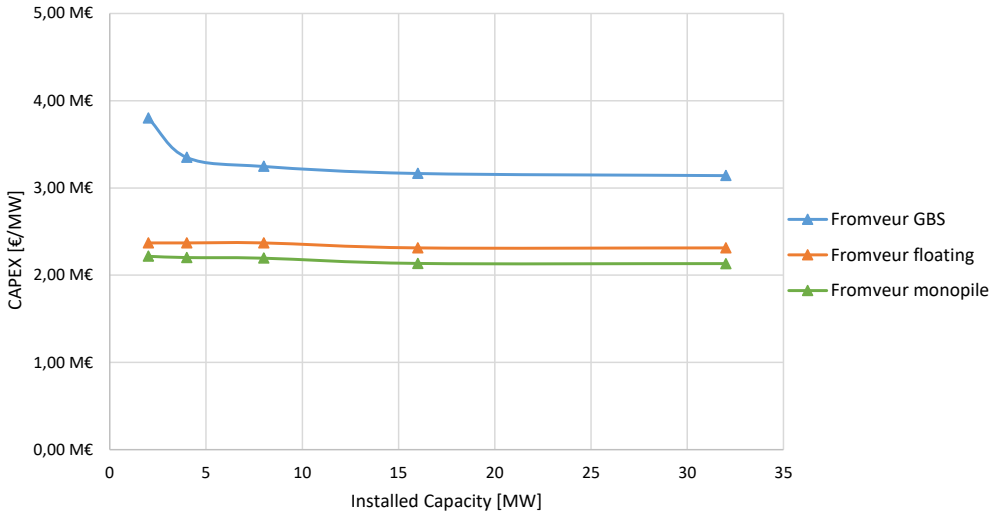

Figure 4.2-6: CapEx values as a function of Installed Capacity generated by GBS, Floating and Monopile TECs at Fromveur

In terms of CapEx the monopile wins also in this location, while the GBS remains the least convenient technology as can be seen in Figure 4.2-6.

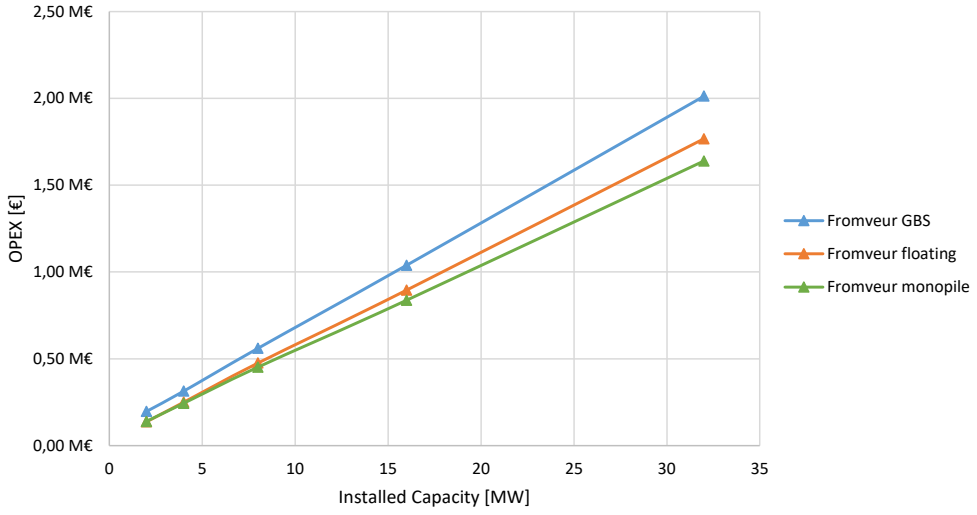

Figure 4.2-7: OpEx values as a function of Installed Capacity generated by GBS, Floating and Monopile TECs at Fromveur

OpEx are really close each other this time, following a sort of linear trend as shown in Figure 4.2-7.

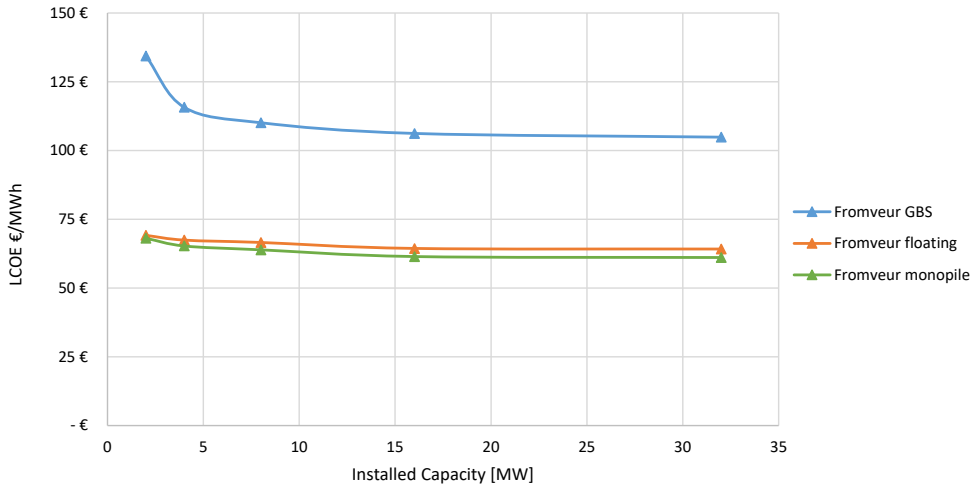

Figure 4.2-8: LCoE values as a function of Installed Capacity generated by GBS, Floating and Monopile TECs at Fromveur

Also for the Fromveur site the monopile TEC is the most convenient technology, producing a minimum LCoE of 61 €/MWh, but it's important to note that monopile and floating configurations produce really similar results as reported in Figure 4.2-8.

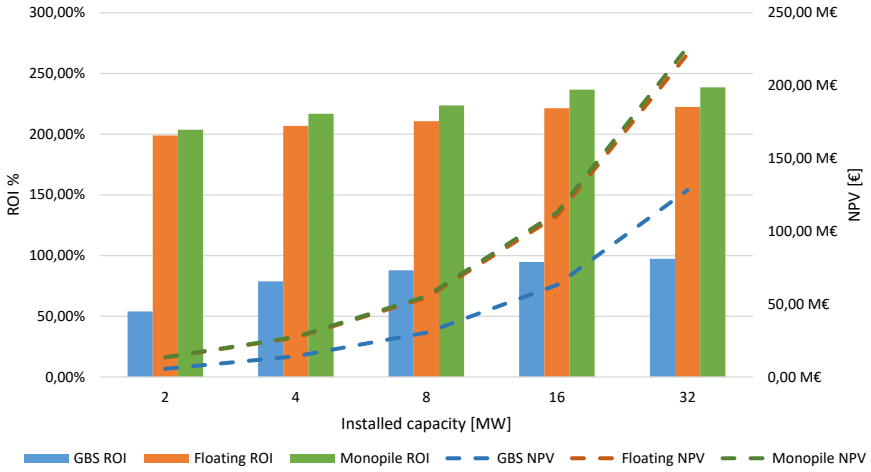

Figure 4.2-9: NPV and ROI as a function of Installed Capacity generated by GBS, Floating and Monopile TECs in Fromveur. Bars and dashed lines represent NPV and ROI values, respectively

Considering NPV and ROI, no negative results are found, meaning that all the plants are profitable, and also in Figure 4.2-9 monopile and floating configurations are really close, in particular in terms of NPV, but, by considering the ROI, the monopile results the most profitable technology. Even though the analysis was performed in France, where a feed-in-tariff for tidal energy is found to be 150 €/MWh [102], the same selling price of UK of 207 €/MWh is considered in order to make a fair comparison of the different case studies, and no cost variation is included in the cost model despite, as an example, steel cost strongly varies among countries.

4.3. Raz Blanchard

Le Raz Blanchard, also known as Alderney Race in English, is another promising location for tidal energy in France, located between Alderney Island and La Hague Cape, characterized by powerful tidal currents due to natural constriction of the flow between these two lands [103]. Location of the exact site is presented in Figure 4.3-1.

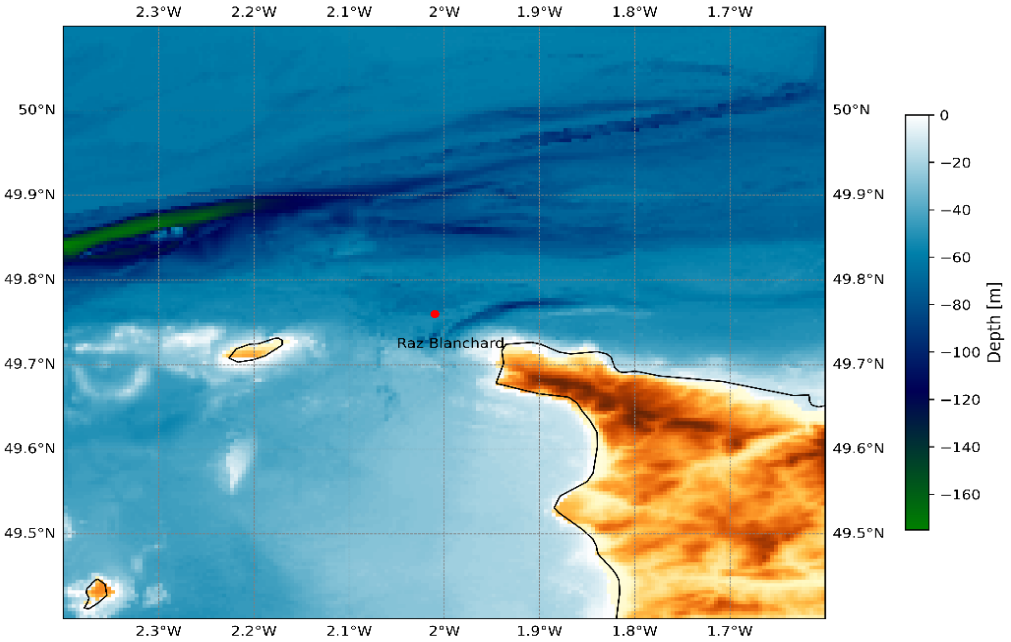

Figure 4.3-1: Bathymetry and location of Raz Blanchard. The red dot represents the selected tidal test site

Additionally, a tidal project called FloWatt is currently under development by HydroQuest company, in which 6 HydroQuest machines will be installed in Raz Blanchard, composing an array of 17 MW [104].

As it occurred for Fromveur, the selection of the exact coordinates of the tidal site depended on the data availability, which also in this case was retrieved from the dataset of DTOceanPlus project.

In this case study, it is hypothesized that the tidal array is the electricity source for the Alderney Island, whose distance is 11 km, as depicted in Figure 4.3-2, despite the selected tidal location is closer to the French mainland compared to the island coast.

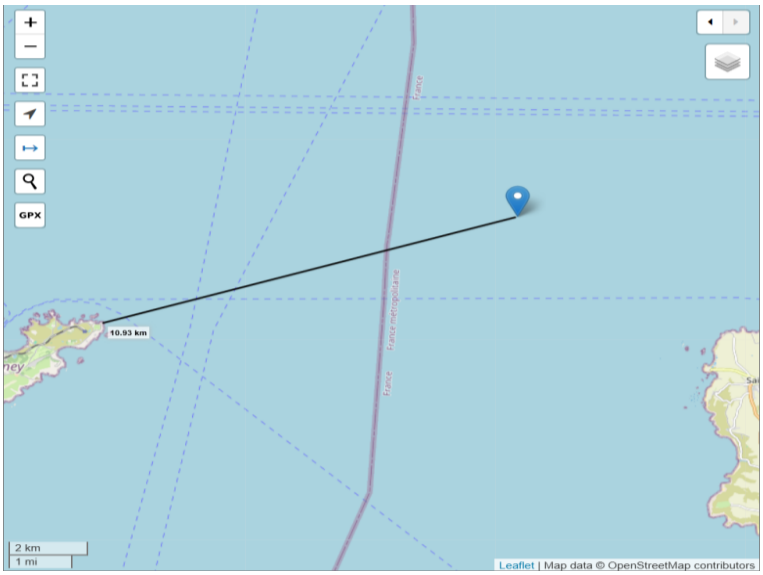

Figure 4.3-2: Raz Blanchard tidal plant distance from the shore

The same tidal resource evaluation has been performed on the dataset from DTOceanPlus, containing data from 1996 to 2014, whose results are reported in Figure 4.3-3.

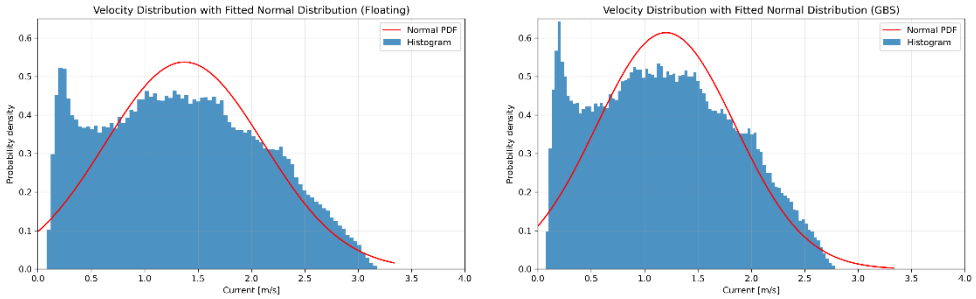

Figure 4.3-3: Resource assessment results (histogram and PDF) of Raz Blanchard tidal site

A really narrow behaviour is encountered in the GBS configuration, reaching over 0.6 of probability density at 1.21 m/s, while in the floating case the occurs at 1.38 m/s.

Maximum values of current reached in this location are 3.2 m/s and 2.8 m/s for floating and GBS respectively, and the 90-percentile is 2.4 m/s and 2.1 m/s.

The same power curve used for the Fromveur case study is involved in Raz Blanchard, meaning the Seagen S 2 MW, and results of the power assessment of the 2008 year is presented in Figure 4.3-4.

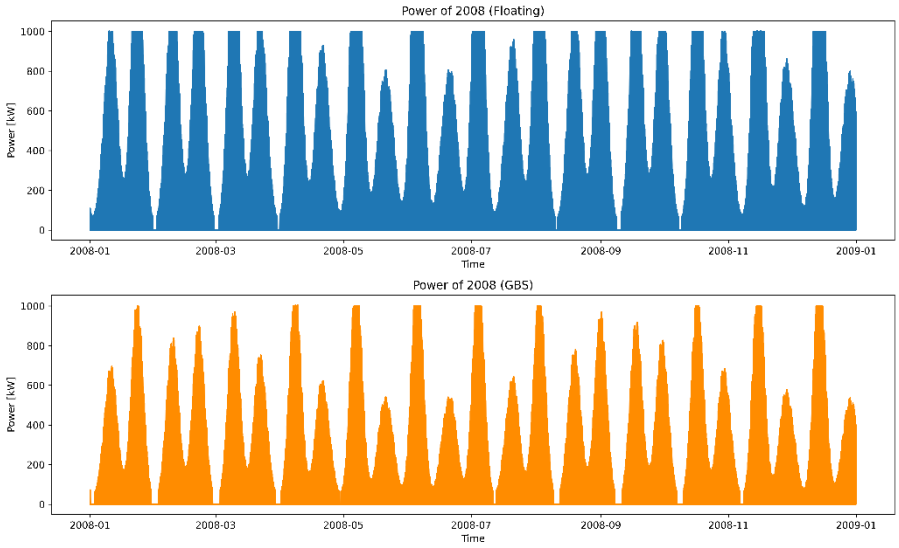

Figure 4.3-4: Power generated by GBS and floating TEC in Raz Blanchard in 2008

This time the rated power, and so rated current, is reached only few times compared to the Fromveur location. This can be easily explained by the lower tidal current resource that is present in this location. An average yearly power of 285 kW and a capacity factor of 28.49% are obtained from the floating TEC analysis, while P_{yearly_mean}=203 kW and CF=20.24% for the GBS one.

Much higher costs are encountered in this tidal location. The main reason of this behaviour is that export power cable cost is high due to the long distance from the shore, and so cable length.

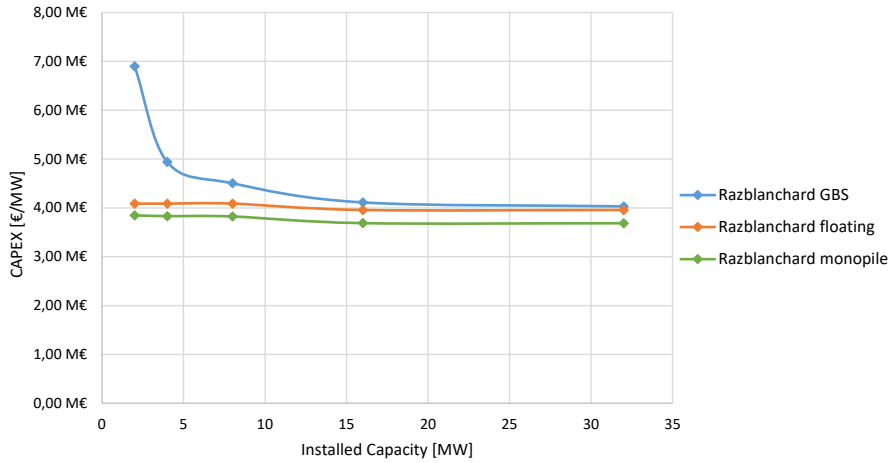

Figure 4.3-5: CapEx values as a function of Installed Capacity generated by GBS, Floating and Monopile TECs at Raz Blanchard

For the CapEx, a strong reduction in cost can be achieved by increasing array size in the GBS configuration (Figure 4.3-5), reaching a CapEx really similar between the three technologies, around 4 M€/MW, with the monopile winning among the others.

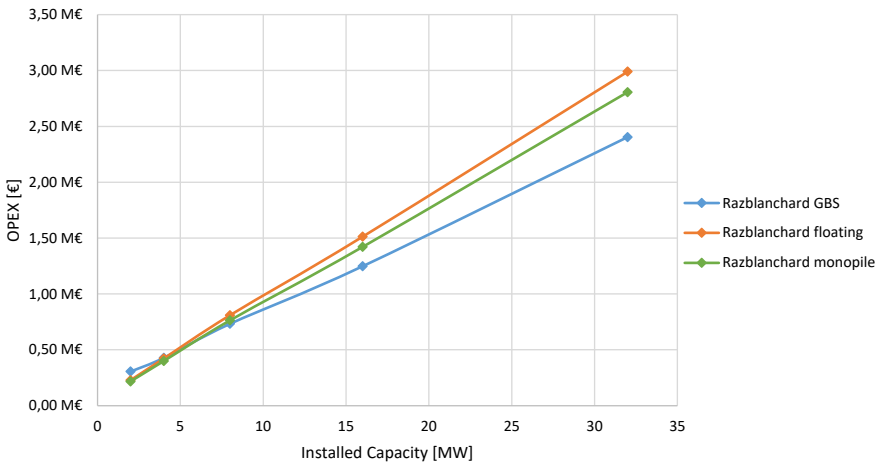

Figure 4.3-6: OpEx values as a function of Installed Capacity generated by GBS, Floating and Monopile TECs at Raz Blanchard

Interesting to note that the increased distance from the shore makes the OpEx of the GBS more advantageous compared to the other two (Figure 4.3-6). This result is always related to the power cable because the GBS requires a single and long cable, due to the present of the offshore substation, while floating and monopile TECs own a single cable for each structure.

Despite the advantage regarding the OpEx, in terms of LCoE the GBS TEC results again the technology with the highest LCoE, while monopile and floating produce almost the same results, reaching a minimum of 143 €/MWh, a much higher value compared to the previous case studies.in which shore distances were about few kms (Figure 4.3-7).

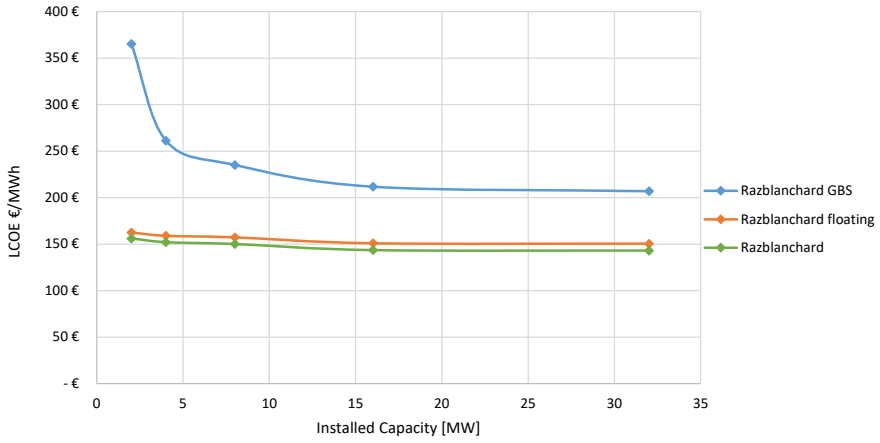

Figure 4.3-7: LCoE values as a function of Installed Capacity generated by GBS, Floating and Monopile TECs at Raz Blanchard

Different profitability metric values can be determinate for Raz Blanchard, in fact negative values of NPV and ROI are encountered for the GBS TEC as can be noted in Figure 4.3-8.

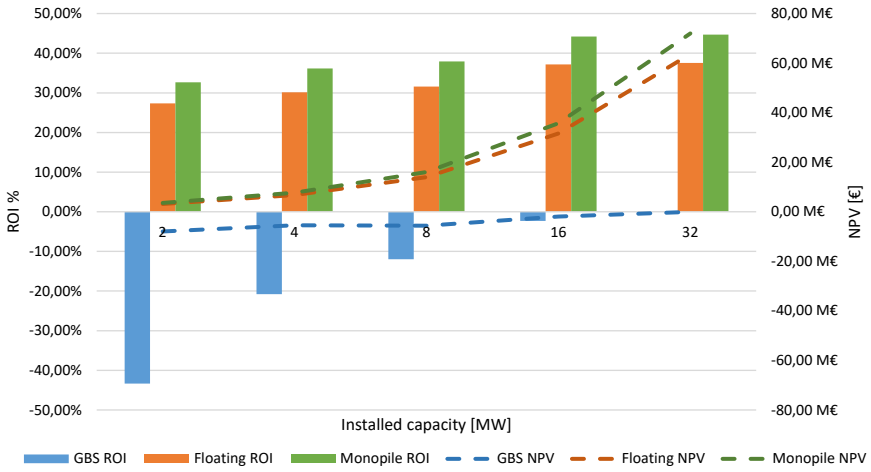

Figure 4.3-8: NPV and ROI as a function of Installed Capacity generated by GBS, Floating and Monopile TECs in Raz Blanchard. Bars and dashed lines represent NPV and ROI values, respectively

A negative value of ROI means that the project is not feasible in economic terms, so a lower investment cost should be obtained, or incentives have to be allocated in selling the renewable energy produced. Only in the 32 MW configuration a positive ROI is obtained, but still really low compared to the monopile configuration that reaches a 45% of ROI.

4.4. Punta Pezzo

Punta Pezzo, located in the Strait of Messina between the Sicily and Calabria region, represents one of the most promising locations for tidal energy exploitation in Italy. The site experiences tidal currents reaching 3 m/s, making it an attractive location not only for the velocities, but also for the proximity to the shore that provides advantages in terms of installation and maintenance [105]. The Strait of Messina is also characterized by a sharply drop in water depth near the coastline as can be noted in Figure 4.4-1.

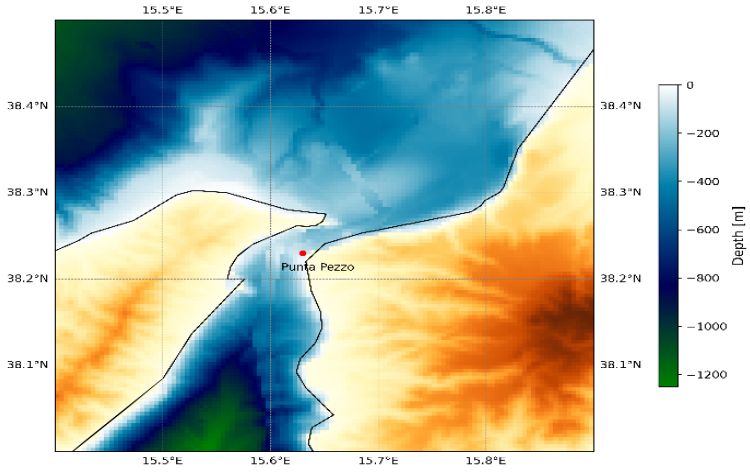

Figure 4.4-1: Bathymetry and location of Punta Pezzo. The red dot represents the selected tidal test site

Water depth in the selected location is 100 m, which could be a much higher value if another location is selected. Despite this, Punta Pezzo remains the tidal site with the highest water depth compared to the other case studies.

An advantage of this location is that the tidal plant is installed less than 1 km far from the coast, 550 m to be precise as depicted in Figure 4.4-2.

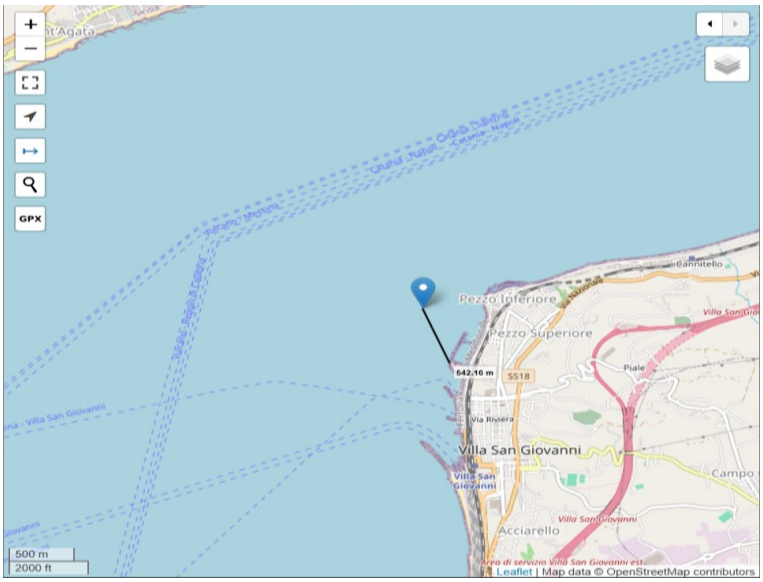

Figure 4.4-2: Punta Pezzo tidal plant distance from the shore

As it occurred for the previous case studies, the exact location was elected based on the available data. This time data was provided in terms of waveform components of the tidal current, meaning amplitude, period and phase, so the resource assessment followed the procedure explained in Case 3: Tidal current harmonic analysis.

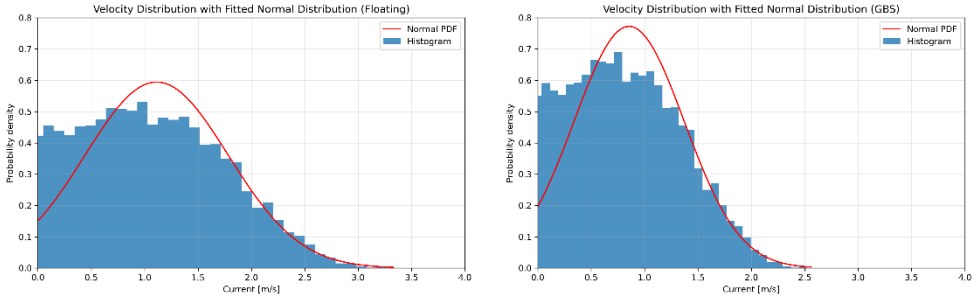

Figure 4.4-3: Resource assessment results (histogram and PDF) of Punta Pezzo tidal site

Results of the resource assessment are provided in Figure 4.4-3, in which a yearly data has been computed (8760 h), and it's possible to notice that much lower values of tidal current are reached in this location compared to previous case studies. In particular, maximum tidal velocity of 3.33 m/s is

reached in the floating configuration, and only 2.56 m/s in the GBS case. This strong difference in velocity, as can also be noted in by the much narrower shape of the PDF for the GBS configuration, is mainly due to the high-water depth characterizing Punta Pezzo, which leads to a great difference in velocity between bottom and upper part of the sea. Additionally, the 90-percentile in floating TEC is 2.03 m/s and in the case of GBS is 1.56 m/s.

For this case study, a less powerful turbine was involved, meaning the turbine employed in the Seagen 1.2 MW, the previous project with respect to the actual one, whose power curve is represented in Figure 4.4-4 [9].

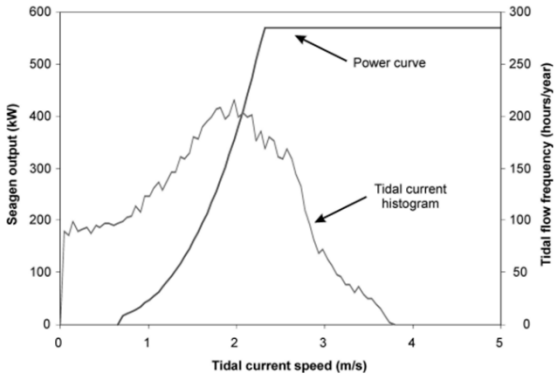

Figure 4.4-4: Original Seagen S-1.2 MW power curve

Seagen S-1.2 MW involved a couple of 2-bladed turbines of 16 m of rotor diameter and 600 kW of rated power at U_{rated}=2.35 m/s. other characteristics are U_{in}=0.7 m/s and U_{out}=4 m/s, meaning a wider range of operation compared to previous turbines. Many points of the power curve were picked up, the Cp was calculated for each point and a variation of Cp was noted, which ranged from 0.4 to 0.45. For this reason, also the Seagen 1.2 MW power curve was modelled with a third law interpolation equation, reported below.

$$P = 59.464 * U^3 - 67.146 * U^2 + 102.5 * U - 51.128 \qquad Eq.(99)$$

Coupling the power curve with the tidal resource resulted in a yearly power trend represented in Figure 4.4-5 for both TEC configuration.

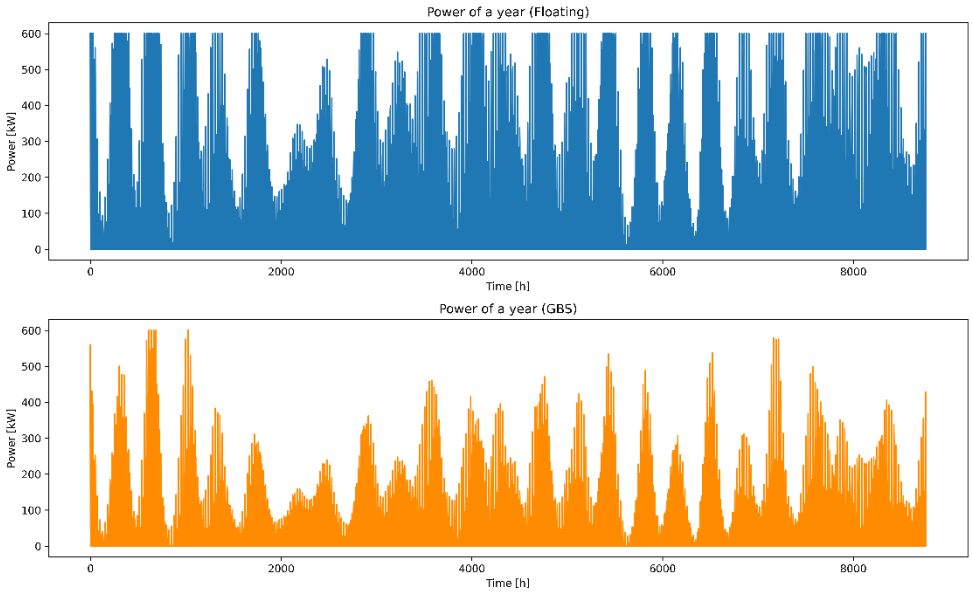

Figure 4.4-5: Power generated by GBS and floating TEC in Punta Pezzo in a year

By remembering the much lower current speeds reaching in the GBS, it's intuitive to say that much less power is generated compared to the floating case, in which many times the rated power is reached. Also in terms of average power and capacity factor a great difference is expected, in fact P_{yearly_mean}=125 kW and CF=20.83% are obtained for floating case, while only P_{yearly_mean}=59 kW and CF=9.76% for the GBS one.

Moving to the cost analysis, interesting considerations can be made for Punta Pezzo.

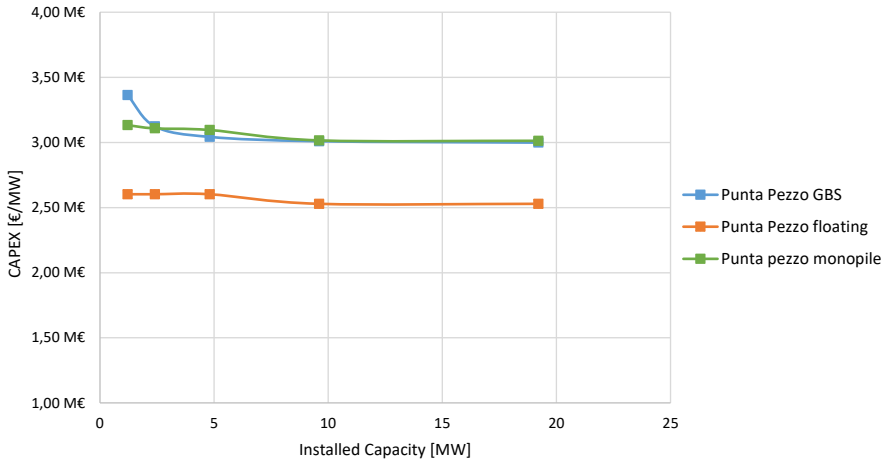

Figure 4.4-6: CapEx values as a function of Installed Capacity generated by GBS, Floating and Monopile TECs at Punta Pezzo

It's possible to notice in Figure 4.4-6 that the TEC that requires less investment cost is the floating one, meaning that floating type of TEC wins against the other in deep water location which makes the cost of the two other configurations to increase. CapEx of the monopile has increased so much that reached the cost of the GBS.

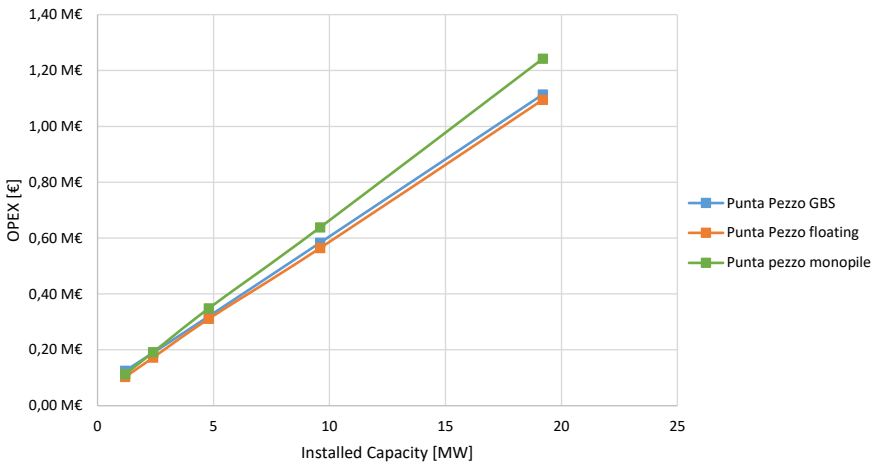

Figure 4.4-7: OpEx values as a function of Installed Capacity generated by GBS, Floating and Monopile TECs at Punta Pezzo

In terms of OpEx, monopile results to be the costliest, while the floating one the most convenient as reported in Figure 4.4-7. In any case, thanks to the proximity to the shore, OpEx are not so high as previous case studies.

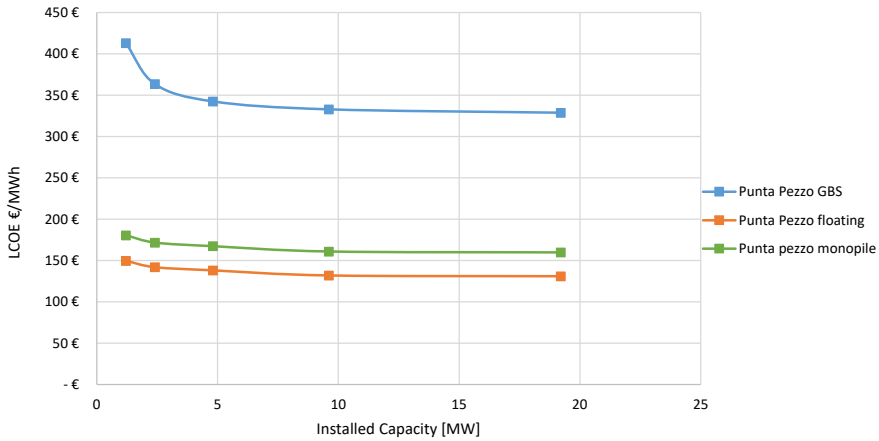

Figure 4.4-8: LCoE values as a function of Installed Capacity generated by GBS, Floating and Monopile TECs at Punta Pezzo

Overall, considering the LCoE, the floating TEC results to be the most convenient technology that produces a minimum LCoE of 131 €/MWh at 19.2 MW of array capacity (Figure 4.4-8). It's important to note that array size in terms of MW is different from the previous case studies because the same number of turbines installed has been used, but due to the lower rated power of the Seagen 1.2 MW power curve, lower values in the x-axis are obtained. In any case, a steady state cost is reached already at 19.2 MW, so increasing the array size wouldn't have led to better results.

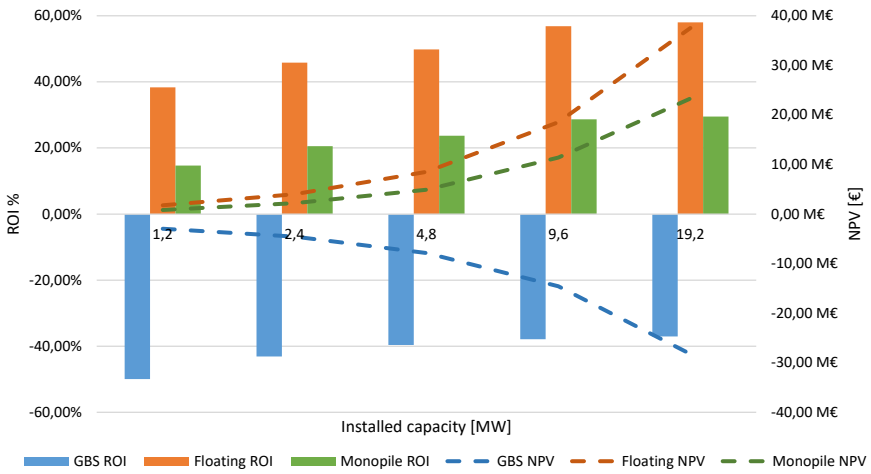

Figure 4.4-9: NPV and ROI as a function of Installed Capacity generated by GBS, Floating and Monopile TECs in Punta Pezzo. Bars and dashed lines represent NPV and ROI values, respectively

Considering the financial point of view, the GBS TEC resulted to be not profitable in all the cases, mostly due to the low yearly energy produced, while the other two configurations are profitable, with the floating TEC being the most profitable technology for this tidal location as visible in Figure 4.4-9.

4.5. Cozumel

The Cozumel channel, located in Mexico, is bordered by the Yucatan Peninsula and Cozumel Island and experiences northward flow velocities reaching up to 2.5 m/s, providing a continuous energy source. In particular, the Cozumel Island's insular shelf offers suitable conditions for a tidal turbine installation, with depths reaching up to 50 m at 250-500 m from the shoreline. Additionally, the growing population and tourism underscores the need of a sustainable energy demand that could be satisfied by tidal energy [89].

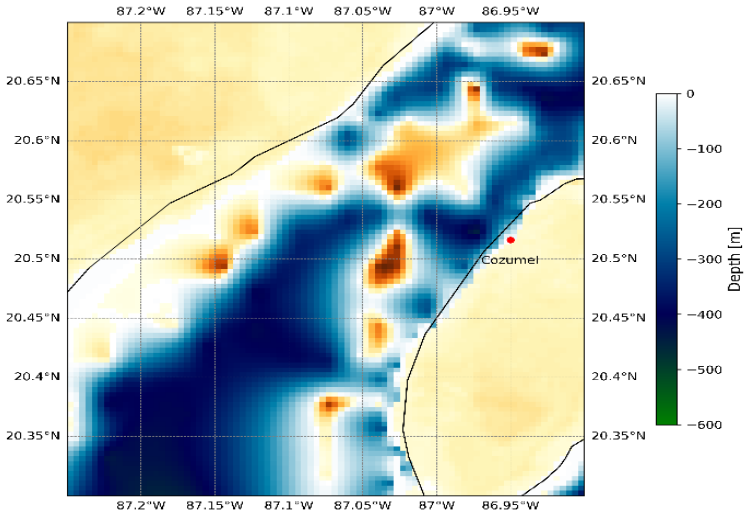

Figure 4.5-1: Bathymetry and location of Cozumel. The red dot represents the selected tidal test site

The location of the site of interest is really close to shore, in fact from Figure 4.5-1 the marker seems to be located onshore, but in reality, is just 220 m from the coast (Figure 4.5-2), which can't be accurately represented in the map.

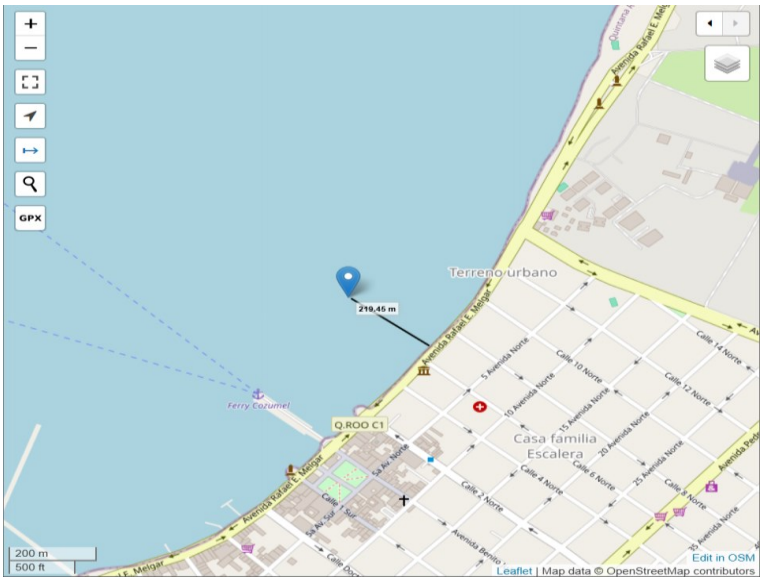

Figure 4.5-2: Cozumel tidal plant distance from the shore

Due to the high proximity to the coast, there's a shallow water depth, in fact for the selected location it's 19.1 m.

As explained in Case 4: Yearly current frequency analysis, statistical data is already present for the Cozumel location, meaning that the tidal current yearly trend is not provided, but directly the relative frequency of occurrence. The original histogram data was rescaled to the depth of interest for floating and GBS and results are reported in Figure 4.5-3.

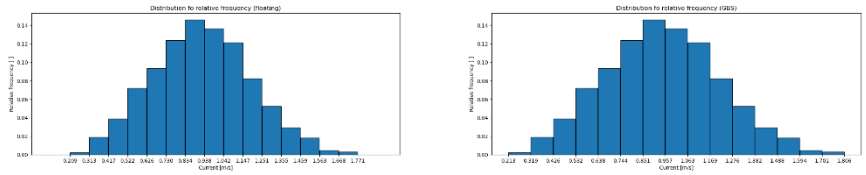

Figure 4.5-3: Resource assessment results (histogram and PDF) of Cozumel tidal site

Due to the scaling, also the bin width has been scaled accordingly, and it's possible to notice that in the GBS case the tidal velocities are slightly higher than the floating one. The reason for this is that it wasn't possible to satisfy both the minimum clearance constraints, so only the clearance from the seabed has been considered, which led to a lower depth of operation (8.11 m) compared to the floating case (9.35 m).

Due to shallow water, it wasn't possible to install a large turbine as it happened in previous case studies, so a smaller one has been selected, meaning the Tocardo T2. Many configurations of this turbine are present, as can be noted from the different power curves in Figure 4.5-4, in which rotor diameter is decreasing, from a maximum D=9.9 to a minimum D=5.3 m as rated current increases [67]. Power curve considered has a U_{in}=0.4 m/s, U_{rated}=2 m/s and U_{out}=2.6 m/s.

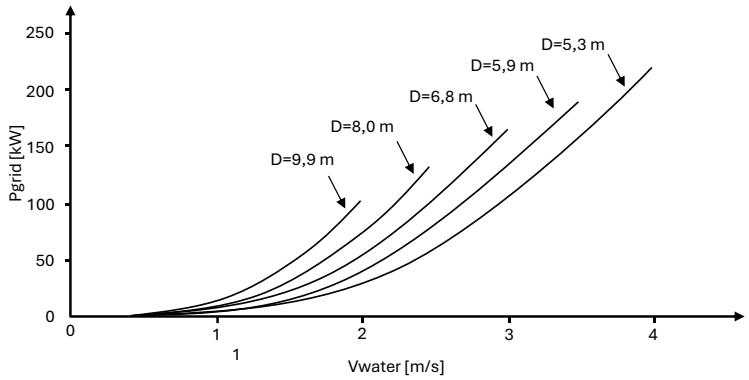

Figure 4.5-4: Tocardo T2 power curves at different rotor diameters

Since not high tidal currents are present in the location, the turbine with lowest rated current has been selected, despite not satisfying one clearance constraint.

Also in this case, the power curve has been modelled with a cubic law equation since Cp varies between 0.1 to 0.35, which is reported below:

$$P = 1.3792 * U^3 + 40.198 * U^2 - 38.414 * U + 9.4614 \qquad Eq.(100)$$

Coupling the power curve into the resource analysis, the n° of occurrences of a certain value of power is obtained, as reported in Figure 4.5-5.

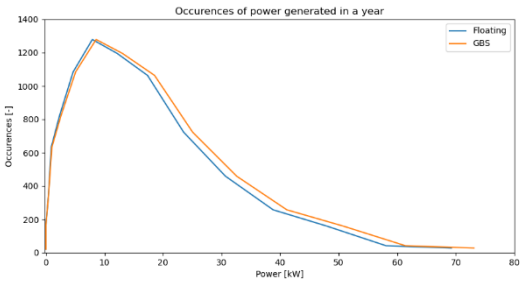

Figure 4.5-5: Occurrences of power values for GBS and floating in Cozumel

By multiplying each power value for the corresponding relative frequency and summing up all the values, the average yearly power is obtained, which resulted in P_{yearly_mean}=11.9 kW and CF=11.51% for floating case, and P_{yearly_mean}=12.7 kW and CF=12.3% for the GBS one.

Moving to the cost analysis, it's important to denote that for the floating case an initial export voltage of 3.3 kV has been selected (no more 11 kV) due to low power exported, and for the array of 16 and 32 turbines it has been reduced to 0.69 kV to show the cost reduction and the necessity to optimize to cable cost with the export power.

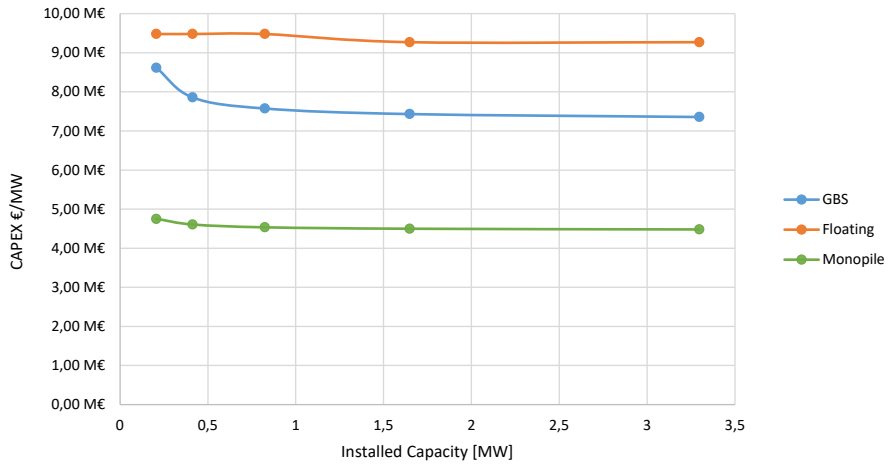

Figure 4.5-6: CapEx values as a function of Installed Capacity generated by GBS, Floating and Monopile TECs at Cozumel

High CapEx costs are present in terms of €/MW because a small and low power turbine is involved in the array (Figure 4.5-6).

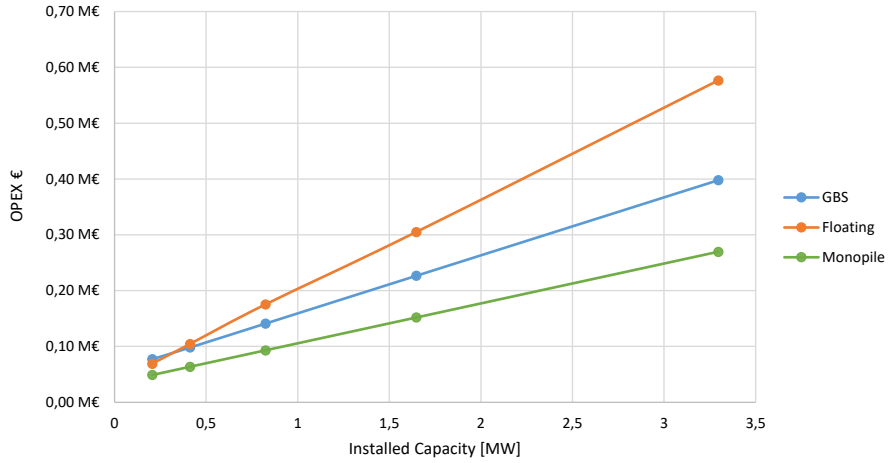

Figure 4.5-7: OpEx values as a function of Installed Capacity generated by GBS, Floating and Monopile TECs at Cozumel

Low OpEx values are encountered thanks to the small array size and the short distance from the shore (Figure 4.5-7).

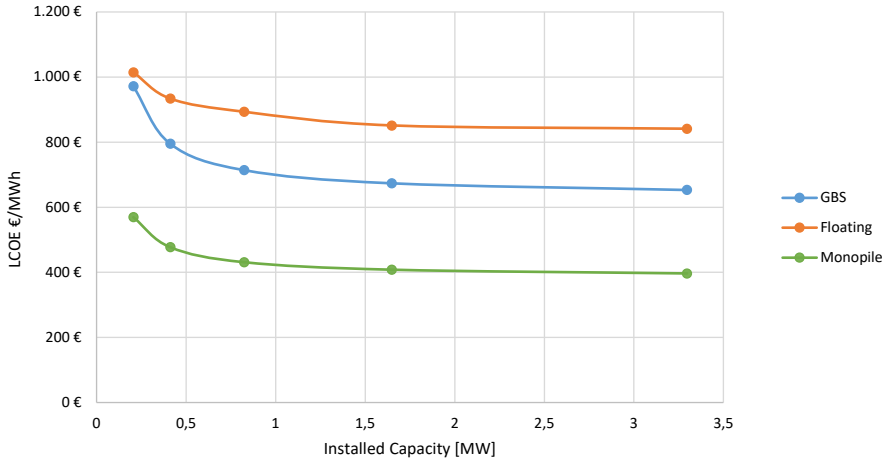

Figure 4.5-8: LCoE values as a function of Installed Capacity generated by GBS, Floating and Monopile TECs at Cozumel

In terms of LCoE, as can be noted in Figure 4.5-8, the monopile configuration is the costless technology, while the floating one is the costliest one. Main reason for the floating TEC of not being cost competitive in this location is that the floating platform has the advantage of reducing costs in high water depths, and this advantage is lost when it is used in a shallow location as Cozumel. For this reason, for example the GBS becomes more advantageous than it, as well as the monopile.

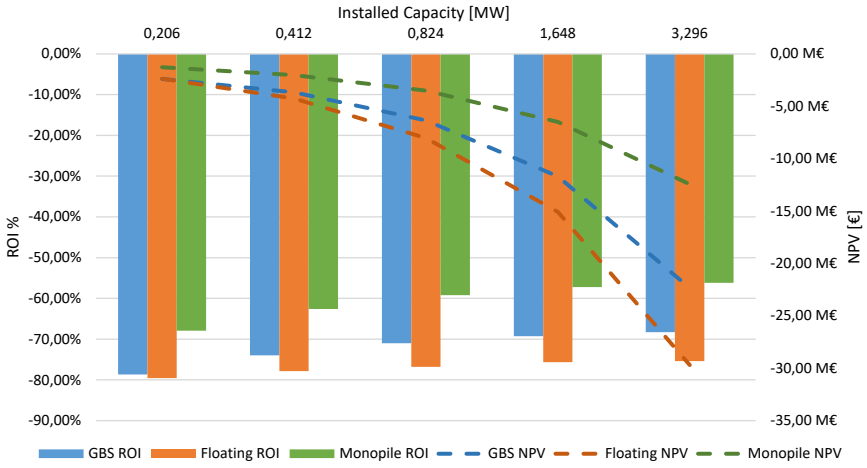

Figure 4.5-9: NPV and ROI as a function of Installed Capacity generated by GBS, Floating and Monopile TECs in Cozumel. Bars and dashed lines represent NPV and ROI values, respectively

Considering the financial metrics, all the TEC configurations result to be not financially feasible in all the evaluated array sizes as reported in Figure 4.5-9. The low power turbine involved doesn't allow to cover costs in a reasonable period, so different solutions should be adopted. A more powerful turbine could be used by moving the tidal plant to a deeper location, in which a larger turbine can be employed, or offering incentives for tidal energy so that revenues are increase and there's more chance to reach a positive NPV.

4.6. Results Summary

A lot of data and results have been obtained from single case studies and are reported in this section to better analyse differences in the locations.

First of all, Table 4.6-1 summarizes the main characteristics of single case study, from the location itself to the turbine parameters.

Table 4.6-1: Summary of main characteristics of tidal locations and turbine parameters

	Fall of Warness	Fromveur	Raz Blanchard	Punta Pezzo	Cozumel
Latitude	59.14°	48.44°	49.76°	38.23°	20.51°
Longitude	-2.82°	-5.03°	-2.01°	15.63°	-86.95°
Water depth [m]	49	51.3	55	100	19.1
Distance from shore [m]	1600	2500	11100	600	200
Turbine name or project name	Orbital O2	Seagen S-2 MW	Seagen S-2 MW	Seagen S-1.2 MW	Tocardo T2
Rotor diameter [m]	20	20	20	16	9.9
Rated power [kW]	1000	1000	1000	600	103
Rated current [m/s]	2.65	2.5	2.5	2.35	2
Cut-in velocity [m/s]	1	1	1	0.7	0.4
Cut-out velocity [m/s]	4	4	4	4	2.6

Additionally, the 4 power curves involved are represented all together in Figure 4.6-1.

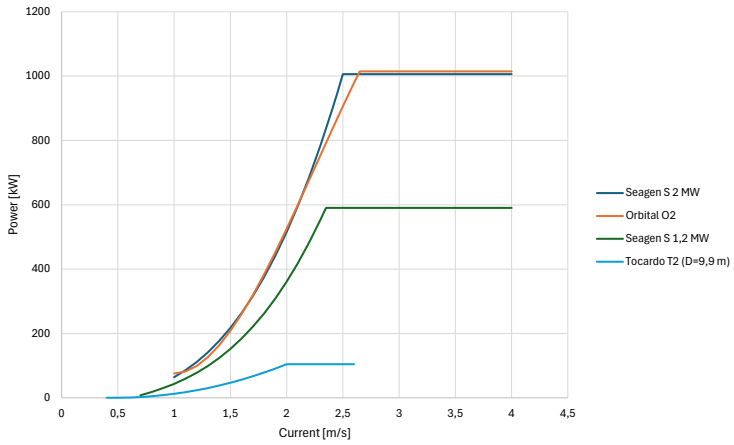

Figure 4.6-1: Power curves involved in the case studies

As previously mentioned, Seagen S 2 MW and Orbital O2 turbines are the most powerful ones, followed by the Seagen 1.2 MW and the Tocardo T2. Only the Seagen S 2 MW turbine power curve

has been computed with a constant Cp, while for the others a cubic polynomial equation has been evaluated.

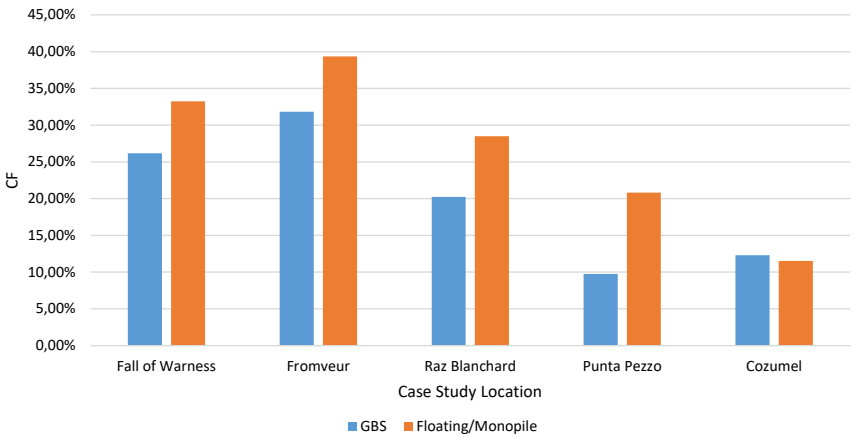

Figure 4.6-2: Capacity factor of different case study location

In Figure 4.6-2 the capacity factor for each location is reported, independently on the array size since no wake effects are considered in this work, which would reduce the incoming flow to the behind turbines. What is possible to note is in Fromveur there's the best exploitation of the selected turbine with the available currents. Higher current values are present in this location and only few exceeds the cut-out velocity, meaning that many times the power produced is at rated level. Additionally, the water depths strongly affect the CF difference between GBS and floating. A high-water depth, as occurs in Punta Pezzo, produces a higher difference in the two configurations compared to a low-water depth location, as in Cozumel channel in which the two CFs are almost the same.

Main results from the techno-economic assessment are reported in Table 4.6-2 and Table 4.6-3, specifically for an array of 32 turbines.

It's possible to additionally evaluate the amount of CO2 that has been saved by using tidal energy converters instead of a fossil fuel to produce electricity, natural gas in this evaluation. The environmental impact of decarbonization is estimated by adopting the following equation [106]:

$$E_{CO_2} = EF * AEP \ , \qquad Eq.(101)$$

where EF is the emission factor equal to 532 g $CO_{2,eq}$/kWh, meaning the amount of CO2 emitted if the electricity was produced through a natural gas power plant, and AEP the annual energy production. Furthermore, another cost metric has been included in the tables, i.e. the Payback Period (PP), which is the time necessary to recover the CapEx, meaning that after PP only profits will be generated. Given its definition, PP can be obtained by solving the following equation:

$$NPV = -CapEx + \sum_{t=1}^{T} \frac{R_t - OpEx}{(1+r)^T} = 0 \quad , \qquad Eq.(102)$$

which becomes:

$$PP = T = \frac{ln\left(\frac{R - OpEx}{R - OpEx - r * CapEx}\right)}{ln(1+r)} \qquad Eq.(103)$$

Table 4.6-2: Summary of main results from techno-economic assessment 1

	Fall of Warness			Fromveur			Raz Blanchard		
	GBS	Float.	Mono	GBS	Float.	Mono	GBS	Float.	Mono
Ip [MW]	32	32	32	32	32	32	32	32	32
CF [%]	26.17	33.24	33.24	31.83	39.35	39.35	20.24	28.49	28.49
AEP [MWh]	73444	93066	93066	10176	12576	12576	56793	79891	79891
CapEx [M€]	97.93	64.15	47.98	100.6	74.77	68.24	128.9	126.6	117.9
OpEx [M€]	2.02	1.60	1.24	2.01	1.78	1.64	2.41	2.99	2.81
LCoE [€/MWh]	124.9	66.7	52.6	104.9	64.8	61.1	207.0	150.5	143.1
NPV [M€]	85.01	184.1	202.5	128.3	220.8	226.5	0.006	63.64	71.99
ROI [%]	65.77	210.6	293.6	97.33	219.4	238.6	0.004	37.56	44.69
PP [year]	10	5	3	8	5	4	24	13	12
E_{CO2} [t_{CO2eq}]	39072	49511	49511	47423	58608	58608	30214	42502	42502

CPI=Ip=Installed capacity, CF=capacity factor, AEP=annual energy production, CapEx=capital expenditure, OpEx=operational expenditure, LCoE=levelized cost of electricity, NPV=net present value, ROI=return of investment, PP=payback period, ECO2=environmental impact of decarbonization

Table 4.6-3: Summary of main results from techno-economic assessment 2

	Punta Pezzo			Cozumel		
	GBS	Float.	Mono	GBS	Float.	Mono
Ip [MW]	19.2	19.2	19.2	3.296	3.296	3.296
CF [%]	9.76	20.83	20.83	12.3	11.51	11.51
AEP [MWh]	16427	34040	34040	3554	3325	3325
CapEx [M€]	57.58	48.56	57.85	24.25	30.56	14.78
OpEx [M€]	1.11	1.09	1.24	0.398	0.577	0.27
LCoE [€/MWh]	328.9	131	159.8	653.1	840.9	396.5
NPV [M€]	-28.22	37.51	23.29	-22.35	-29.7	-12.45
ROI [%]	–	57.97	29.51	–	–	–
PP [year]	–	11	14	–	–	–
E_{CO2} [t_{CO2eq}]	8739	18641	18641	1891	1769	1769

4.7. Case studies with Tocardo T2

Up to now different tidal turbines were employed in the different locations, but in order to enable a direct comparison of site performance and to better understand how local characteristics influence power production, it is necessary to use the same turbine, thus eliminating the variables related to different turbine designs. Since the main constraint is the water depth in the Cozumel Island, the Tocardo T2 has been employed in all locations despite being a low powerful turbine. The purpose of this analysis is not focusing on providing financial feasibility, otherwise a more powerful turbine should be employed, but rather compare the different tidal locations.

In Figure 4.7-1, the capacity factor is reported. It's possible to notice how the turbine works in the different locations independently on the type of turbine. Interesting considerations can be made by looking at the Fromveur location, in fact the CF of the floating TEC is lower than the GBS one. This is the opposite of what is expected, but this reduction is due to the fact that the tidal current overcomes the cut-out velocity more times than in the GBS case, making the turbine to shut off. For this reason, Fromveur location is no longer the location with the highest CF as it occurred in previous case studies but now Fall of Warness is the best one.

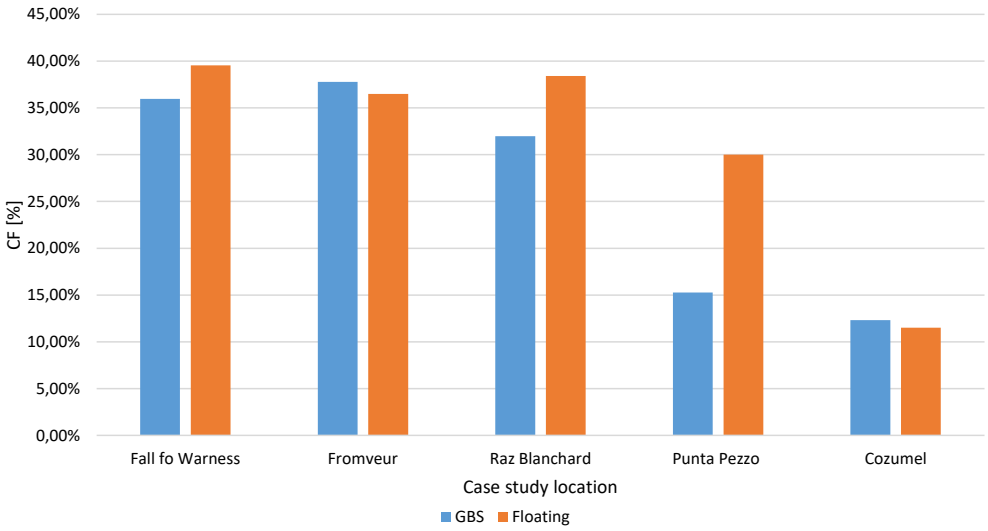

Figure 4.7-1: Capacity factor for the 32 turbines array in different case study locations

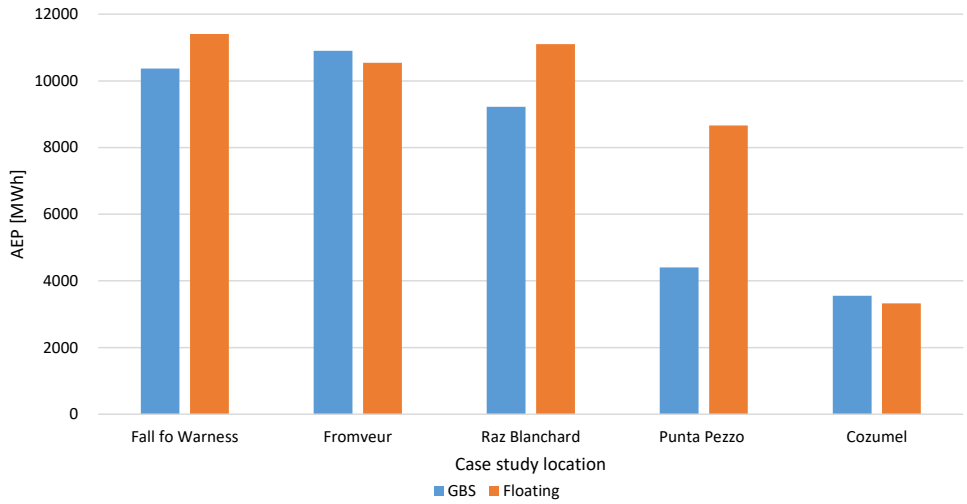

Figure 4.7-2: AEP for the 32 turbines array in different case study locations

Same consideration can be made for the AEP (Figure 4.7-2). It's possible to notice that the bar chart shape is the same as the CF since no longer variations due to different turbines involved are present. About the cost analysis, the same cost metrics are reported in the following figures and it's important to remark that due to the low power produced, the voltage of the export cables has been reduced. In particular, for the GBS a 6.5 kV export cable is used until the 16 turbines array, after which it is increased to 11 kV, and for the floating and monopile TECs the voltage involved is 3.3 kV, which is reduced to 0.69 kV after an array size of 16 turbines.

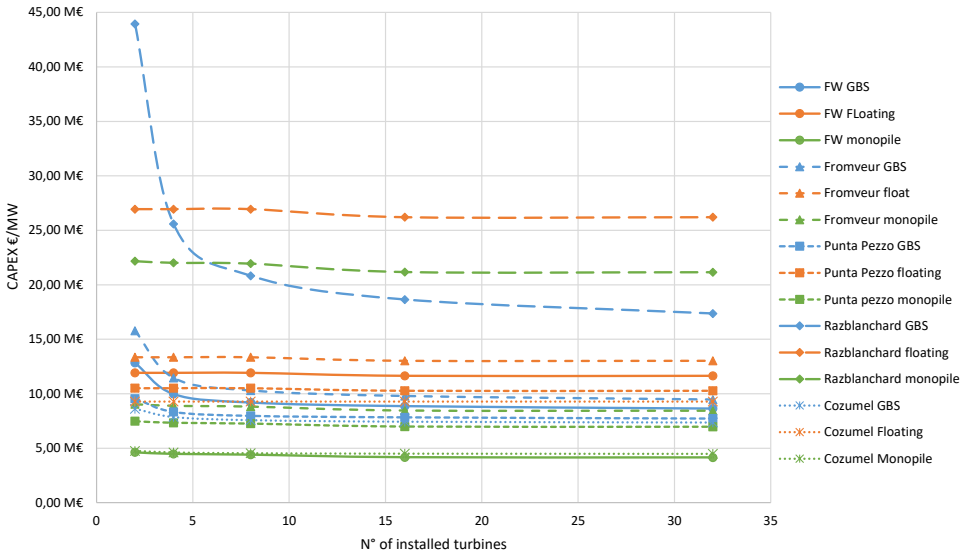

Figure 4.7-3: CapEx in €/MW vs n° of installed turbines in all case study locations

As expected, the CapEx in terms of €/MW is really high, reaching up to 44 M€/MW for the GBS TEC in Raz Blanchard, as visible in Figure 4.7-3, while the minimum one is reached by the monopile TEC in Fall of Warness (4.15 M€/MW), followed by Cozumel.

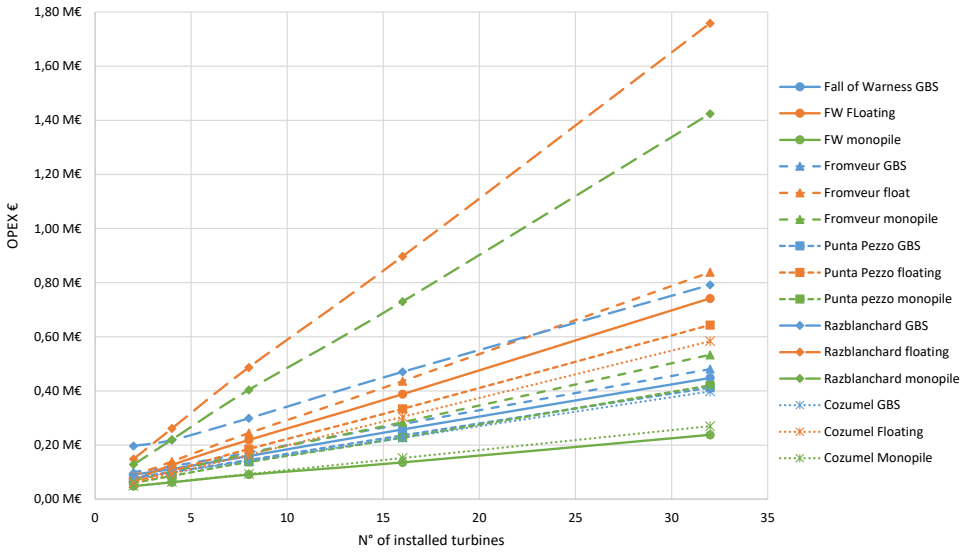

Figure 4.7-4: OpEx vs n° of installed turbines in all case study locations

OpEx are not as high as previous case studies since a smaller turbine is involved, so the OpEx cost reflects more the environmental characteristics and location of the tidal site with respect to shore. For this reason, Raz Blanchard remains the highest OpEx location due to the high distance from the land. Monopile configuration of Fall of Warness and Cozumel remains the OpEx costliest ones (Figure 4.7-4).

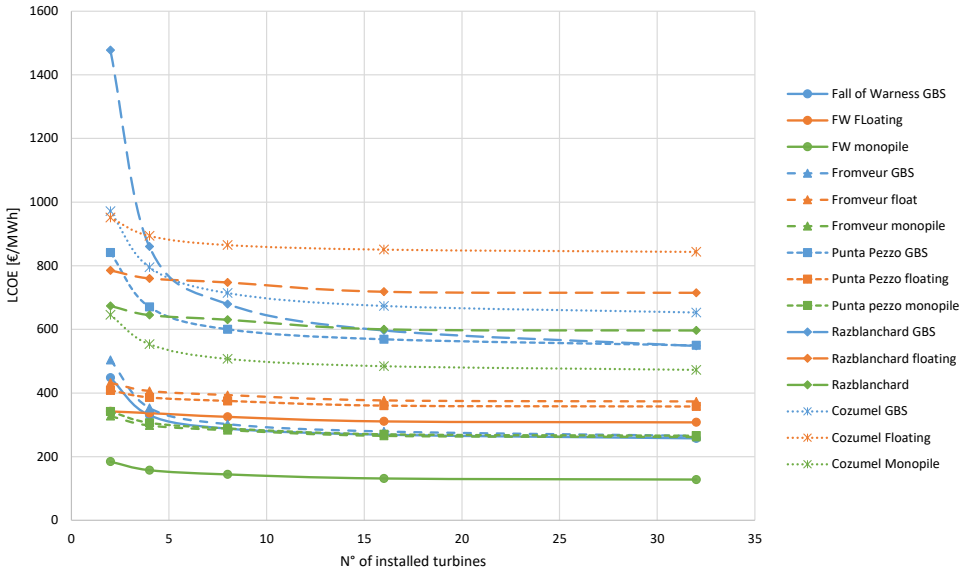

Figure 4.7-5: LCoE vs n° of installed turbines in all case study locations

Moving to the LCoE, as expected, the monopile TEC in Fall of Warness is the lowest one, reaching a value of 128 €/MWh, while the floating one in Cozumel Island is the worst one at a 32 turbines array (Figure 4.7-5). Overall, LCoE values are high compared to what obtained in previous case studies, and for this reason almost all the locations don't result to be profitable, as can be seen in Figure 4.7-6. There's only one configuration that generates a positive NPV, which is the monopile in Fall of Warness, while all the others will generate an economic loss if the plant would be installed.

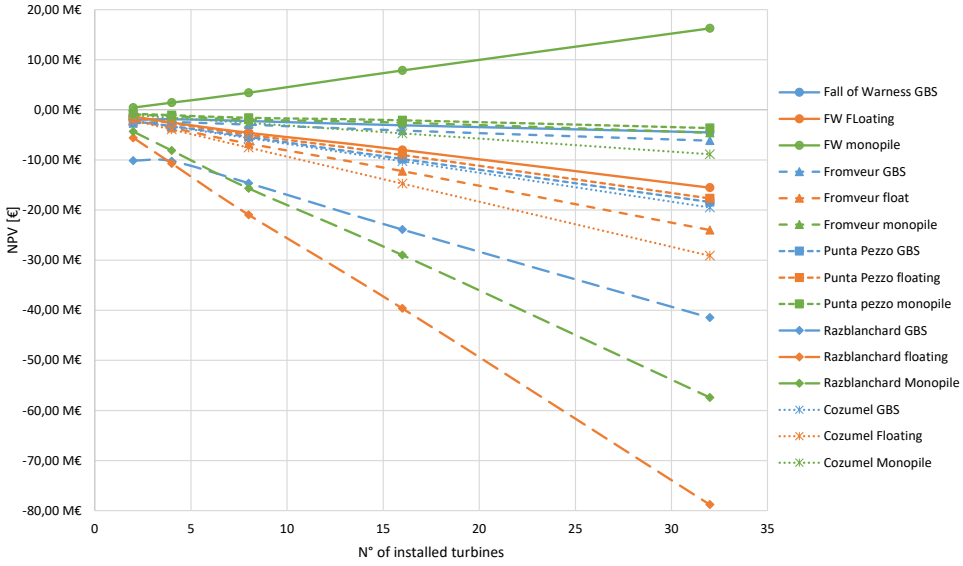

Figure 4.7-6: NPV vs n° of installed turbines in all case study locations

The analysis performed in this section allowed a better understanding on the difference between the potential tidal locations, allowing a correct comparison. Since almost none of the configurations

allowed an economic profitability, due to the undersized turbine involved. These results remark the importance of designing a powerful turbine specifically for that tidal location to better exploit the resource and to reduce costs (cost decreasing as power is increasing).

5. Summary

This work presented a model to estimate costs of a tidal energy converter plant using a bottom-up approach, in which cost functions were retrieved from literature or interpolated with available data for each single component composing the plant. Cost model was applied to a real case study, the ATIR floating platform owned by Magallanes Renovables, in which costs were available for different categories of components of the TEC, and, if necessary, model was corrected. An additional application of the model could be possible to a gravity-based TEC plant, i.e. Meygen tidal array, but it a validation of the cost functions would have led to underestimated results because Meygen project encountered really high costs, for being one the first and biggest project in the tidal energy sector.

Four cases of tidal resource assessment methodology were presented depending on the form of the available tidal resource data, as well as the application of the power curve to the data, retrieved from existing projects.

Five different locations were selected for performing the techno-economic analysis in which a proper turbine was selected, and different power and cost metrics were evaluated. In particular, most important indicators are Capacity Factor (CF), Levelized Cost of Electricity (LCoE), Net Present Value (NPV), and return on investment (ROI). For a correct comparison of the different tidal site locations, the same turbine was involved that satisfied all location constraints, so the Tocardo T2 was selected due to its small rotor diameter, satisfying the low water depth present in Cozumel Island.

Considering the single case studies, in almost all cases the monopile TEC resulted in the lowest LCoE with the expect of the Punta Pezzo location, in which the high water depth affected the foundation costs for this configuration, leading to a more profitable plant with the usage of the floating TEC. On the contrary, GBS resulted to be the least profitable configuration in all cases with the expect of Cozumel Island in which the low water depth makes the GBS and monopile TEC more convenient than the floating one. In fact, it's important to remember that the mass of the platform is assumed to be constant, as well as mooring system design, so in reality a shallow water depth and lower currents would reduce mass and cost.

In the Tocardo T2 case study, only one technology and tidal site resulted to be profitable, meaning the monopile TEC in Fall of Warness, while all the others resulted in a negative NPV. In particular, Raz Blanchard was the most expensive and less profitable tidal site mainly due to the far distance from shore that increased a lot power cables cost.

In any case, GBS was one of the first technologies to be implemented in the tidal sector which allowed the retrieval of a lot of knowledge about this field, but in recent years the floating TECs seemed to be

more convenient and efficient in terms of productivity, in fact they're also called second-generation tidal devices [75].

Despite the convenience of the monopile TEC obtained from this work, this tidal configuration hasn't gained so much popularity as the other two, probably because the others are more adaptable to varying seabed conditions. GBS can be just laid onto the seabed, staying fixed due to gravity, the floating TEC requires only the mooring system to be in contact with the ground, while the monopile installation requires drilling into the seabed. For this reason, noise pollution is generated, which may affect the neighbour ecosystem in terms of habitat as well as sediment plumes that travel with currents [107].

As previously mentioned, the proposed cost model has been obtained with a bottom-up approach under different hypothesis. A list of possible improvements is following proposed, which could refine and better estimate costs under this model:

- Tidal platform and mooring system design: as mentioned different times, platform and mooring system design for the floating TEC has been considered fixed, independently on the currents available on that site. In reality, having a low or high currents would change the design of these systems, so introducing naval engineering knowledge would allow a correct design parameters, and so costs;
- Steel price: a correct steel price was obtained through the cost model validation phase based on costs related to the ATIR floating platform. By making some considerations and hypothesis, steel price costs for the platform and the mooring system were obtained, while steel price used for monopile and GBS foundations was assumed based on what obtained from the floating one. An additional real case study cost distribution would improve the validity of the model and steel prices. In any case, it's really important to note that steel price has a huge variability in time and country, and is affected by the geopolitical situation, like trade restrictions and regulations, and many parameters such as demand, global economic conditions and raw material costs [108];
- Decommissioning cost: cost for dismantling the TEC was retrieved from literature and considered as a fixed price since the study published an average cost. It's intuitive to say that the larger the TEC is, the higher the decommissioning costs will be, as well as the distance from the shore which would require more time to dismantle it if far from the port;
- Onshore substation: only the offshore part of the tidal plant has been considered in the cost model evaluation. In reality, an onshore substation is needed to transform and effectively distribute electrical energy to the designated load or grid [28], so its inclusion in the cost

evaluation depends on the purpose and the cost area of interest, because it may be possible that the onshore substation already exists and there's no need to build a new one;

- OpEx: as mentioned in the relative chapter, OpEx typically are provided in terms of % of the overall CapEx, however, this work attempted to produce a dynamic OpEx model that included the failure probabilities of single elements composing the TEC. Given the significant uncertainty in marine conditions, further refinements of this model are necessary, like including a probabilistic weather modelling to quantify costs related to bad weather downtimes, or performing Monte Carlo simulations to quantify ranges of different maintenance scenarios;
- TEC availability: in this work no downtime of the turbine has been considered, so characterized by a 100% of availability. It's unrealistic that the turbine continuously operates because it requires preventive and corrective maintenance, which would require the turbine to stop, producing less energy. Based on the fact that proper planning of the preventive maintenance is required and that downtime values are unknown, no decrease in availability has been considered. By introducing an accurate OpEx model, costs could be better estimated as well as downtime values, so availability.

In summary, this study provides important technological and economical comparisons between the three main TEC configurations around the world, and assesses the economic feasibility of tidal energy plants, highlighting the importance of a proper tidal turbine selection to enhance cost-effectiveness. Future research should focus in improving the cost model to make it more adaptable to environmental conditions and country location.

References

[1] "THE RANCE MEMOGUIDE The Rance Tidal Power Station is in the Rance Estuary in the department of Ille-et-Vilaine," 2012.

[2] A. Etemadi, Y. Emami, O. AsefAfshar, and A. Emdadi, "Electricity generation by the tidal barrages," in *Energy Procedia*, Elsevier Ltd, 2011, pp. 928–935. doi: 10.1016/j.egypro.2011.10.122.

[3] Joint Research Centre (JRC), "Ocean Energy in the European Union STATUS REPORT ON TECHNOLOGY DEVELOPMENT, TRENDS, VALUE CHAINS & MARKETS," 2024. doi: 10.2760/1244922.

[4] Ocean Energy Europe, "Sabella," https://www.oceanenergy-europe.eu/annual/sabella/.

[5] M. H. Khanjanpour and A. A. Javadi, "Optimization of the hydrodynamic performance of a vertical Axis tidal (VAT) turbine using CFD-Taguchi approach," *Energy Convers Manag*, vol. 222, Oct. 2020, doi: 10.1016/j.enconman.2020.113235.

[6] D. Coiro, "Resource assessment for the GEMSTAR tidal current energy harvester deployment in the strait of Messina," 2019. [Online]. Available: https://www.researchgate.net/publication/337275969

[7] E. Segura, R. Morales, J. A. Somolinos, and A. López, "Techno-economic challenges of tidal energy conversion systems: Current status and trends," 2017, *Elsevier Ltd*. doi: 10.1016/j.rser.2017.04.054.

[8] Atlantis Resources, "AR1500 TIDAL TURBINE." [Online]. Available: https://simecatlantis.com/wp-content/uploads/2016/08/AR1500-Brochure-Final-1.pdf

[9] C. A. Douglas, G. P. Harrison, and J. P. Chick, "Life cycle assessment of the Seagen marine current turbine," *Proceedings of the Institution of Mechanical Engineers Part M: Journal of Engineering for the Maritime Environment*, vol. 222, no. 1, pp. 1–12, 2008, doi: 10.1243/14750902JEME94.

[10] EMEC, "Magallanes ATIR Project Information Summary," 2021.

[11] L. Fingersh, M. Hand, and A. Laxson, "Wind Turbine Design Cost and Scaling Model," 2006. [Online]. Available: http://www.osti.gov/bridge

[12] T. Ashuri, "Integrated Aeroservoelastic Design and Optimization of Large Offshore Wind Turbines Turaj Ashuri."

[13] H. Liu, Y. Gu, Y. G. Lin, Y. J. Li, W. Li, and H. Zhou, "Improved blade design for tidal current turbines," *Energies (Basel)*, vol. 13, no. 10, May 2020, doi: 10.3390/en13102642.

[14] E. Segura, R. Morales, and J. A. Somolinos, "Cost assessment methodology and economic viability of tidal energy projects," *Energies (Basel)*, vol. 10, no. 11, Nov. 2017, doi: 10.3390/en10111806.

[15] R. N. Clark, "Wind Turbine Components and Descriptions: Essential Components to Have a Productive, Reliable, and Safe Wind Machine," *Small Wind: Planning and Building Successful Installations*, pp. 39–67, Jan. 2014, doi: 10.1016/B978-0-12-385999-0.00003-5.

[16] D. J. Malcolm and A. C. Hansen, "WindPACT Turbine Rotor Design Study: June 2000--June 2002 (Revised)," 2000. [Online]. Available: http://www.osti.gov/bridge

[17] Claire Legrand, Black & Veatch Ltd, and EMEC, "Assessment of Performance of Tidal Energy Conversion Systems," 2009.

[18] "Tidal turbine braking systems."

[19] K. Rajambal, B. Umamaheswari, and C. Chellamuthu, "Electrical braking of large wind turbines," *Renew Energy*, vol. 30, no. 15, pp. 2235–2245, Dec. 2005, doi: 10.1016/j.renene.2004.11.002.

[20] G. Li and W. Zhu, "A Review on Up-to-Date Gearbox Technologies and Maintenance of Tidal Current Energy Converters," Dec. 01, 2022, *MDPI*. doi: 10.3390/en15239236.

[21] H. Li and Z. Chen, "Design Optimization and Evaluation of Different Wind Generator Systems," 2008.

[22] F. Wani and H. Polinder, "A Review of Tidal Current Turbine Technology: Present and Future", doi: 10.13140/RG.2.2.26857.44640.

[23] A. Hydro, "ANDRITZ HYDRO Hammerfest - Renewable energy from tidal currents." [Online]. Available: www.andritz.com

[24] A. Benlevi, "Engineering Model for Automatic Design of Rotor Nacelle Assem-blies For Offshore and Onshore Applications."

[25] V. S. Neary, Y.-H. Yu, and A. E. Copping, “Methodology for Design and Economic Analysis of Marine Energy Conversion (MEC) Technologies,” 2014, doi: 10.13140/RG.2.2.10201.95846.

[26] G. B. Sinclair and J. E. Helms, “A review of simple formulae for elastic hoop stresses in cylindrical and spherical pressure vessels: WHAT can be used when,” Apr. 01, 2015, *Elsevier Ltd*. doi: 10.1016/j.ijpvp.2015.01.006.

[27] SAE Renewables, “SeaGen-S 2MW Proven and commercially viable tidal energy generation.”

[28] A. Y. Nakhai, “Electrical Infrastructure Cost Model for Marine Energy Systems,” 2023. [Online]. Available: www.nrel.gov/publications.

[29] A. J. Collin *et al.*, “Electrical components for marine renewable energy arrays: A techno-economic review,” *Energies (Basel)*, vol. 10, no. 12, Dec. 2017, doi: 10.3390/en10121973.

[30] A. Y. Nakhai, “Electrical Infrastructure Cost Model for Marine Energy Systems,” 2023. [Online]. Available: www.nrel.gov/publications.

[31] Marine Technology, “SAE Deploys Upgraded Turbine at MeyGen Tidal Power Site,” https://www.marinetechnologynews.com/news/deploys-upgraded-turbine-meygen-629369.

[32] Cable Solutions Worldwide Ltd, “Electrical Cable Design & Manufacture,” https://www.cable-solutions-worldwide.com/electrical-cables/.

[33] “Comparison Between HVDC and HVAC Transmission System,” https://www.electricaldeck.com/2021/08/comparison-between-hvdc-and-hvac-transmission-system.html.

[34] F. Sharkey and F. Sharkey, “ARROW@TU Dublin ARROW@TU Dublin Offshore Electrical Networks and Grid Integration of Wave Energy Offshore Electrical Networks and Grid Integration of Wave Energy Converter Arrays-Techno-economic Optimisation of Array Converter Arrays-Techno-economic Optimisation of Array Electrical Networks, Power Quality Assessment, and Irish Market Electrical Networks, Power Quality Assessment, and Irish Market Perspectives Perspectives Recommended Citation Recommended Citation,” 2015, doi: 10.21427/D7VG7F.

[35] E. Giglio, E. Petracca, B. Paduano, C. Moscoloni, G. Giorgi, and S. A. Sirigu, “Estimating the Cost of Wave Energy Converters at an Early Design Stage: A Bottom-Up Approach,” *Sustainability (Switzerland)*, vol. 15, no. 8, Apr. 2023, doi: 10.3390/su15086756.

[36] “XLPE Submarine Cable Systems Attachment to XLPE Land Cable Systems-User´s Guide Rev 5 2 XLPE Submarine Cable Systems | ABB.” [Online]. Available: www.abb.com/cables

[37] Simec Atlantis Energy, “SUBSEA HUB MARINE LICENCE | SUPPORTING INFORMATION,” 2019. [Online]. Available: www.simecatlantis.com

[38] France Energies Marines, “Dynamic cable: the umbilical for heavy-duty ORE floating systems,” https://www.france-energies-marines.org/en/ore-engineering/dynamic-cable/.

[39] Farinia Group, “TIDAL TURBINE BALLAST AND OTHER TIDAL TURBINE FOUNDATIONS,” https://www.farinia.com/blog/tidal-turbine-ballast-and-other-tidal-turbine-foundations.

[40] Marine Current Turbines, “SeaGen-S 2MW Proven and commercially viable tidal energy generation.”

[41] F. Nash, “Review of Technical Assumptions and Generation Costs Levelised Cost of Electricity from Tidal Stream Energy Issue: 1.1 SYSTEMS • ENGINEERING • TECHNOLOGY,” 2023.

[42] R. Starzmann, I. Goebel, and P. Jeffcoate, “Field Performance Testing of a Floating Tidal Energy Platform-Part 1: Power Performance.”

[43] M. S. Licensing, O. Team, and J. Murray, “Orbital Marine Power Orbital O2.2 Tidal Turbine EMEC Berth 6, Fall of Warness, Eday, Orkney Project Information Document,” 2021.

[44] A. Martinez and G. Iglesias, “Multi-parameter analysis and mapping of the levelised cost of energy from floating offshore wind in the Mediterranean Sea,” *Energy Convers Manag*, vol. 243, Sep. 2021, doi: 10.1016/j.enconman.2021.114416.

[45] Y. Bai and Q. Bai, “Subsea Surveying, Positioning, and Foundation,” *Subsea Engineering Handbook*, pp. 91–137, Jan. 2010, doi: 10.1016/B978-1-85617-689-7.10004-4.

[46] F. Correia Da Fonseca and F. Arede, “DTOceanPlus Deliverable D5.7-Logistics and Marine Operations Tools-Alpha version,” 2020. [Online]. Available: https://www.researchgate.net/publication/342003106

[47] F. Johnson, “Operations Phase Emergency Response Cooperation Plan between Operation Phase Emergency Response Cooperation Plan.” [Online]. Available: www.meygen.com

[48] Black & Veatch, “Lessons Learnt from MeyGen Phase 1A Final Summary Report Lessons learnt from the design, installation and initial operations phases of the 6MW 4-turbine tidal array in Scotland’s Pentland Firth THE TIDE OF CHANGE IN CAITHNESS,” 2020.

[49] “Cable Laying Vessels.” Accessed: Jul. 15, 2024. [Online]. Available: https://ulstein.com/ship-design/cable-laying-vessels

[50] “MV C-Odissey Leask Marine specifications.”

[51] “Neptune DP2 offshore installation vessel,” https://www.deme-group.com/technologies/neptune. Accessed: Dec. 31, 2024. [Online]. Available: https://www.deme-group.com/technologies/neptune

[52] “Aker Wayfarer Multipurpose Offshore Vessel, Norway,” https://www.ship-technology.com/projects/aker-wayfarer-multipurpose-construction-vessel/?utm_source=chatgpt.com&cf-view.

[53] D. Manson, “ODIN OF SCAPA FRYA OF SCAPA THOR OF SCAPA.”

[54] Leask Marine, “MV-USKMOOR.” [Online]. Available: www.leaskmarine.com

[55] Scaldis, “TECHNICAL INFORMATION CHARACTERISTICS HEAVY LIFT VESSEL RAMBIZ.” [Online]. Available: www.scaldis-smc.com

[56] “5 Project Description MeyGen Tidal Energy Project Phase 1 Environmental Statement.”

[57] Atlantis, “MeyGen Update – AR1500 Turbine Deployed in Record Time.” Accessed: Jul. 18, 2024. [Online]. Available: https://saerenewables.com/2225/

[58] W. Guachamin-Acero, Z. Jiang, and L. Li, “Numerical study of a concept for major repair and replacement of offshore wind turbine blades,” *Wind Energy*, vol. 23, no. 8, pp. 1673–1692, Aug. 2020, doi: 10.1002/we.2509.

[59] “EQUIPMENT SHEET.” [Online]. Available: www.boskalis.com/offshore

[60] “MeyGen Tidal Energy Project | Tethys.” Accessed: Jul. 17, 2024. [Online]. Available: https://tethys.pnnl.gov/project-sites/meygen-tidal-energy-project

[61] Aalborg University, “LiftWEC DEVELOPMENT OF A NEW CLASS OF WAVE ENERGY CONVERTER BASED ON HYDRODYNAMIC LIFT FORCES Deliverable D8.1 Cost Database,” 2020.

[62] “EVERYTHING YOU NEED TO KNOW ABOUT TUGBOATS, THEIR TYPES, AND THEIR USES.” Accessed: Jul. 17, 2024. [Online]. Available: https://dexteroffshore.com/what-are-tugboats/

[63] et al. Núñez L.R., “Comparative analysis of life cycle costs between the 2nd generation TEC,” 2015.

[64] M. Kamidelivand, P. Deeney, F. Devoy McAuliffe, K. Leyne, M. Togneri, and J. Murphy, “Scenario Analysis of Cost-Effectiveness of Maintenance Strategies for Fixed Tidal Stream Turbines in the Atlantic Ocean,” *J Mar Sci Eng*, vol. 11, no. 5, May 2023, doi: 10.3390/jmse11051046.

[65] Ove Arup & Partners Ltd, “Marine Scotland Review of Approaches and Cost of Decommissioning Small Scale Offshore Renewable Energy Developments,” 2018. [Online]. Available: www.arup.com

[66] “SABELLA SABELLA D10 tidal turbine MARIINE ENERGY Partners PROJECT ACCOMPAGNED BY ADEME UNDER ECOLOGY AND ENERGY TRANSITION PROGRAMME OF THE INVESTMENTS FOR THE FUTURE PROGRAMME (PIA).” [Online]. Available: www.ademe.fr/invest-avenir

[67] “Typical energy yield Why Tocardo?,” 2014. [Online]. Available: www.tocardo.com

[68] N. M. Nasab, J. Kilby, and L. Bakhtiaryfard, “The potential for integration of wind and tidal power in New Zealand,” *Sustainability (Switzerland)*, vol. 12, no. 5, pp. 1–21, Mar. 2020, doi: 10.3390/su12051807.

[69] E. Fernandez-Rodriguez, T. J. Stallard, and P. K. Stansby, “Experimental study of extreme thrust on a tidal stream rotor due to turbulent flow and with opposing waves,” *J Fluids Struct*, vol. 51, pp. 354–361, Nov. 2014, doi: 10.1016/j.jfluidstructs.2014.09.012.

[70] W. Finnegan, E. Fagan, T. Flanagan, A. Doyle, and J. Goggins, “Operational fatigue loading on tidal turbine blades using computational fluid dynamics,” *Renew Energy*, vol. 152, pp. 430–440, Jun. 2020, doi: 10.1016/j.renene.2019.12.154.

[71] EMEC, “Assessment of Tidal Energy Resource,” 2009.

[72] U.S. Bureau of Labor Statistics, “Consumer Price Index,” https://www.bls.gov/cpi/factsheets/escalation.htm.

[73] “Magallanes Renovables,” https://www.magallanesrenovables.com/.

[74] “MAGALLANES RENOVABLES S.L. Floating energy generation platform-ATIR Initial Decommissioning Programme,” 2020.

[75] M. Bianchi, A. J. Arnal, M. Astorkiza-Andres, J. Clavell-Diaz, A. Marques, and M. Isasa-Sarralde, “Life cycle and economic assessment of tidal energy farms in early design phases: Application to a second-generation tidal device,” *Heliyon*, vol. 10, no. 12, Jun. 2024, doi: 10.1016/j.heliyon.2024.e32515.

[76] E. Díaz-Dorado, C. Carrillo, J. Cidras, D. Román, and J. Grande, “Performance evaluation and modelling of the Atir marine current turbine,” *IET Renewable Power Generation*, vol. 15, no. 4, pp. 821–838, Mar. 2021, doi: 10.1049/rpg2.12071.

[77] “Magallanes Array EMEC Fall of Warness Test Site Navigational Risk Assessment Addendum Document History,” 2023.

[78] A. Marques, “Global Problem 2 Energy transition Challenges Investor Deck.”

[79] A. Ghigo, L. Cottura, R. Caradonna, G. Bracco, and G. Mattiazzo, “Platform optimization and cost analysis in a floating offshore wind farm,” *J Mar Sci Eng*, vol. 8, no. 11, pp. 1–26, Nov. 2020, doi: 10.3390/jmse8110835.

[80] “Steel (USA) Prices,” https://www.focus-economics.com/commodities/base-metals/steel-usa/.

[81] Penny Haire, “Did you know that 90% of coastal seas have no tidal data available?,” https://www.tidetechmarinedata.com/news/90-percent-coastal-sea-have-no-tidal-data-available.

[82] NOAA, “How do we monitor currents? National Ocean Service website,” https://oceanservice.noaa.gov/facts/currentmon.html. Accessed: Feb. 01, 2025. [Online]. Available: https://oceanservice.noaa.gov/facts/currentmon.html

[83] “Copernicus Marine Data Store,” https://data.marine.copernicus.eu/products.

[84] University of Wisconsin–Madison, “How Big is a Degree?,” https://www.sco.wisc.edu/2022/01/21/how-big-is-a-degree/.

[85] M. Lewis, S. P. Neill, P. Robins, M. R. Hashemi, and S. Ward, “Characteristics of the velocity profile at tidal-stream energy sites,” *Renew Energy*, vol. 114, pp. 258–272, 2017, doi: 10.1016/j.renene.2017.03.096.

[86] “DTOceanPlus Site Characterisation (SC) module databases,” https://gitlab.com/dtoceanplus/dtop_sc_databases.

[87] European Commission, “DTOceanPlus, Design Tools for Ocean Energy Systems Innovation,” https://cinea.ec.europa.eu/featured-projects/dtoceanplus_en.

[88] France Energies Marines, “Advanced Design Tools for Ocean Energy Systems Innovation, Development and Deployment Deliverable D5.2,” Apr. 2020.

[89] J. C. Alcérreca-Huerta *et al.*, “Energy yield assessment from ocean currents in the insular shelf of Cozumel Island,” *J Mar Sci Eng*, vol. 7, no. 5, May 2019, doi: 10.3390/jmse7050147.

[90] “Probability Density Function,” https://www.geeksforgeeks.org/probability-density-function/.

[91] K. A. Abed T’ and A. A. El-Mallah, “CAPACITY FACTOR OF WIND TURBINES,” 1997.

[92] “Environmental Technology AS LEVEL Energy from the Wind (2).” Accessed: Feb. 04, 2025. [Online]. Available: https://ccea.org.uk/

[93] “SeaGen Installation Set for Strangford Lough,” https://www.maritimejournal.com/seagen-installation-set-for-strangford-lough/470879.article.

[94] “EMEC Fall of Warness Grid-Connected Tidal Test Site,” https://tethys.pnnl.gov/project-sites/emec-fall-warness-grid-connected-tidal-test-site#description.

[95] “GEBCO Gridded Bathymetry data,” https://www.gebco.net/data_and_products/gridded_bathymetry_data/.

[96] “SammysHP,” https://www.sammyshp.de/fsmap.

[97] European Marine Energy Centre (EMEC), “FloTEC - lessons learnt from developing the world’s most powerful tidal stream turbine,” https://youtu.be/Mj_czIIGHQk?si=fqbjfJb_SNFgEKEi.

[98] “Carbon Steel Prices,” https://agmetalminer.com/metal-prices/carbon-steel/.

[99] A. Gallo, “A Refresher on Net Present Value,” 2014. [Online]. Available: www.business-literacy.com.

[100] “UK awards six tidal stream projects with Contracts for Difference in Allocation Round 6 .” Accessed: Feb. 06, 2025. [Online]. Available: https://www.offshore-energy.biz/uk-awards-six-tidal-stream-projects-with-contracts-for-difference-in-allocation-round-6/

[101] M. H. Nabil *et al.*, “Techno-economic analysis of commercial-scale 15 MW on-grid ground solar PV systems in Bakalia: A feasibility study proposed for BPDB,” *Energy Nexus*, vol. 14, Jul. 2024, doi: 10.1016/j.nexus.2024.100286.

[102] Hydro Review Content Directors, “Joint venture to launch French tidal energy project.” Accessed: Feb. 07, 2025. [Online]. Available: https://www.renewableenergyworld.com/wind-power/offshore/joint-venture-to-launch-french-tidal-energy-project/

[103] R. Campbell, A. Martinez, C. Letetrel, and A. Rio, “Methodology for estimating the French tidal current energy resource,” *International Journal of Marine Energy*, vol. 19, pp. 256–271, Sep. 2017, doi: 10.1016/j.ijome.2017.07.011.

[104] HydroQuest, “FloWatt – Les hydroliennes du Raz Blanchard,” https://www.hydroquest.fr/en/flowatt-en/.

[105] S. Barbarelli, G. Florio, M. Amelio, N. M. Scornaienchi, A. Cutrupi, and G. Lo Zupone, “Design procedure of an innovative turbine with rotors rotating in opposite directions for the exploitation of the tidal currents,” *Energy*, vol. 77, pp. 254–264, Dec. 2014, doi: 10.1016/j.energy.2014.08.044.

[106] M. Corrales-Gonzalez, G. Lavidas, A. Lira-Loarca, and G. Besio, “Wave energy assessment and wave converter applicability at the Pacific coast of Central America,” *Front Energy Res*, vol. 12, Sep. 2024, doi: 10.3389/fenrg.2024.1454275.

[107] S. Horwath, J. Hassrick, R. Grismala, and E. Diller, “Comparison of Environmental Effects from Different Offshore Wind Turbine Foundations,” 2020.

[108] R. Venkat and J. Raina, “What is driving the fluctuation in steel prices?” Accessed: Feb. 24, 2025. [Online]. Available: https://pricevision.ai/blog/what-is-driving-the-fluctuation-in-steel-prices/